

Summer 5-2014

# IDENTIFICATION OF NOVEL NATURAL COMPOUNDS WITH ANTI-BREAST CANCER ACTIVITIES

YUSRA SAIF AL DHAHERI

Follow this and additional works at: [https://scholarworks.uaeu.ac.ae/all\\_dissertations](https://scholarworks.uaeu.ac.ae/all_dissertations)

Part of the [Biology Commons](#)

---

## Recommended Citation

DHAHERI, YUSRA SAIF AL, "IDENTIFICATION OF NOVEL NATURAL COMPOUNDS WITH ANTI-BREAST CANCER ACTIVITIES" (2014). *Dissertations*. 30.  
[https://scholarworks.uaeu.ac.ae/all\\_dissertations/30](https://scholarworks.uaeu.ac.ae/all_dissertations/30)

This Dissertation is brought to you for free and open access by the Electronic Theses and Dissertations at Scholarworks@UAEU. It has been accepted for inclusion in Dissertations by an authorized administrator of Scholarworks@UAEU. For more information, please contact [fadl.musa@uaeu.ac.ae](mailto:fadl.musa@uaeu.ac.ae).

**United Arab Emirates University**

**College of Science**

**IDENTIFICATION OF NOVEL NATURAL COMPOUNDS WITH  
ANTI-BREAST CANCER ACTIVITIES**

**YUSRA SAIF AL DHAHERI**

**This dissertation is submitted in partial fulfillment of the  
requirements for the degree of Doctor of Philosophy**

**Under the direction of Dr. Rabah Iratni**

**May 2014**

## DECLARATION OF ORIGINAL WORK

I, Yusra Saif Al Dhaheri, the undersigned, a graduate student at the United Arab Emirates University (UAEU) and the author of the dissertation entitled "Identification of novel natural compounds with anti-breast cancer activities", hereby solemnly declare that this dissertation is an original research work done and prepared by me under the guidance of Dr. Rabah Iratni, in the College of Science at UAEU. This work has not been previously submitted as the basis for the award of any academic degree, diploma or similar title at this or any other university. The materials borrowed from other sources and included in my dissertation have been properly cited and acknowledged.

Student's Signature..... Date.....

Copyright © 2014 by Yusra Saif Al Dhaheri

All Rights Reserved

## ABSTRACT

Breast cancer continues to be the leading cause of cancer-related death in women worldwide. In this dissertation, natural compounds with anti-breast cancer activities were identified. We investigated the effect of Salinomycin, a potassium ionophore isolated from *Streptomyces albus*, on the survival of three human breast cancer cell lines MCF-7, T47D and MDA-MB-231. High concentrations of Salinomycin induced a G2 arrest, down regulation of survivin and triggered apoptosis. Interestingly, treatments with low concentrations of Salinomycin induced a transient G1 arrest at an earlier time and G2 arrest and senescence, associated with enlarged cell morphology, at a later time. There was also an upregulation of p21 protein, an increase in Histone H3 and H4 hyperacetylation and expression of SA- $\beta$ -Gal activity. Furthermore, it was found that Salinomycin was able to potentiate the killing of the MCF-7 and MDA-MB-231 cells, by the chemotherapeutic agents, 4-Hydroxytamoxifen and frondoside A. We also investigated the effect of *Origanum majorana*, a culinary herb, ethanolic extract (OME) on the survival, migration, invasion and tumor growth of the highly proliferative and invasive triple-negative p53 mutant breast cancer cell line MDA-MB-231. We found that OME inhibited the viability of MDA-MB-231 breast cancer cells both *in vitro* and *in vivo*. OME was found to elicit anti-breast cancer activity by inducing mitotic arrest, DNA damage and triggering the extrinsic apoptotic pathway.

Moreover, OME was found to induce down regulation of survivin, an important therapeutic target against breast cancer.

OME was also found to inhibit cell migration and invasion, two major events required for tumor metastasis. Our data are the first to link senescence and histone modifications to Salinomycin which provides a new insight to better understand the mechanism of action of Salinomycin, at least in breast cancer cells. Moreover, our findings provide strong evidence that *O. majorana* may be a promising chemopreventive and therapeutic candidate against cancer especially for highly invasive triple negative p53 mutant breast cancer; thus validating its use in alternative medicine.

**Keywords:** Breast Cancer, Apoptosis, DNA Damage, Histone Hyperacetylation, p21, Salinomycin, *Origanum majorana*, Senescence-Associated Beta Galactosidase (SA- $\beta$ -Gal), Mitotic Arrest.

## المخلص

لايزال سرطان الثدي السبب الرئيسي للوفيات المرتبطة بالسرطان بين النساء في جميع أنحاء العالم . في هذه الأطروحة ، تم دراسة تأثير نشاط بعض المركبات الطبيعية المضادة لسرطان الثدي. في هذه الأطروحة تم دراسة تأثير السالينومييسين ، مركب حامل لأيون البوتاسيوم و الممعزول من السلالة *Streptomyces albus* ، على حيوية و تكاثر ثلاثة أنواع من الخلايا البشرية لسرطان الثدي: MCF-7 ، T47D و MDA- MB- 231. أظهرت نتائج البحث أن التركيزات العالية من السالينومييسين أدى إلى وقف دورة حياة الخلايا عند مرحلة ال G2 ، وانخفاض تنظيم بروتين ال survivin و تسبب في تحفيز موت الخلايا المبرمج. ومن المثير للاهتمام أن المعاملة مع تركيزات منخفضة من السالينومييسين نتج عنه توقف دورة حياة الخلايا عند مرحلة ال G1 في خلال 24 ساعة من المعالجة و وقف دورة حياة الخلايا في مرحلة ال G2 و الشيخوخة المرتبطة بكبر في حجم الخلايا في خلال 48 ساعة من المعالجة ، زيادة في تنظيم البروتين P21 ، وزيادة في هيستون H3 H4 (hyperacetylation) و زيادة في نشاط تعبير من SA- $\beta$ -Gal. علاوة على ذلك ، وجدنا أن السالينومييسين كان قادرا على تحفيز قتل خلايا الثدي السرطانية MCF- 7 و MDA- MB- 231 ، عند الإستخدم مع أدوية العلاج الكيميائي، 4- Hydroxytamoxifen و frondoside A ، على التوالي. في الجزء الثاني من الأطروحة تم دراسة تأثير مستخلص أوراق نبتة البرقوش (*Origanum majorana*) ، و هي نبتة منتشرة في كافة أنحاء العالم و تستخدم في الطهي و كدواء عشبي تقليدي ، على حيوية، تكاثر، هجرة والغزو و نمو الورم من خلايا سرطان الثدي واسع الإنتشار/ الثلاثي السلبي (MDA- MB- 231) . أظهرت نتائج البحث أن نبتة البردقوش تحول دون جدوى على تكاثر و حيوية خلايا الثدي السرطانية MDA- MB- 231 على حد سواء في المختبر و نمو الورم في الجسم الحي (الحيوانات المخبرية). أظهرت النتائج المخبرية أن نبتة البردقوش تقوم بنشاطها المضاد لسرطان الثدي عن طريق حفز وقف دورة حياة الخلايا الإنقسامية ، تحفيز تلف الحمض النووي (DNA) و التسبب في الموت المبرمج للخلايا عن طريق المسار الخارجي للموت المبرمج للخلايا. علاوة على ذلك، أظهرت النتائج أيضا أن مستخلص هذه النبتة تحت على تقليل من تنظيم بروتين ال survivin ، هدفا علاجيا هاما ضد سرطان الثدي. كذلك وجدنا ان هذا المستخلص فعال في منع هجرة الخلايا السرطانية و غزوها لأماكن أخرى في الجسم ، اثنتين من الأحداث الكبرى الأساسية لل ورم الخبيث.

تقدم النتائج التي توصلنا إليها أدلة قوية على أن مستخلص نبتة البرقوش قد تكون وقائية كيميائية واعدة و مرشح العلاجية ضد السرطان وخاصة بالنسبة لخط خلايا سرطان الثدي ثلاثي السلبية متحولة البروتين p53 الغازية للغاية ؛ وبالتالي التحقق من صحة استخدامه الطبية التكميلية والبديلة . الأهم من ذلك، البيانات المتوفرة لدينا هي الأولى التي تربط بين السالينوميسين الشيوخة و التغير في تعبير الهيستون و الذي يوفر رؤية جديدة لفهم أفضل لآلية عمل السالينوميسين ، على الأقل على خلايا سرطان الثدي.

## **ACKNOWLEDGMENTS**

I am especially grateful to my mentor Dr. Rabah Iratni. Dr. Iratni kindly shared his wisdom and experience. It is with his expert guidance and honest criticism, that I have begun the journey of thinking logically and creatively in the world of molecular biology and cancer. He has provided deep insights into the powers of molecular biology in understanding human cancer. Dr. Iratni was an excellent mentor.

Also, I would like to thank the chair of the Department of Biology and all members at the United Arab Emirates University for assisting me throughout my studies and research.

I would also like to thank my family; Finally, I would like to thank the dissertation committee for their guidance, support, and assistance throughout the preparation of this dissertation.

## **DEDICATION**

To my beloved father, mother, sisters and brothers who believed in me  
and who made my future brighter

## TABLE OF CONTENTS

DECLARATION OF ORIGINAL WORK	ii
COPYRIGHT	iii
ABSTRACT	iv
ACKNOWLEDGMENTS	viii
DEDICATION	ix
TABLE OF CONTENTS	x
LIST OF TABLES	xi
LIST OF FIGURES	xii
LIST OF ABBREVIATIONS	xviii
CHAPTER 1: INTRODUCTION	1
CHAPTER 2: MATERIALS AND METHODS	25
CHAPTER 3: RESULTS AND DISCUSSIONS	39
GENERAL CONCLUSION	131
REFERENCES	132

## **LIST OF TABLES**

Table 1. Viability of MDA-MB-231 Cells in Response to Salinomycin Determined by Trypan Blue Exclusion Assay.

## LIST OF FIGURES

Figure 1. Inhibition of Cellular Viability of MDA-M-231 Cells by Salinomycin.

Figure 2. Inhibition of Cellular Viability of MCF-7 cells by Salinomycin.

Figure 3. Inhibition of Cellular Viability of T47-D Cells by Salinomycin.

Figure 4. Cell Viability of MDA-MB-231 Cells in Response to Various Concentrations of Salinomycin Using Trypan Blue Exclusion Dye Assay.

Figure 5. Cell Viability of the MDA-MB-231 Cells in Response to Salinomycin after 24 hours Determined by Trypan Blue Exclusion Dye and CellTiter-Glo Assays.

Figure 6. Cell Viability of the MDA-MB-231 Cells in Response to Salinomycin after 48 hours Determined by Trypan Blue Exclusion Dye and CellTiter-Glo Assays.

Figure 7. Morphological changes Observed in the MDA-MB 231 Cells After 24 Hours of Treatment with Various Concentration of Salinomycin.

Figure 8. Western Blot Analysis of Vimentin and E-cadherin Expression in Salinomycin Treated MDA-MB-231 Cells.

Figure 9. Immunofluorescence Staining for Vimentin in Salinomycin Treated MDA-MB-231 Cells.

Figure 10. Morphological Changes Observed in the MDA-MB 231 Cells After 72 Hours of Treatment with Various Concentrations of Salinomycin.

Figure 11. Salinomycin Induced Apoptosis in the MDA-MB-231 Cells. Annexin V binding was carried out using Annexin V-FITC Detection Kit.

Figure 12. Immunofluorescence Staining for Annexin V-FITC in Salinomycin Treated MDA-MB-231 Cells.

Figure 13. Stimulation of Caspase 3/7 Activity in MDA-MB-231 Cells After Exposure to Salinomycin (10 and 25  $\mu$ M) for 24 and 48 Hours.

Figure 14. Western Blot Analysis Showing Dose-and Time-Dependent Induction of PARP Cleavage in Salinomycin Treated MDA-MB-231 Cells.

Figure 15. Inhibition of Proliferation by Salinomycin in MDA-MB-231 Cells.

Figure 16. Induction of Growth Arrest by Salinomycin in MDA-MB-231 Cells.

Figure 17. Flow Cytometry Analysis of Salinomycin-Induced G2 Cell-Cycle Arrest in MDA-MB-231 Cells.

Figure 18. Western Blot Analysis of p(ser10) Histone H3, cyclin B1 and cyclinD1 Expression in Salinomycin Treated MDA-MB-231.

Figure 19. Salinomycin Induced Senescence in MDA-MB-231 Cells After Incubated with 5  $\mu$ M Salinomycin for 96 Hours and Stained for SA- $\beta$ -Galactosidase Activity.

Figure 20. Western Blot Analysis of Phosphor-H2AX (Ser 139) in MDA-MB-231 Cells Treated for 6, 24 and 48 Hours with DMSO or Indicated Concentrations of Salinomycin.

Figure 21. Immunofluorescence Staining for  $\gamma$ H2AX in Salinomycin Treated MDA-MB-231 Cells.

Figure 22. Western Blot Analysis of p21 Expression in Salinomycin Treated MD-MB 231 Cells.

Figure 23. Immunofluorescence Staining for p21 in Salinomycin Treated MDA-MB-231Cells.

Figure 24. Western Blot Analysis of p27 Expression in MDA-MB-231 Cells upon Salinomycin Treatment.

Figure 25 . Western Blot Analysis of Survivin Expression in Salinomycin-Treated MDA-MB 231 Cells.

Figure 26. Western Blot Analysis of Ac-H3 and Ac-H4 Expression in Salinomycin Treated MDA-MB 231 Cells.

Figure 27. Immunofluorescence Staining of Ac-H3 and Ac-H4 in MDA-MB-231 Cells Treated with 10 and 25  $\mu$ M Salinomycin for 24 Hours.

Figure 28. Salinomycin Enhanced Cell Death Induced by Frondoside A in MDA-MB-231 Cells.

Figure 29. Salinomycin Enhanced Cell Death Induced by 4 Hydroxy-Tamoxifen in MCF-7 Cells.

Figure 30. Salinomycin Induced Synergistic Apoptosis Against MCF-7 Cells.

Figure 31. Hypothetic Model for the Differential Effect of Salinomycin in MDA-MB-231 Breast Cancer Cells.

Figure 32. Inhibition of Cell Viability of MDA-MB-231 Cells by *O. majorana* Extract.

Figure 33 Micrograph of MDA-MB-231 Cells After 24 Hours Incubation with Various Concentrations of OME.

Figure 34. Flow Cytometry Analysis Showing a G2/M Cell Cycle Arrest Induced by *O. majorana* Extract in MDA-MB-231 Cells.

Figure 35 . Western Blot Analysis of Phosphor(ser10)-H3, and Cyclin B1 in OME Treated MDA-MB231 Cells.

Figure 36. Stimulation of Caspase 3/7 Activity in OME Treated in MDA-MB-231 Cells.

Figure 37. Concentration-Dependent Induction of PARP Cleavage in OME Treated MDA-MB231 Cells.

Figure 38. Western Blot Analysis Showing A differential Effect on Survivin Expression by Different Concentrations of OME in MDA-MB-231 Cells.

Figure 39 . *O. majorana* Induced Apoptosis by Activation of Caspase 8 and but not Caspase 9 in MDA-MB-231 Cells.

Figure 40. Western Blot Analysis Showing An increase in Cellular TNF- $\alpha$  Protein in the MDA-MB-231 Cells Treated with OME.

Figure 41. Immunofluorescence Staining for TNF- $\alpha$  in OME Treated MDA-MB- 231 Cells.

Figure 42. Western Blot Analysis Showing Expression Levels of Mutant p53 and p21 in *O. majorana* Treated MDA-MB-231 Cells.

Figure 43. Western Blot Analysis Showing Protein Levels of Ac-H3 and Ac-H4, Extracted from OME Treated Cells.

Figure 44. Immunofluorescence Staining of Ac-H3 and Ac-H4 in MDA-MB231 Cells Treated with OME for 24 Hours.

Figure 45. Western Blot Analysis of Phosphor-H2AX (Ser 139) in MDA-MB231 Cells Exposed to OME.

Figure 46. Immunofluorescence Staining for  $\gamma$ H2AX in OME Treated MDA-MB 231 Cells.

Figure 47 . Caspase 3/7 Activation in OME Treated MDA-MB-231 Cells After 6 Hours.

Figure 48. Inhibition of Colony Growth by *O. majorana* Extract.

Figure 49. Wound Healing Assay Showing that OME Inhibited the Migration of MDA-MB-231 Breast Cancer Cells in Dose-Dependent Manner.

Figure 50. Cell Viability After Incubation of MDA-MB-231 Cells with OME For 10 Hours.

Figure 51. Boyden Chamber Transwell Assay Indicating that OME inhibited the Migration of MDA-MB-231 Cells.

Figure 52. Quantification of Migrated MDA-MB-231 Cells.

Figure 53. Photograph Under Phase-Contrast Microscope (x100 Magnification) Showing Aggregated Cells After OME Treatment.

Figure 54. Western Blot Analysis of E-cadherin expression in OME Treated MD-MB-231 Cells.

Figure 55. Immunofluorescence Staining for E.cadherin in OME Treated MDA-MB 231 Cells.

Figure 56 . E. cadherin Promoter Activity Following transfection with A Luciferase Reporter Gene Containing E-cadherin promoter in MDA-MB-231 Cells.

Figure 57. *O. majorana* Inhibited the Invasive Activity of MDA-MB-231 Cells.

Figure 58. Quantification of Invaded MDA-MB-231 into the Matrigel.

Figure 59 . Effects of OME on the Secretions of MMP-2 and MMP-9 in the Collected Conditioned Medium of OME Treated MDA-MB-231 Cells.

Figure 60. RT-PCR Analysis of the mRNA Levels of MMP-2 and MMP-9 in MDA-MB-231 Cells Treated with OME for 24 Hours.

Figure 61 . Activities of MMP-2 and MMP-9 in OME Treated MDA-MB 231 Cells.

Figure 62. Western Blot Analysis of uPAR Expression in OME Treated MD-MB-231 Cells.

Figure 63. Inhibition of Adhesion of MDA-MB-231 Cells to HUVEC by *O. majorana*.

Figure 64. Western Blot Analysis of ICAM-1 Expression in OME Treated MD-MB-231 Cells.

Figure 65. *O. majorana* Inhibited Migration of MDA-MB-231 Cells A cross Monolayer of TNF-  $\alpha$  Activated HUVECs.

Figure 66. Quantification of Basal Level of VEGF Secretion in Conditioned Medium from Vehicle or OME Treated MDA-MB-231 Cells.

Figure 67. Quantification of VEGF Secretion in TNF- $\alpha$  Induced MDA-MB-231 Cells Cultured in Presence of Vehicle or Indicated Concentrations of OME.

Figure 68 . Quantification of VEGF Secretion in TNF- $\alpha$  Induced HUVECs Cultured in Presence of Vehicle or Indicated Concentrations of OME.

Figure 69. Western Blot Analysis of the Phosphorylation Status of I $\kappa$ B $\alpha$ .

Figure 70. Western Blot Analysis of the Nuclear p65 (NF $\kappa$ B).

Figure 71. Quantification of NO levels in OME Treated MDA-MB-231 Cells.

Figure 72 . Anti-tumor Growth of *O. majorana* on Breast Tumor in a Chick Embryo Chorioallantoic Membrane Model System.

Figure 73 . Quantification of Tumor Weight in Vehicle, Colchicine and Indicated Concentrations of OME Treated Chick Embryo.

Figure 74. Anti-Metastatic Effect of *O. majorana*. Quantification of Nodules Observed in the Lower CAM of Chick Embryo Treated with Vehicle, Colchicine or OME.

Figure 75. Proposed Mechanisms of Action of *O. majorana* on MDA-MB-231 Cells.

## LIST OF ABBREVIATIONS

**4-HT**, 4-Hydroxy-Tamoxifen

**AP-1**, Activator Protein-1

**CAM**, Chorioallantoic Membrane

**CDKs**, Cyclin Dependent Kinases

**COX-2**, Cyclooxygenase-2

**DMEM**, Dulbecco Minimal Essential Medium

**DMSO**, Dimethyl Sulfoxide

**ECM**, Extra Cellular Matrix

**EGFR**, Epidermal Growth Factor Receptor

**FACS**, Fluorescence-Activated Cell Sorting

**Fr**, Frondoside A

**IAP**, Inhibitor of Apoptosis Protein

**ICAM-1**, Intracellular Adhesion Molecule-1

**HDAC**, Histone Deacetylase

**HUVECs**, Human Umbilical Vein Endothelial Cells

**GSK**, Glycogen Synthase Kinase

**MAPK**, Mitogen-Activated Protein Kinases

**MMPs**, Matrix Metalloproteinases

**NF $\kappa$ B**, Nuclear Factor  $\kappa$ B

**OME**, *Origanum majorana Extract*

**PARP**, Poly (ADP-ribose) Polymerase

**PCR**, Polymerase Chain Reaction

**PI3K**, Phosphoinositide 3-Kinase

**PKC**, Protein Kinase C

**RIPA**, Radioimmunoprecipitation Assay Buffer

**ROS**, Reactive Oxygen Species

**SA- $\beta$ -Gal**, Senescence-Associated  $\beta$ -Galactosidase

**SDS-PAGE**, Sodium Dodecyl Sulfate-Polyacrylamide Gel Electrophoresis

**TBST**, Tris Buffered Saline Containing/ 0.05% Tween 20

**TNF- $\alpha$** , Tumor Necrosis Factor-  $\alpha$

**TNBC**, Triple Negative Breast Cancer

**uPA**, Urokinase Plasminogen Activator

**uPAR**, Urokinase-type Plasminogen Activator Receptor

**VEGF**, Vascular Endothelial Growth Factor

**X-gal**, 5-Bromo-4-Chloro-Indolyl- $\beta$ -D-Galactopyranoside.

# **CHAPTER 1: INTRODUCTION**

## **1.1 Breast Cancer**

Breast cancer is the leading cause of cancer-related death in women worldwide. Approximately one-third of all women with breast cancer develop metastasis and ultimately die as a result of the effects of the disease. The American cancer society estimated nearly 232,670 new cases and about 40,000 deaths estimated due to breast cancer in women in 2014 [1]. According to the UAE Ministry of Health, breast cancer is the most common malignancy diagnosed among women in the UAE. Women in the UAE tend to develop breast cancer at least a decade earlier than their counterparts in the West, according to a study [210]. Remarkable progress has been made in the treatment of breast cancer over the years with hormonal therapy for estrogen receptors and/or progesterone receptors positive tumors, as well as other therapies. However, despite these advances, breast cancer remains a frequent cause of death in women.

## **1.2 Triple Negative Breast Cancer**

Triple-Negative Breast Cancer (TNBC) is a subtype of breast cancer characterized by tumors that do not express estrogen receptors (ER), progesterone receptors (PR), or human epidermal growth factor membrane receptors (HER-2). It comprises about 15% of all breast cancer cases [2]. It is characterized by its unique molecular profile, aggressive behavior, and distinct pattern of metastasis, including lung, liver and brain metastasis [3]. Epidemiological studies showed a high prevalence of triple negative breast cancer among younger women and those of African

descent. TNBC has a poor prognosis and relapse quickly compared with other subtypes of breast cancer that are positive for hormonal receptors or HER2 membrane receptors [4].

Gene-expression profiling approaches demonstrated that TNBC is a heterogeneous group of diseases composed of different, molecularly distinct subtypes [4, 5]. Although not synonymous, the majority of TNBC share morphological and genetic abnormalities with basal-like breast cancer, a subgroup of breast cancer defined by gene-expression profiling, where TNBC constitutes approximately 80% of all basal-like tumors. However, several studies have shown that TNBC includes tumors with a non-basal expression profile and, in particular, normal-breast, the multiple markers negative, as well as the recently identified claudin-negative subtype [4, 5]. TNBC also has molecular features that overlap with breast cancer, BRCA-1 germline mutation, and is also associated with p53 mutations [2, 6].

TNBC represents an important clinical challenge because these types of cancer do not respond to hormonal therapy or other available treatments. Despite advances in the treatment of hormone receptors (HR) and human epidermal growth factor receptors (HER2)-positive breast cancers, the prospects for women with TNBC remains poor and conventional chemotherapy remains the main treatment of TNBC even though TNBC becomes highly resistant [7]. Preclinical and clinical studies have suggested several agents that are active in TNBC. These agents include DNA-damaging agents and poly (ADP-ribose) polymerase (PARP) inhibitors which are active in TNBC associated with BRCA1 dysfunction.

Anti-epidermal growth factor receptors (EGFR) antibodies and EGFR tyrosine kinase inhibitors are active in TNBC with EGFR gene amplification. Dasatinib is active in TNBC with activated Src tyrosine kinase and inhibitors of mammalian target of rapamycin (mTOR) are active in TNBC with loss of PTEN tumor suppressors. Anti-angiogenic therapies were shown to enhance antitumor activity of chemotherapeutic agents in hypervascular TNBC. To develop novel strategies against TNBC, it is essential to understand the pathways driving the aggressive behavior of these types of cancer [8-10].

### **1.3. Cancer Metastasis**

Cancer metastasis starts in the primary tumor site when cancer cells start to invade and degrade the basement membrane and extracellular matrix (ECM) to get into the vascular or lymphatic circulation system. Loss of cell to cell adhesion, induces the disassembly of cancer cells from the primary tumor, disseminating to distant sites through blood vessels and lymphatics, and eventually they leave the circulation to establish metastasis in distant organs [11, 12]. E-cadherin, a cell–cell adhesion molecule, plays a major role in the establishment and maintenance of normal tissue architecture. It is expressed predominantly on the surface of normal epithelial cells. For cancer cells to become metastatic, they must decrease E-cadherin expression and break cell-cell adhesions and induce cell mobility triggering a transition from tumorigenic (epithelial) to migratory/invasive (mesenchymal) phenotype ending in tumor metastasis. Hence, the expression level of the epithelial cadherin (E-cadherin) has become an important indicator of these transitions [13,

14]. Therefore, searching for agents that could enhance E-cadherin expression is therapeutic aim in order to repress the metastatic potential of cancer cells.

The adherence of tumor cells to endothelial cells is an essential step during cancer progression and metastasis. Several adhesive molecules, such as intracellular adhesion molecule-1 (ICAM-1), have been identified as being responsible for the endothelial adhesion of cancer cells [15]. While ICAM-1 expression was found at low basal levels in many cell types, including epithelial and endothelial cells [16], its expression as a soluble serum ICAM-1 were found to be high in metastatic breast cancer patients [16]. Therefore, agents that repress ICAM-1 expression in breast cancer cells, and subsequently block the interaction between cancer and endothelial cells, might be an important therapeutic target for repressing the metastatic potential of cancer cells.

### **1.3.1. Tumor Cell Invasion in Cancer Metastasis**

Degradation of the extracellular matrix (ECM) surrounding the primary tumor is an essential step in tumorigenesis. This degradation is important for tissue remodeling and the induction of angiogenesis, and is mainly mediated by specific proteolytic enzyme systems mainly matrix metalloproteinase (MMPs) and urokinase plasminogen activator (uPA). Among MMPs, upregulation of MMP-2 and MMP-9 was shown to be associated with breast cancer metastasis and poor clinical outcomes [17]. Northern blot analysis revealed that the level of MMP-2 and MMP-9 mRNA was higher in breast cancer tissues compared to normal breast

tissue [18]. In addition, higher MMP-9 protein concentration was detected in breast cancer tissue when compared to normal breast tissue [19]. Similarly, higher protease activity for MMP-2 and MMP-9 was detected by zymography in tumor tissues compared to normal tissues [20].

MMPs are directly activated by Serine Protease Plasmin, which is activated from its proenzyme form (plasminogen) by serine protease urokinase-type plasminogen activator (uPA) upon binding to cell surface receptors (uPAR). Overexpression of uPA has been found in many tumor types and is correlated to a poor prognosis. Moreover, binding of uPA to uPAR also induces signal transduction, allowing enhanced cell migration [17, 21, 22]. Therefore, regulating the expression of ECM degradation enzymes is another therapeutic target to control breast cancer.

### **1.3.2. Angiogenesis in Cancer Metastasis**

Angiogenesis is a complex multistep process involving soluble factors, adhesion molecules, proteases and cytokines. The process of tumor angiogenesis starts when tumor cells secrete and activate angiogenic factors, thereby activating proteolytic enzymes. At this time, endothelial cells proliferate, migrate, and differentiate.

Vascular endothelial growth factor (VEGF) is the most prominent mediator in tumor angiogenesis that is induced in breast cancer [23]. Up-regulation of VEGF expression has been reported in a variety of malignant human cancers including breast, colon, and lung cancers. An in situ hybridization study of human breast samples showed high VEGF expression in tumor cells but not in the normal duct epithelium [24].

Hence, VEGF might be a good target in the treatment of breast cancer patients.

### **1.3.3. Nuclear Factor $\kappa$ B (NF $\kappa$ B) in Cancer Progression and Metastasis**

Nuclear Factor  $\kappa$ B (NF $\kappa$ B), (a transcription factor), is a key player in cancer metastasis [11]. It has been shown that several genes involved in tumor metastasis are directly regulated by NF $\kappa$ B. The frequent over-expression of NF $\kappa$ B in tumor cells suggests that selected tumor cells may acquire metastatic activity via aberrant expression of metastasis relevant genes during their progression. In fact, studies showed that MMP-2 and MMP-9 [25, 26], uPA [27, 28], uPAR [29] and ICAM-1 [30] are downstream targets of the NF $\kappa$ B signaling pathway. NF- $\kappa$ B provides mechanistic links between inflammation and cancer, and moreover, regulates tumor angiogenesis and invasiveness, indicating that signaling pathways that mediate their activation provide attractive targets for new chemotherapeutic approaches [11].

### **1.4. Programmed Cell Death through Apoptosis**

Apoptosis, a major form of programmed cell death, is a defense mechanism and a tumor suppressor pathway essential for the development and maintenance of cellular homeostasis. When deregulated apoptosis leads to an uncontrolled proliferation of damaged cells. It also leads to resistance to chemo and radio therapy [31]. Apoptosis can be triggered by diverse cellular signals. These include intracellular signals produced in response to cellular stress, such as increased intracellular

Ca<sup>2+</sup> concentration, DNA damage and high levels of reactive oxygen species (ROS). Extrinsic inducers of apoptosis include bacterial pathogens, toxins, nitric oxide, growth factors and hormones [32]. Apoptosis is regulated by a series of signaling cascades and occurs via two connected pathways. The extrinsic pathway is initiated by cell surface death receptor stimulation and activation of caspase-8, while the intrinsic pathway involves cytochrome c release from mitochondria and subsequent caspase-9 activation. Activated caspase-8 and-9 activate executioner caspases, including caspase-3, which in turn activate a cytoplasmic endonucleases and proteases that degrades nuclear materials and nuclear and cytoskeletal proteins, respectively, resulting in elimination of abnormal cells [33]. Evasion from apoptosis is a hallmark of cancer cells leading to an uncontrolled proliferation of damaged cells and contributing to cancer development that enhances resistance to conventional anti-cancer therapies, such as radiation and cytotoxic therapies. Most chemotherapeutic agents induce cancer cell death by the activation of the apoptotic pathway. However, most current chemotherapeutic drugs are associated with cytotoxic side-effects and the development of chemo-resistance [34, 35].

### **1.5. Cell Cycle Control**

The cell cycle is series of integrated events controlled by a complex series of cellular and molecular signaling pathways by which a cell grows, replicates its DNA and divides. This process also includes mechanisms to ensure the fidelity of genetic material and corrects errors through checkpoints; if not, the cells commit suicide (apoptosis) [36, 37].

The cell cycle consists of four phases (G1, S, G2 and M). It governs the transition from quiescence (G0) to cell proliferation. As a cell approaches the end of the G1 phase, it is controlled at a checkpoint, called G1/S, where the cell determines whether or not to replicate its DNA. At this checkpoint the cell is checked for DNA damage to ensure that it has all the necessary cellular machinery to allow for successful cell division. As a result of this checkpoint, which involves the interaction of various proteins, a molecular switch is switched on or off. Cells with intact DNA continue to S phase while cells with damaged DNA are arrested and commit suicide through apoptosis, or programmed cell death. A second such checkpoint occurs at the G2 phase following the synthesis of DNA in S phase but before cell division in M phase [38, 39].

In eukaryotes, regulation of the cell cycle is controlled, in part, by a family of protein kinase complexes, and each complex is composed minimally of a catalytic subunit, the Cyclin Dependent Kinases (CDKs), a specific enzyme family that uses signals to switch on cell cycle mechanisms. At least nine structurally related CDKs (CDK1- CDK9) have been identified. CDKs themselves are activated by forming complexes with an essential activating partner, cyclin, and another group of regulatory proteins that are only present for short periods in the cell cycle. These complexes are activated at specific intervals during the cell cycle by phosphorylation at specific sites on the CDK by CDK-activating kinase (CAK), but can also be induced and regulated by exogenous factors. During the progression of the cell cycle, the cyclin-CDK complexes are subject to inhibition through binding with a class of proteins known as

Cyclin Dependent Kinase Inhibitors (CDKIs), such as the CIP/KIP and INK4 families of proteins [37, 40-42].

In mammalian cells CDKIs are grouped into two classes: (1) p21 (Cip1/Waf1/Cap20/Sdi1/Pic1), p27 (Kip1), and p57 (Kip2) are related proteins with a preference for Cdk2-and Cdk4-cyclin complexes, (2) also p16Ink4a, p15Ink4b, p18Ink4c, and p19Ink4d are closely related CDKIs specific for Cdk4- and Cdk6-cyclin complexes [43]. For instance, following stress signals or DNA damage, p21 and p27 bind to cyclin-CDK complexes to inhibit their catalytic activity, stop the cell from proceeding to the next phase of the cell cycle and induce cell-cycle arrest at different phases [44].

A considerable number of cyclins have been identified (cyclin A–cyclin T). The pattern of cyclin expression varies with a cell's progression through the cell cycle, and this specific cyclin expression pattern defines the relative position of the cell within the cell cycle [45]. Cyclin D interacts with CDK2, -4, and -6 and drives cell progression through G1. The association of cyclin E with CDK2 is active at the G1/S transition and directs entry into S phase. S phase progression is directed by the cyclin A/CDK2 complex, and the complex of cyclin A with CDK1 is important in G2. CDK1/cyclin B is necessary for mitosis to occur [40, 46].

When functioning properly, cell cycle regulatory proteins act as the body's own tumor suppressors by controlling cell growth and inducing the death of damaged cells [40]. However, any genetic mutations that cause the malfunction or absence of one or more of the regulatory proteins at cell cycle checkpoints can result in a molecular switch being turned

permanently on, permitting uncontrolled multiplication of the cell, leading to carcinogenesis, or tumor development [38].

## **1.6. Cell Cycle Control and Cancer**

A dysregulation of the cell cycle is a hallmark of cancer in which, contrary to normal cells, tumor cells undergo unrestricted growth without stopping at predetermined points in the cell cycle. This is due to the inactivation of critical CDKs, or to overexpression of cyclins. For instance, overexpression of cyclin D1 has been associated with the development and progression of breast cancer [37, 47]. Thus, abrogation of cell cycle checkpoints through targeting CDKs, CDKIs and/or cyclins would recapitulate cell cycle checkpoints that limit a tumor cell's ability to cycle, and this may induce an apoptotic cascade leading to cell death [48]. Recent studies have suggested that cell cycle arrest in malignant cells is often associated with apoptotic cell death. In recent years, many studies have shown the involvement of cell cycle regulation-mediated apoptosis as a mechanism of cell growth inhibition [59-51] and such targeted therapy against cancer has become important as an ideal compound for the management of cancer. In clinical trials a series of targeted agents directly abrogate the cell cycle checkpoints at critical times and induce growth arrest to ultimately make the tumor cell susceptible to apoptosis [52, 53]. Examples of such agents include synthetic cell cycle inhibitors such as flavopiridol, olomoucine, roscovitine and puvalanol B which are considered to be a new generation of anticancer drugs [41, 54].

Interestingly, a number of natural compounds exerted their anti-cancer activities through the induction of cell cycle arrest at different phases, which is considered as a promising chemopreventive and chemotherapeutic strategy, using more efficient and less toxic agents. Examples of some naturally occurring compounds that have induced cell cycle arrest, include capsaicin (chili peppers ), kaempferol (broccoli and tea), apigenin (parsley and celery), tangeretin (citrus peels), catechins (tea), cyaniding (cherries and strawberries), 6-gingerol (ginger) and resveratrol (grapes and red wine) [55- 57].

### **1.7. Cell Senescence**

Cell senescence is a stable cell cycle arrest that occurs in normal cells after a limited number of cell divisions. However, it is now broadly defined as a physiological program of terminal growth arrest [58]. It can be triggered by genetic manipulations or by different forms of stress such as treatment with chemotherapeutic drugs, radiation or differentiating agents [59]. Cells that undergo senescence do not proliferate even under mitogen stimulation, they remain viable and metabolically active but are permanently growth-arrested and produce secreted proteins such as ECM components that affect the growth of their neighboring cells (with both tumor-suppressing and tumor-promoting activities) as well as tissue organization. Even if not all of the tumor cells are rendered senescent as a result of an inducing agent (i.e. treatment), such cells may provide a reservoir of tumor-suppressing factors that will inhibit the growth of non-senescent cells [60]. Growth arrest is achieved and maintained in either

the G1 or G2/M stage of the cell cycle, in part, by increased expression of specific cyclin-dependent kinase inhibitors (CDKIs), including p16<sup>Ink4a</sup>, p21<sup>Waf1</sup> and p27<sup>Kip1</sup> [61].

Senescent cells develop distinct and recognizable flattened and enlarged cell morphology with a prominent nucleus and increased cytoplasmic granularity. Most notably, these cells can be visualized with a staining technique that is a widely accepted and used as a marker, senescence-associated  $\beta$ -galactosidase (SA- $\beta$ -gal) activity, which is detectable by X-gal staining at pH 6.0, reflecting an increased lysosomal mass of senescent cells, and stains the perinuclear compartment blue [62].

### **1.8. Senescence in Cancer Therapy**

Cancer therapy has traditionally been based on drug cytotoxicity that aims to complete the destruction of tumor cells to improve patient survival. This involves treatment with a high dose of toxic compounds or/ radiation. These approaches may produce complete cell death within a tumor, however, they have been found to cause severe side effects in patients and often develop drug resistance and relapse or progress to advanced primary and metastatic tumors [60]. An alternative strategy is the induction of senescence, which permanently stop the proliferative capacity of cells without inducing cancer cell death (cytostatic therapy). It is of clinical interest that cancerous cells can be induced to a senescent state *in vitro* and *in vivo* with specific conventional anticancer treatments. The induction of senescence in cancerous cells can sensitize cancerous

cells more to chemotherapy or radiation but by using lower doses. A senescence-induced response to chemotherapy has been found to be induced by a wide variety of anticancer agents under conditions of minimal cytotoxicity. Recently, clinical studies utilizing cytostatic treatments have shown promising preliminary results where therapy induced senescence has been identified in tumors after radiation or chemotherapy [63-65]. Although senescence occurs only in a subset of treated cells, suggesting that these treatments may be as effective as cytotoxic therapies in inducing permanent growth inhibitory response in both early and late stage cancers, limiting tumor progression and providing equivalent or prolonged survival with reduced toxicity related side effects. Moreover, evidence suggests that therapy inducing senescence may function as a back-up response to therapy in cancer cells in which apoptotic pathways are disabled [66]. Therefore, activating senescence in tumor cells is another attractive approach to cancer treatment.

Senescence is not the only anti-proliferative response that determines treatment responses in the absence of apoptosis. Another principal mechanism for anticancer agents is mitotic catastrophe; cell death resulting from abnormal mitosis; which usually ends in the formation of large cells with multiple micronuclei and uncondensed chromatin [67]. Etoposide-induced mitotic catastrophe in HeLa cells was greatly increased when apoptosis was inhibited by BCL-2 [68]. Also, both mitotic catastrophe and senescence were shown to be induced in irradiated tumor cells when apoptotic responses were suppressed [69].

## **1.9. Natural Sources As Potential Anti-Cancer Agents**

Among the potential alternatives for treating cancer are anti-cancer agents from natural sources such as plants and dietary phytochemicals, marine organisms and microorganisms. Throughout history, nature has been an attractive and rich source of new therapeutic compounds that have found many applications in cancer therapy, as a tremendous chemical diversity can be found in millions of species of plants, animals, marine organisms and microorganisms [70]. Over 70% of all anti-cancer compounds are either natural products, or natural product-derived substances or their derivatives (chemically-altered products) that were developed on the basis of knowledge gained from small molecules or macromolecules that exist in nature [71]. Chemoprevention and chemotherapy by naturally occurring agents is now considered to be more effective, and they do not have large side-effect consequences compared to synthetic drugs. It is an inexpensive, readily applicable, acceptable and accessible approach to cancer prevention and treatment [72].

Recent studies have shown that compounds isolated from natural sources have cytotoxic effects on several types of cancer cells, like breast, colon, melanoma, uterine, lung and leukemia cells. Moreover, studies suggest that the consumption of food rich in fruit, vegetables and spices results in a lower incidence of cancers (stomach, oesophagus, lung, oral cavity and pharynx, endometrium, pancreas and colon) [56, 70, 71].

Between 2001 and 2005, four new drugs derived from natural products were approved as anti-cancer agents. The approved anti-cancer

agents doxorubicin, estradiol in 2002, chlorophyll and L-aspartic acid in 2004 and taxol nanoparticles in 2005 [73]. The marine alkaloid trabectedin, epothilone derivative ixabepilone and temsirolimus are three new drugs introduced in 2007 that originated from microbial sources for the treatment of cancer [74].

### **1.9.1. Phytochemicals: Dietary Source of Anti-Cancer Agents**

Phytochemicals are natural plant-derived compounds that have been shown to influence human health in many ways. Plants have been a rich source of highly effective phytochemicals which offer great potential in the fight against cancer. More than 1,000 different phytochemicals have already been proved to possess interesting chemo-preventing activities. Phytochemicals are becoming more attractive for cancer prevention and treatment because they were proven to be very effective, and do not have serious side-effects compared to synthetic drugs and most importantly, they can act on specific and/or multiple molecular and cellular targets. Recently, these natural compounds have become of increasing interest thanks to their health promoting properties, especially with regard to breast cancer treatment and prevention [71, 75].

Identification and development of new chemotherapeutic agents from plants have been recognized in cancer therapy, and have become major areas for experimental cancer research. Various phytochemicals present in the diet were found to (i) kill breast cancer cells *in vitro* and (ii) prevent and/or suppress breast cancer progression in various preclinical animal models [76]. Phytochemicals have been shown to target breast cancer development and progression through inhibiting cellular

proliferation, suppressing inflammatory processes, arresting cell cycles, inducing apoptosis, modulating gene expression such as upregulation of cytoprotective genes that encode for carcinogen detoxifying enzymes and antioxidant enzymes and/or upregulation of tumor suppressing genes that encode for tumor suppressor proteins that play an important roles in cellular signaling pathways, and inhibiting angiogenesis and invasion potential of many metastatic cancer cell line [77].

Thus, cell signaling cascades and their interacting factors have become important targets of chemoprevention and chemotherapy in which phytochemicals and plant based agents seem to be effective. The mechanistic insight into chemoprevention further includes induction of cell cycle arrest and apoptosis, or inhibition of signal transduction pathways, mainly the mitogen-activated protein kinases (MAPK), protein kinases C (PKC), phosphoinositide 3-kinase (PI3K), glycogen synthase kinase (GSK) which lead to abnormal cyclooxygenase-2 (COX-2), activator protein-1 (AP-1), NF- $\kappa$ B and c-Myc expression. The effectiveness of chemopreventive agents reflects their ability to counteract certain upstream signals that lead to genotoxic damage, redox imbalances and other forms of cellular stress [77].

Bioactive natural compounds and the modulated molecular targets identified through extensive research can be the basis for how these anti-cancer agents can potentially be used for the prevention and treatment of cancer. However, a lack of success with targeted monotherapy, resulting from evading mechanisms, has forced researchers to employ either combination therapy or agents that interfere with multiple cell-signaling

pathways. Numerous anti-cancer agents and phytochemicals identified from plants can interfere with cell-signaling pathways. Examples of anticancer drugs derived from plants and currently in clinical use include the *vinca* alkaloids (vinblastine and vincristine) isolated from *Catharanthus roseus*. The *Vinca* alkaloid was responsible for an increase in the cure rates of some forms of leukemia [78]. Vincristine was shown to inhibit microtubule assembly, inducing tubulin self-association into coiled spiral aggregates [78]. Etoposide is an epipodophyllotoxin, derived from the mandrake plant *Podophyllum peltatum* and the wild chervil *Podophyllum emodi* [79] and displayed significant promise against small-cell lung carcinomas [80]. Etoposide is a topoisomerase II inhibitor, stabilizing enzyme–DNA cleavable complexes leading to DNA breaks [81]. The taxanes paclitaxel and docetaxel show antitumor activity against breast, ovarian and other types of tumor in clinical trials. Paclitaxel stabilizes microtubules leading to mitotic arrest [82]. In addition, the camptothecin derivatives irinotecan and topotecan, have shown significant antitumor activity against colorectal and ovarian cancer, respectively [83, 84]. These later compounds were initially obtained from the bark and wood of *Nyssaceae Camptotheca acuminate* and act by inhibiting topoisomerase [85]. The taxanes and the camptothecins are approved for human use in various countries.

Synthetic flavone, a cyclin-dependent kinase inhibitor, derived from rohitukine, is a plant alkaloid isolated from the leaves and stems of *Dysoxylum binectariferum* [86, 87]. Flavopiridol represents the first cyclin-dependent kinase inhibitor to enter clinical trials [88]. Its mechanism

involves interfering with the phosphorylation of cyclin-dependent kinases and arresting cell-cycle progression at the growth phases G1 or G2 [89, 90].

Homoharringtonine, another alkaloid isolated from the *Cephalotaxus harringtonia* tree, is efficient against various forms leukemia [91, 92]. Its mechanism involves the inhibition of protein synthesis and blocking cell-cycle progression [93]. DNA topoisomerase I inhibitor  $\beta$ -lapachone, originally obtained from the Lapacho tree, induces cell-cycle delay at the G1 or S phase before inducing either apoptotic or necrotic cell death in a variety of human carcinoma cells, including ovaries, colon, lungs, prostate and breast [94]. Moreover, there are many plants which are known to suppress cancers that need further studies to validate their potential anticancer activities. Examples include *Salvia officinalis*, *Viscum album*, *Broussonetia papyrifera*, *Euphorbia heterophylla*, and *Viscum calcaratum*. About 117 plants were reviewed in ref. [70] for their anti-cancer activity.

#### **1.9.1.1. *Origanum majorana***

*Origanum majorana* belongs to the family Lamiaceae. It is commonly known as marjoram. It is a perennial herb and widespread worldwide. A large number of known species of the genus *Origanum* are utilized worldwide as spices and flavoring agents and have a long history of both culinary and medicinal use. *O. majorana* is used as a home remedy for chest infections, coughs, sore throats, rheumatic pains, nervous disorders, stomach disorders, cardiovascular disease and skin

care [95, 96]. Many such traditional uses of the marjoram species were confirmed in several studies utilizing both *in vitro* and *in vivo* approaches.

Several reports indicate that *O. majorana* is very rich in phenolic compounds. The high phenolic content in *Origanum* has a capacity to scavenge free radicals to be associated with strong antioxidant activity [97]. *O. majorana* contains phenolic terpenoids (thymol and carvacrol), flavonoids (diosmetin, luteolin, and apigenin), tannins, hydroquinone, phenolic glycosides (arbutin, methyl arbutin, vitexin, orientin, and thymonin) and triterpenoids (ursolic acid and oleanolic acid) [98].

*O. majorana* has been reported to exhibit significant anti-microbial activity [99]. Several studies have also demonstrated that ethanolic, aqueous extracts and the essential oil of *O. majorana* could protect against liver and kidney damage and genotoxicity induced by lead acetate [100-102]. *O. majorana* has also been found to inhibit platelet adhesion aggregation and secretion [103]. Furthermore, this plant exerts a low cytotoxicity on several hepatoma cell lines [104]. It has been shown by Al Harbi that an extract of *O. majorana* reduced the side effects induced by cyclophosphamide, an established anticancer drug, without altering its cytotoxicity [96].

In the present study, we investigated the effect of *Origanum majorana* ethanolic extract (OME) on breast cancer cells. We examined the effects of OME on cell viability, cell cycle, apoptosis and tumor invasion and metastasis in the highly proliferative and invasive Estrogen Receptor (ER)-negative mutant p53 breast cancer cell line MDA-MB-231.

### 1.9.2. Microorganisms as Source of Anti-Cancer Agents

Many anti-cancer agents have been discovered by screening natural products from a wide range of microorganisms. Toxins that originally evolved to kill competing microorganisms can have a variety of physiological effects in animals. In many cases, the targets of these compounds are components of signal transduction cascades that are conserved in many species, and that have been considered novel targets for anticancer drug discovery [105].

Anti-tumor antibiotics are among the most important cancer chemotherapeutic agents, and include members of the anthracycline, bleomycin (isolated from *Streptomyces verticillus* and used in treatment of germ-cell, cervix and head and neck cancers), actinomycin (isolated from *Streptomyces* spp. and used to treat sarcoma and germ-cell tumors) [106]. Clinically useful agents from these above families are the daunomycin (isolated from *Streptomyces coeruleorubidus* and used to treat leukemia) and related agents like doxorubicin, idarubicin, and epirubicin (isolated from *Streptomyces Pneuceticus* and used in lymphoma, sarcomas, breast, ovary, lung cancers).

Rapamycin and its analogs are products of *Streptomyces hygrosopicus* that have potent immunosuppressive activity. They inhibit the signaling pathways required for T-cell activation and proliferation. Rapamycin blocks progression of the cell cycle at the middle-to-late G1 phase in T cells and B cells, and osteosarcoma and rhabdomyosarcoma cell lines, among others [107]. Geldanamycin is a benzoquinone

ansamycin natural fermentation product and inhibits the heat-shock protein HSP 90 [108].

Wortmannin is a product of the fungus *Talaromyces wortmanni* and inhibits signal transduction pathways by forming a covalent complex with an active-site residue of phosphoinositide 3 kinase (PI3K), inhibiting PI3K activity [109]. Others include also the peptolides (i.e. dactinomycin), the mitosanes (such as mitomycin C) and the glycosylated anthracenone mithramycin. The anthracyclines are among the most used anti-tumor antibiotics in the clinic and exert anti-tumor activity mainly by inhibiting topoisomerase II [110].

Anti-cancer agents from natural sources exert their toxicity through modulation of several pathways and induction of different mechanisms of cell death and growth inhibition. Such anti-cancer agents from natural sources induce apoptosis, necrosis, growth arrest, senescence, and autophagocytosis in several types of cancer. Growth inhibition and induction of cell death are among the major objectives of anti-cancer therapies.

#### **1.9.2.1. Salinomycin**

Salinomycin is a monocarboxylic polyether antibiotic, isolated from *Streptomyces albus*, widely used as an antibiotic to prevent anticoccidiosis in poultry and as growth promoter for ruminants and swine. Screening for compounds that specifically target cancer stem cells has led to the identification of Salinomycin as potential anticancer agent. Salinomycin was shown to (i) selectively induce cell death in breast

cancer stem cells in cell culture assay and (ii) inhibit breast tumor growth in mice [111]. More recent investigations have reported that Salinomycin possesses a potent anticancer activity against other cancer stem cells such as the ALDH positive A549 lung cancer cells [112], ALDH gastric cancer cells [113], and CD133+ subpopulations in human CRC HT29 and SW480 colorectal cancer cells [114]. However, the mechanism of Salinomycin's activity on cancer stem cells is yet to be elucidated.

More recent studies reported that Salinomycin shows efficacy against other human cancer cells including those displaying drug resistance [115]. Salinomycin was shown to act as a p-glycoprotein inhibitor to overcome apoptosis resistance in cancer cells [116]. Lu, et al., 2010, have shown that Salinomycin inhibits Wnt signaling and selectively induces apoptosis in chronic lymphocytic leukemia cells [117]. Salinomycin was also shown to induce apoptosis in human prostate cancer cells by inducing an elevation in the intracellular reactive oxygen species (ROS) levels and mitochondrial membrane depolarization [118]. Very recent studies have also shown that Salinomycin inhibits prostate cancer growth and migration through the induction of oxidative stress [119].

A combination treatment using Salinomycin with gemcitabine has proven to be more effective than individual drugs against pancreatic cancer cells [120]. It appears that Salinomycin sensitizes cancer cells to the effects of etoposide and doxorubicin treatments by enhancing apoptosis, increasing DNA damage and reducing the level of p21 protein [121]. Indeed, Salinomycin sensitizes radiation-treated cells by inducing

G2 arrest and causing DNA damage [122]. More recently, Salinomycin was reported to sensitize cancer cells to antimitotic drugs (paclitaxel, docetaxel, vinblastin and colchicine) by enhancing apoptosis as well as preventing G2 arrest [123].

Despite the recent findings, the mechanisms underlying the anticancer activity of Salinomycin are still poorly understood. In the present study, we have investigated the effect of Salinomycin on MCF-7, T47D and the triple negative MDA-MB-231 human breast cancer cell lines.

## **SPECEIFIC AIMS OF THE STUDY (OBJECTIVES)**

**1. Testing the efficacy of *Origanum majorana* plant extract and Salinomycin against different types of human breast cancer *in vitro* (cancer cell lines) and *in vivo* (chick embryo tumor growth and metastasis assay).**

In this study, the effects of this plant extract and this compounds on cell viability, apoptosis, migration and invasion *in vitro* and the progression and metastasis of human solid breast tumors *in vivo* were evaluated.

**2. Identification of downstream biomarkers associated with response to the treatment with selected active plant extracts.**

Because most anticancer drugs are known to alter gene expression, we examined the effects of the *O. majorana* extract and Salinomycin on the expression of pathways (apoptosis, cell cycle...)- specific genes in several breast cancer cell lines using western blot, immunofluorescence and RT-PCR analysis.

## CHPATER 2: MATERIALS AND METHODS

### 2.1. Preparation of the *Origanum majorana* Ethanolic Extract

*Origanum majorana* commonly known as “marjoram” and used as a culinary herb was obtained from a private commercial farm located in the Tyre region of Lebanon. All necessary permits were obtained for the harvesting of the leaves. 5.0 g of the dried leaves were ground to a fine powder using a porcelain mortar and pestle. The powder was suspended in 100 mL of 70% absolute ethanol and the mixture was kept in the dark for 72 hours at 4°C in a refrigerator without stirring. The mixture was then filtered through a glass sintered funnel and the filtrate was evaporated using a rota-vapor at room temperature. The green residue was kept under vacuum conditions for 2–3 hours and its mass was recorded.

### 2.2. Cell Culture and Reagents

Human breast cancer cells MDA-MB-231 and MCF-7 were maintained in DMEM (Hyclone, Cramlington, UK) and the MDA-MB-23-GFP used in this study was maintained as previously described [124]. The T47-D breast cancer cells were maintained in RPMI 1640 (Hyclone). All media were supplemented with 10% fetal bovine serum and 100U/ml penicillin/streptomycin (Invitrogen). HUVECs (Invitrogen, Carlsbad, CA, USA) were maintained in MEM 199 supplemented with 20% FBS, penicillin/streptomycin, 2 mM L-glutamine, 5U/ml heparin and 50 µg/ml endothelial cell growth supplements (BD Biosciences, Bedford, MA, USA). Salinomycin and 4-Hydroxy-Tamoxifen were purchased from Sigma-Aldrich (Saint-Quentin Fallavier; France). Antibodies for p21

(556431), PARP (556494) were obtained from BD Pharmingen. Antibodies for phosphor-H2A.X (ser139) (07-164), acetyl-Histone H3 (06-599), acetyl-Histone H4 (06-866), phosphor-Histone H3 (ser10) (05-1336), P53 (E26, 04-241), Cyclin B1 (05-373) and cyclin D1 (04-1151) were obtained from Millipore. Antibodies for survivin (sc-1779), ICAM-1 (sc-107),  $\beta$ -actin (C4, sc-47778), goat anti-mouse IgG-HRP (sc-2005) and goat anti-rabbit IgG-HRP (sc-2004) were obtained from Santa Cruz Biotechnology, Inc. Antibodies to E-cadherin (ab15148), TNF- $\alpha$  (ab9739) and uPAR (ab103791) from Abcam. Antibodies to p27 (3686), NF- $\kappa$ B p65 (3034), pI $\kappa$ B- $\alpha$  (ser32) (2859) from Cell Signaling (Cell Signaling Technology, Inc., Danvers, MA, USA). AlexaFluor 488 goat anti-rabbit IgG (H+L) (A11008) and AlexaFluor 594 goat anti-mouse IgG (H+L) (A11005) were obtained from Invitrogen.

### **2.3. Cellular Viability**

Cells were seeded in triplicate in 96-well plates at a density of 5,000 cells/well. After 24 hours of culture, cells were treated with increasing concentrations of Salinomycin or OME and incubated for the indicated time periods. Control cells were exposed to DMSO cells (in case of Salinomycin) at a concentration equivalent to that of the Salinomycin-treated or equal volume of 70% ethanol (in case of OME). In combination experiments, MCF-7 and MDA-MB-231 cells were subjected to simultaneous treatment with 20  $\mu$ M 4-hydroxy-tamoxifen A and 1 $\mu$ M frondoside A, respectively, plus DMSO or increasing concentrations of Salinomycin for 48 hours. The effects of Salinomycin, alone or in

combination, on cell viability was determined using a CellTiter-Glo Luminescent Cell Viability Assay (Promega Corporation, Madison, USA), based on quantification of ATP, which signals the presence of metabolically active cells. Luminescent signals were measured using a Berthold FB12 Luminometer. The Data were presented as proportional viability (%) by comparing the treatment group with the untreated cells, the viability of which is assumed to be 100%.

Cell viability was also assessed using Trypan Blue Exclusion Assay. Cells were plated onto 24-well plates ( $20 \times 10^4$  cells/well). The day of the treatment the cells were counted to estimate the approximate number of cells per well. Following Salinomycin treatment at indicated times, cells were trypsinized, pelleted by centrifugation and resuspended in serum free DMEM and stained with trypan blue. Dead (stained blue) and live (unstained) cells were counted on a Neubauer Hemacytometer. Three independent assays were performed in triplicate, and results were reported as the means  $\pm$  SEM.

#### **2.4. Caspase 3/7, 8 and 9 activities**

MDA-MB-231, MCF-7 cells were seeded at a density of 5,000 cells / well into a 96-well plate in triplicate and treated with the drugs for 24 hours and 48 hours. Caspase-3/7, 8 and 9 activities were measured using a luminescent Caspase-Glo 3/7, Caspase8 and Caspase 9 assay kits (Promega Corporation, Madison, USA) following the manufacturer's instructions. Caspase reagents were added to triplicate in the 96 wells. The plate was mixed on an orbital shaker and incubated for 2.5 hours at

room temperature in the dark. A luminescent signal was measured as described above.

## **2.5. Senescence Associated- $\beta$ -Galactosidase (SA- $\beta$ -gal) Staining**

$2.5 \times 10^5$  MDA-MB-231 cells were cultured in 60mm culture dishes for 24 hours and then exposed to Salinomycin  $10\mu\text{M}$  or DMSO for 96 hours. Treatment and control cells were then washed in PBS, and fixed with 2% formaldehyde/ 0.2% glutaraldehyde for 5 minutes at room temperature. The SA- $\beta$ -gal staining was conducted as previously described [125]

## **2.6. Flow Cytometric Analysis of Cell Cycle**

MDA-MB-231 cells ( $1.8 \times 10^6$ ) were seeded in 100mm culture dishes and cultured for 24 hours before the addition of either OME extract or Salinomycin at the concentrations indicated in the results part. After incubation, cells were harvested, washed twice with ice-cold PBS, resuspended in  $500\mu\text{l}$  PBS, fixed with an equal volume of 100% ethanol and incubated for at least 12 hours at  $-20^\circ\text{C}$ . Cells were then pelleted, washed twice with PBS, permeabilized in 0.1% Triton X-100/PBS for 15 minutes on ice, pelleted and then resuspended in PBS containing  $40\mu\text{g/ml}$  propidium iodide and  $25\mu\text{g/ml}$  RNase A, at  $37^\circ\text{C}$  for 30 minutes. Cells were analyzed using BD FACSCanto II (Becton Dickinson). Data acquisition was conducted using FACSDiva 6.1 software. The percentage of cells in the G1, S and G2/M phases were determined using the FlowJo software.

## **2.7. Quantification of Apoptosis by Annexin V /Propidium iodide (PI)**

### **Staining**

DMSO and Salinomycin-treated MDA-MB231 ( $1.8 \times 10^6$ ) cells grown in 100mm culture dishes were harvested by trypsin release and washed twice with ice-cold PBS. Apoptotic cell death was determined using the BD FITC Annexin V Apoptosis Detection Kit II (BD Biosciences) according to the manufacturer's instructions. Cell samples were analyzed using the BD FACSCanto II (Becton Dickinson).

## **2.8. Immunofluorescence Staining**

MDA-MB 231 cells ( $4 \times 10^4$ ) were grown on 4 well labtek chamber slide (Becton Dickinson) for 24 hours, and then treated with vehicle as control or either OME extract or Salinomycin for 24 hours at the concentrations indicated in the results come later. Cells were then fixed in 10% formalin solution (4% paraformaldehyde) (Sigma-Aldrich; Saint-Quentin Fallavier, France) for 5 minutes at room temperature followed by permeabilization in PBS containing 0.1% Triton X-100 for 5 minutes at room temperature. Cells were then washed three times with PBS, blocked with 5% non-fat dry milk in PBS for 30 minutes at room temperature and then incubated with the primary antibody diluted in 1% non-fat dry milk/PBS overnight at 4°C. Following incubation, cells were washed three times with PBS and incubated for 1 hour at room temperature in the presence of rhodamine-conjugated or fluorescein-conjugated secondary antibody diluted at 1:200 in 1% non-fat dry milk/PBS. After washing with PBS, cells were mounted in Fluoroschild with DAPI (Sigma-Aldrich) and examined under Nikon Ti U fluorescence microscope.

## **2.9. Colony Formation Assay in Soft Agar**

Assays were performed in six-well plates. The lower (base) layer consisted of 1 ml 2.4% Noble Agar. The base layer was overlaid with a second layer consisting of 2.9 ml growth medium, 0.3% Noble Agar, and  $3 \times 10^4$  MDA-MB-231 cells. Agar at 50°C was mixed with the medium at 37°C, plated, and left to set for 10 minutes. Growth medium was then added and plates incubated at 37°C. Cells were allowed to grow to form colonies for 14 days before treatment with either Salinomycin or OME extract. Colonies were allowed to grow for one more week. Following treatment, plates were washed twice with PBS and then colonies were fixed with 10% ice-cold methanol for 10 min and washed once with PBS. Colonies were allowed to stain for 1 hour in a solution containing 2% Giemsa. The size of the colonies was measured, using a microscope (10X) and the colony size was categorized as Large (>400  $\mu\text{m}$ ), medium (200-400  $\mu\text{m}$ ), or small (50-200  $\mu\text{m}$ ). Colony sizes were expressed as a percentage of total counted colonies and then compared to the vehicle treated controls (DMSO). The experiment was repeated three times.

## **2.10. Nuclear and whole Cell Extract and Western Blot Analysis**

Cells ( $1.8 \times 10^6$ ) were seeded in 100mm culture dishes and cultured for 24 hours before the addition of various concentrations of either Salinomycin or OME extract. For whole cell lysates, following incubation, cells were washed twice with ice-cold PBS, scraped, pelleted and lysed in RIPA buffer (89900, Pierce) supplemented with a protease/phosphatase inhibitor cocktail (1861281, Pierce). After incubation for 30 minutes on ice, cell lysates were centrifuged at 14,000

rpm for 20 minutes at 4°C. Nuclear extract were prepared from vehicle-or OME-treated MDA-MB-231 cells using the NE-PER extraction reagents (Thermo Scientific, Rockford, IL, USA). The protein concentration of the lysates was determined using BCA Protein Assay Kit (23225, Thermo Scientific) and the lysates were adjusted with lysis buffer. Aliquots of 25 µg of total cell lysate were resolved onto 10-12% SDS-PAGE. Proteins were transferred to nitrocellulose membranes (88018, Thermo Scientific) and blocked for 1 hour at room temperature with 5% non-fat dry milk in TBST (TBS and 0.05% Tween 20). Incubation with specific primary antibodies was conducted in a blocking buffer overnight at 4°C. Horseradish peroxidase-conjugated anti-IgG was used as secondary antibody. Immunoreactive bands were detected by ECL chemiluminescent substrate (32209, Thermo Scientific). Also when needed, membranes were stripped in a Restore Western Blot Stripping Buffer (21059, Thermo Scientific) according to the manufacturer's instructions.

### **2.11. Wound Healing Migration Assay**

MDA-MB-231 cells were grown in six-well tissue culture dishes until confluence. A scrape was made through the confluent monolayer with a sterile plastic pipette tip of 1mm diameter. Afterwards, the dishes were washed twice with PBS and incubated at 37°C in fresh DMEM complemented with 10% fetal bovine serum in the presence or absence of the indicated concentrations of OME. At the bottom side of each dish, three arbitrary places were marked where the width of the wound was measured with an inverted microscope (objective x 10). Wound closure

was expressed as the average  $\pm$  SEM of the difference between the measurements at time zero and a 10 hours' time period.

### **2.12. Migration Chamber Assay**

$5 \times 10^4$  cells were seeded in the upper chamber, HTS Multiwell Insert System (BD Biosciences, Franklin Lakes, NJ, USA), in serum-free medium, with or without OME and migration assay, A serum-containing medium was added to the lower chamber to act as a chemotactic attractant. After 6 hours of incubation, cells were washed with PBS, and fixed with formaldehyde. Cells were then stained with 1% crystal violet for 10 minutes. After washing with PBS, cells from at least 5 different random fields were counted under a microscope.

### **2.13. Aggregation Assay**

Growing cells were detached using a 2mM EDTA in calcium magnesium-free PBS (CMF-PBS). A cell suspension of  $1 \times 10^6$  cells/ml was aliquoted into microcentrifuge tubes, washed with PBS, resuspended in a 1ml culture media and incubated with or without OME on a rocker for 1 hour at 37°C. Cells were then fixed with 1% formaldehyde and pictures taken under an inverted microscope (Olympus IX71). Aggregation was calculated as previously reported [126] using the following equation: % aggregation =  $(1 - N_t/N_c) \times 100$ , where  $N_t$  and  $N_c$  represent the number of single cells in treatment and untreated groups, respectively.

#### **2.14. Adhesion Assay**

Adhesion of MDA-MB-231 to HUVECs was performed as previously described [127] with minor modifications. Cell culture plates were coated with collagen and HUVECs grown to confluent monolayers. TNF- $\alpha$  (25ng/ml) was added for 6 hours to stimulate HUVECs prior to the addition of MDA-MB-231 cells. MDA-MB-231 transfected with *Renilla* Luciferase were resuspended in HBSS containing a 1% BSA at a concentration of  $2 \times 10^5$  cells/ml. 150  $\mu$ l of this cell suspension was added to the upper chamber containing confluent HUVECs in the absence or presence of OME. After 1 hour, unattached cells were removed by gently washing the plates three times with PBS. Adherent cells were lysed using a luciferase lysis buffer (Promega, Madison, WI, USA) and light units were measured.

#### **2.15. Matrigel Invasion Assays**

The invasiveness of the MDA-MB-231 cell was treated with the indicated concentrations of OME and tested using a BD Matrigel Invasion Chamber (8- $\mu$ m pore size: BD Biosciences, Bedford, MA, USA). MDA-MB-231 ( $1 \times 10^5$ ) cells were placed in 0.5 mL of media containing vehicle or the indicated concentrations of OME were seeded into the upper chambers of the system. The bottom wells in the system were filled with DMEM complemented with 10% fetal bovine serum as a chemo-attractant and then incubated at 37°C for 24 hours. Non-penetrating cells were removed from the upper surface of the filter with a cotton swab. Cells that have migrated through the matrigel were fixed with 4% formaldehyde,

stained with DAPI and counted in 6 random fields under a microscope. For quantification, the assay was done in duplicate then and repeated three times.

### **2.16. Measurement of Matrix Metalloproteinases by ELISA**

Cells were seeded in 6-well plates in the absence of vehicle or OME for 24 hours. The conditioned medium was collected and the levels of MMP-2 and MMP-9 secreted were determined using immunoassay kits (Invitrogen, Camarillo, CA, USA). The experiments were repeated three times and the average of the three means was represented as  $\pm$  SEM.

### **2.17. Gelatin Zymography**

Gelatin zymography was conducted as previously described [128]. MDA-MB-231 ( $2.5 \times 10^6$ ) cells were incubated in serum-free DMEM for 24 hours in the presence of vehicle or OME (150 and 300  $\mu\text{g}/\text{mL}$ ). The conditioned medium was collected, concentrated and 30  $\mu\text{g}$  of total protein was resolved in 10% polyacrylamide gel containing 0.1% gelatin. After electrophoresis, the gel was washed for 1 hour in 2.5% (v/v) Triton X-100 to remove SDS and then incubated overnight at 37°C in 50 mM Tris-HCl (pH 7.5), 150 mM NaCl, 0.5 mM  $\text{ZnCl}_2$  and 10 mM  $\text{CaCl}_2$  to allow proteolysis of the gelatin substrate. Bands corresponding to activity were visualized by negative staining using 0.5% Coomassie brilliant blue R-250 (Bio-Rad, Hercules, CA, USA). Representative results from two independent experiments are shown. Densitometry was conducted using ImageJ software and the band density was normalized to the non-specific band staining on the gel.

## **2.18. Quantitative Immunoassay for Human Vascular Endothelial Growth Factor (VEGF)**

MDA-MB-231 cells ( $1.5 \times 10^5$ ) were seeded in 24-well plates. The conditioned medium was collected and the level of VEGF measured using a VEGF Enzyme-Linked Immunosorbent Assay Kit (R&D Systems, Minneapolis, MN, USA). Assays were performed in triplicate and three independent experiments were conducted. The data is presented as mean values  $\pm$  SEM.

## **2.19. Quantification of Nitrate/Nitrite Production**

The amount of nitrate/nitrite production was determined with a colorimetric ELISA Kit (Cayman Chemical, Ann Arbor, Michigan, USA), which is based on the Griess reaction. The value of nitrate/nitrite presented is the total value measured in the presence of cells minus the value determined from the media alone in the absence of any growing cells.

## **2.20. Luciferase Activity**

MDA-MB-231 cells were seeded in 12-well plates the day before transfection. Cells were then transfected with the E-cadherin Luciferase Reporter Expression Plasmid [129] using Lipofectamine 2000 (Life Technologies, Inc. Grand Island, NY, USA). Cells were allowed to recover for 4 hours after transfection in OPTI-MEM (Life Technologies, Inc., Grand Island, NY, USA) which was then replaced with a complete medium. Luciferase activity was measured using Dual Luciferase Reporter Assay

System (Promega, Madison, WI, USA). *Renilla* Luciferase reporter was used as an internal control, to which firefly luciferase values were normalized. Experiments were repeated three times and the average of the three means was represented  $\pm$  SEM.

### **2.21. Transendothelial Migration Assay**

Transendothelial migration of MDA-MB-231 through HUVEC was conducted as previously described [130]. Transwell filters were coated with collagen and allowed to dry overnight. HUVECs ( $2 \times 10^5$ /well) were then seeded onto the rehydrated membrane and allowed to grow until a confluent monolayer was formed. TNF- $\alpha$  (25ng/ml) was added for 6 hours to stimulate HUVECs. Then, MDA-MB -231 cells ( $1 \times 10^6$ ) were loaded on top and incubated overnight in the absence, or presence, of OME. Cells on the upper chamber were removed with a cotton swab, whereas MDA-MB-231 on the bottom were stained and quantified as previously reported [130].

### **2.22. RNA Extraction and RT-PCR**

Total RNA from vehicle- or OME-treated MDA-MB-231 cells were prepared using Trizol reagent (Life Technologies, Inc. Grand Island, NY, USA). The RNA expression of MMP-2 and MMP-9 was determined by RT-PCR. RT-PCR was performed using the Qiagen OneStep RT-PCR Kit (Qiagen, Hilden, Germany). Equal amounts of RNA (500 ng) were used as templates in each reaction. The sequences of specific primers were as follows: MMP-2 sense, 5'-TCTCCTGACATTGACCTTGGC-3', and antisense: 5'-CAAGGTGCTGGCTGAGTAGATC-3'; MMP9 sense, 5'-

TTGACAGCGACAAGAAGTGG-3', and antisense, 5'-  
CCCTCAGTGAAGCGGTACAT-3'; GAPDH sense, 5'-  
GGCCTCCAAGGAGTAAGACC-3', and antisense: 5'-  
AGGGGTCTACATGGCAACTG-3'. The PCR products were separated by  
1.5% agarose gel and visualized by ethidium bromide staining.  
Representative results from two independent experiments are shown.

### **2.23. Chick Embryo Tumor Growth and Metastasis Assay**

The chick embryo tumor growth assay was performed as previously described [131] with slight modifications. According to French legislation, no ethical approval is needed for scientific experimentation using oviparous embryos (decree n°2013-118, February 1, 2013; art. R-214-88). This work was done under animal experimentation permit N°381029 issued to Jean Viallet and animal experimentation permit N° B3851610001 issued to Institute Albert Bonniot. Fertilized White Leghorn eggs (Société Française de Production Agricole, St. Briec, France), were incubated at 38°C with 60% relative humidity for 10 days. At stage E10, the chorioallantoic membrane (CAM) was dropped by drilling a small hole through the eggshell into the air sac and a 1 cm<sup>2</sup> window was cut in the eggshell above the CAM. Cultured MDA-MB-231-GFP were detached by trypsinization, washed with complete medium and suspended in serum free DMEM. A 50 µl inoculum of 1 X 10<sup>6</sup> MDA-MB-231-GFP cells was added onto the CAM of each egg (eggs were randomized in 4 groups of 15). One day later, tumors that began to be detectable were treated every second day at E11, E13, E15 and E17 by dropping 100 µl of either OME (300 µg/mL or 450 µg/mL), colchicine (2µM) or 0.02 % ethanol (vehicle) in

PBS onto the tumor. At E19 the upper portion of the CAM was removed, transferred in PBS and the tumors were then carefully cut away from normal CAM tissue and weighted. In parallel, a 1 cm<sup>2</sup> portion of the lower CAM was collected to evaluate the number of nodules, containing GFP-expressing cells. The fluorescent nodules were visualized *in situ* using whole mounts of tissue fixed in 4% formaldehyde in PBS and flattened between a hollow glass slide and a thick coverslip. In order to number the nodules, a thorough and complete visual scan of the piece of the lower CAM was done using a fluorescent microscope. Chick embryos were sacrificed by decapitation.

#### **2.24. Statistical Analysis**

Results were expressed as means  $\pm$  SEM of the number of experiments. A *p* value of  $< 0.05$  was considered statistically significant. Student's *t*-test was used to detect the difference between the two values.

## CHAPTER 3: RESULTS AND DISCUSSION

### Part I. Anti-breast cancer activity of Salinomycin

#### 3.1 Growth Inhibitory Effect of Salinomycin on MDA-MB-231, MCF-7 and T47D Breast Cancer Cell Lines

To examine the anticancer activity of Salinomycin on breast cancer cells, we first measured the effect of various concentrations of Salinomycin (1, 2.5, 5, 10, 25 and 50  $\mu\text{M}$ ) on the proliferation of three different breast cancer cell lines (MDA-MB-231, MCF-7 and T47D). The data obtained is summarized in figure 1. Our results show that exposure of the three cell lines to Salinomycin decreased cellular viability in concentration and in a time-dependent manner. However, the growth inhibitory effect of Salinomycin appears to be more pronounced in MCF-7 and T47D than in MDA-MB-231. The  $\text{IC}_{50}$  (producing half-maximal inhibition) at 24 hours was approximately 40  $\mu\text{M}$  for the MCF-7 and T47D (fig. 2 and 3) while the same concentration gave only about 35% inhibition of proliferation in the MDA-MB-231 cells (fig. 1). Following 48 hours of treatment,  $\text{IC}_{50}$  was 15  $\mu\text{M}$  for the MCF-7 and T47D (fig. 2 and 3) and approximately 35  $\mu\text{M}$  for the MDA-MB-231 cells. Maximal inhibition (90%,  $P < 0.05$ ) of cell growth was observed with 50  $\mu\text{M}$  for the MCF-7 and T47D cell lines. The same concentration gave approximately 70% inhibition of proliferation of the MDA-MB-231 cell lines (fig.1). Taken together, our data show that Salinomycin inhibits cell growth of breast cancer cell lines in a concentration and time-dependent manner and that MCF-7 and T47D exhibit a greater sensitivity to Salinomycin compared to the MDA-MB-231 cells.

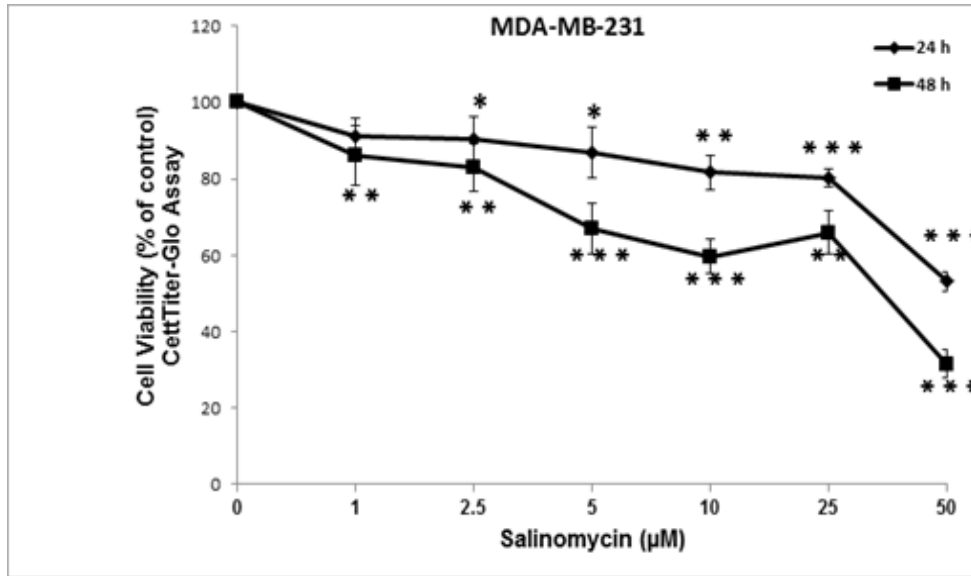


Figure 1. Inhibition of Cellular Viability of MDA-M-231 Cells by Salinomycin.

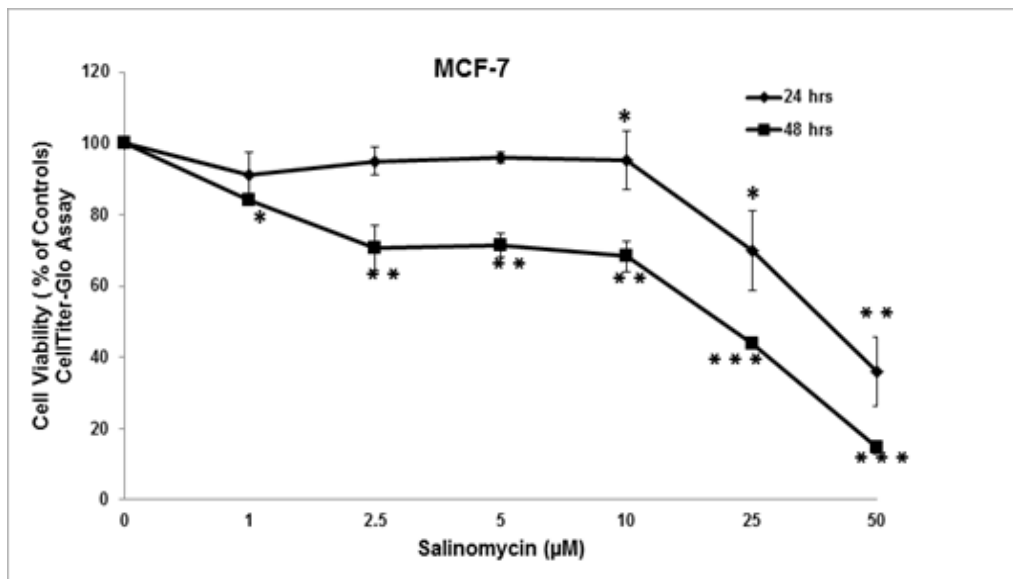


Figure 2. Inhibition of Cellular Viability of MCF-7 Cells by Salinomycin.

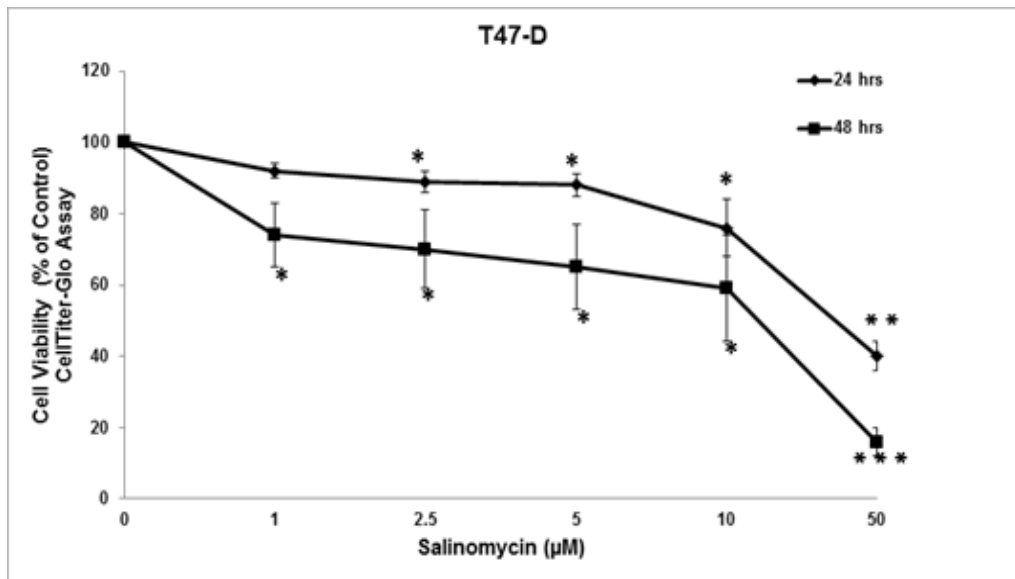


Figure 3. Inhibition of Cellular Viability of T47-D Cells by Salinomycin.

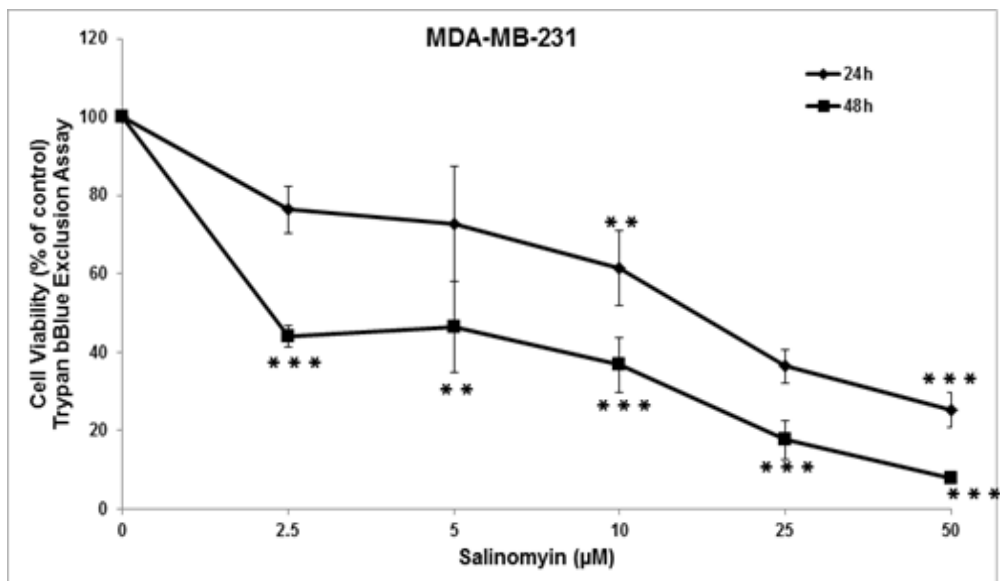


Figure 4. Cell Viability of MDA-MB-231 Cells in Response to Various Concentrations of Salinomycin Using Trypan Blue Exclusion Dye Assay.

We next focused only on the highly proliferative and invasive Estrogen Receptor (ER)-negative, mutant p53 breast cancer cell line MDA-MB-231 to investigate the mechanism by which Salinomycin decreased cell viability.

In order to distinguish between cell death and the possible growth arrest effects of Salinomycin, cell viability of the MDA-MB-231 cells was monitored by using the trypan blue exclusion dye assay at 24 and 48 hours after the Salinomycin treatment. As it is shown in Figure 4, Trypan Blue Assay also showed a dose- and time-dependent decrease in viability in Salinomycin-treated cells when compared to the control cells. However, a closer look to the number of viable (Trypan Blue Negative) cells counted in each treatment, revealed that the number of cells after treatment with 2.5, 5 and 10  $\mu\text{M}$  did not significantly change at 24 and 48 hours and moreover, was comparable to the number of cells counted at the day of treatment (Table 1) with a very low percentage of cell death (Trypan Blue Positive) suggesting that proliferation of the MDA-MB-231 at these concentrations is inhibited and cell death is minimal (Table 1) . Interestingly, at higher concentrations of Salinomycin (25 and 50  $\mu\text{M}$ ), the number of viable MDA-MB-231 cells showed a steady decline after 24 and 48 hours indicative of cell death. The number of viable cells compared to the day of treatment, dropped to 58% and 42% at 25  $\mu\text{M}$  and to 48 and 28% at 50  $\mu\text{M}$ .

Comparative analysis of cell viability between CellTiter-Glo and Trypan Blue Exclusion assay shows that cell viability data obtained by CellTiter-Glo and trypan blue exclusion assays are not perfectly super-

imposable (fig. 5 and 6). As a matter of fact, the same concentration of Salinomycin gave slightly different IC50 between Trypan Blue Exclusion and CellTiter-Glo assay.

Salinomycin ( $\mu\text{M}$ )	Dead cells (number and %)		Viable cells (number and %)	
	24 hours	48 hours	24 hours	48 hours
<b>Control</b>	<b>589 (1.0%)</b>	<b>2311 (2%)</b>	<b>64122 (100%)</b>	<b>143055 (100%)</b>
<b>2.5</b>	<b>1078 (2.0%)</b>	<b>1444 (2.0%)</b>	<b>48822 (76%)</b>	<b>63688 (45%)</b>
<b>5</b>	<b>1844 (4.0%)</b>	<b>2700 (4.0%)</b>	<b>46877 (73%)</b>	<b>55400 (39%)</b>
<b>10</b>	<b>2244 (6%)</b>	<b>3244 (7%)</b>	<b>39322 (61%)</b>	<b>43844 (31%)</b>
<b>25</b>	<b>4478 (17%)</b>	<b>6978 (27%)</b>	<b>23288 (36%)</b>	<b>19377 (41%)</b>
<b>50</b>	<b>2156 (12%)</b>	<b>12089 (50%)</b>	<b>16244 (25%)</b>	<b>11333 (8%)</b>
<b>* Number of cells counted at the day of treatment (0h) approximately 39000</b>				

Table 1. Viability of MDA-MB-231 Cells in Response to Salinomycin Determined by Trypan Blue Exclusion Assay.

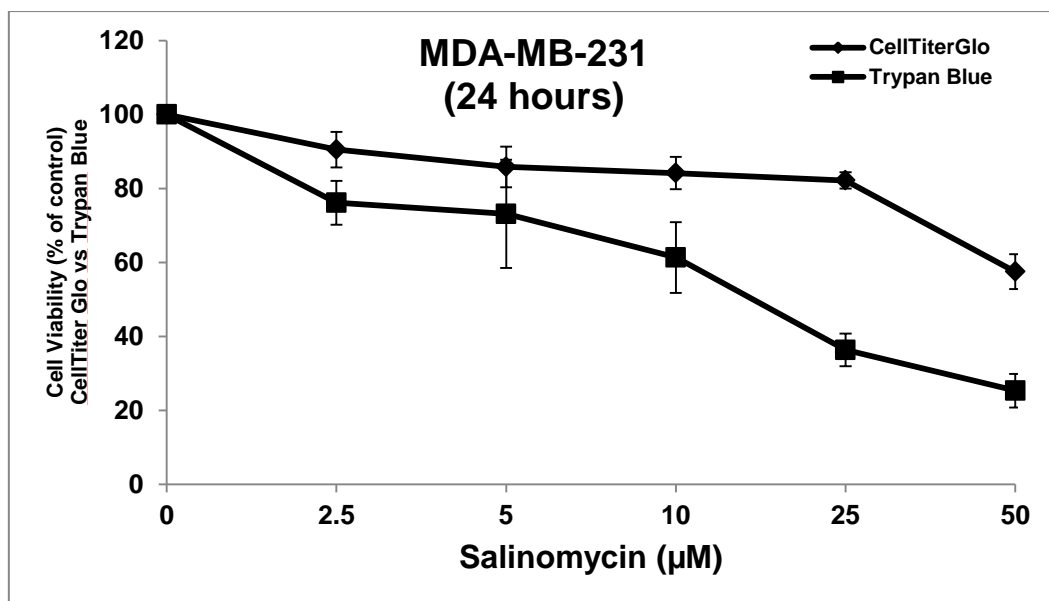


Figure 5. Cell Viability of the MDA-MB-231 Cells in Response to Salinomycin After 24 Hours Determined by Trypan Blue Exclusion Dye and CellTiter-Glo Assays.

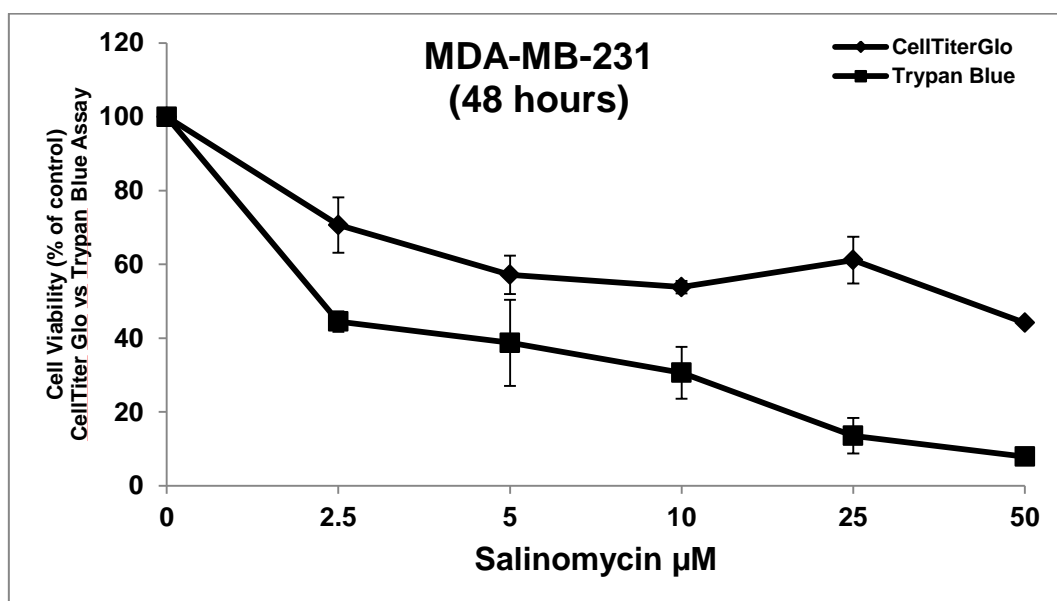


Figure 6. Cell Viability of MDA-MB-231 Cells in Response to Salinomycin After 48 Hours Determined by Trypan Blue Exclusion Dye and CellTiter-Glo Assays.

### **3.2 Salinomycin Induces Morphological Changes in MDA-MB-231 Cells**

Light microscopy observation of Salinomycin-treated MDA-MB-231 cells revealed morphological changes induced by this compound. As shown in figure 7, MDA-MB-231 cells treated with concentrations of Salinomycin 5, 10 and 25  $\mu\text{M}$ , underwent morphological changes characterized by a loss of their epithelial morphology visible after 24 hours of treatment. These cells appeared dispersed and exhibited fibroblast-like morphology with filopodia-like extensions and central nuclei. However, the fibroblast-like morphology observed in these cells is not due to an epithelial-mesenchymal transition, since no changes in levels of vimentin and E.cadherin proteins was detected by a western blot analysis (fig. 8) and immunofluorescence (fig. 9). Interestingly, a subpopulation of MDA-MB-231 cells treated with low concentration of Salinomycin exhibited a senescence-like phenotype characterized by cell size increase and flattening shape compared to the control cells (fig. 7 arrows). At higher concentrations of Salinomycin (25 and 50 $\mu\text{M}$ ), cells appeared smaller and rounded, characteristic of cells undergoing apoptosis. Strikingly, lower concentrations of Salinomycin up to 10  $\mu\text{M}$  did not lead to further change in cell morphology nor to cell density after 72 hours exposure to Salinomycin (fig 10). In contrast higher concentrations (25 and 50) led to fewer cells on the plate and further rounded cells. These morphological changes seem to be specific to MDA-MB-231 cells, since no obvious changes were observed in the MCF-7 and T47D cell lines.

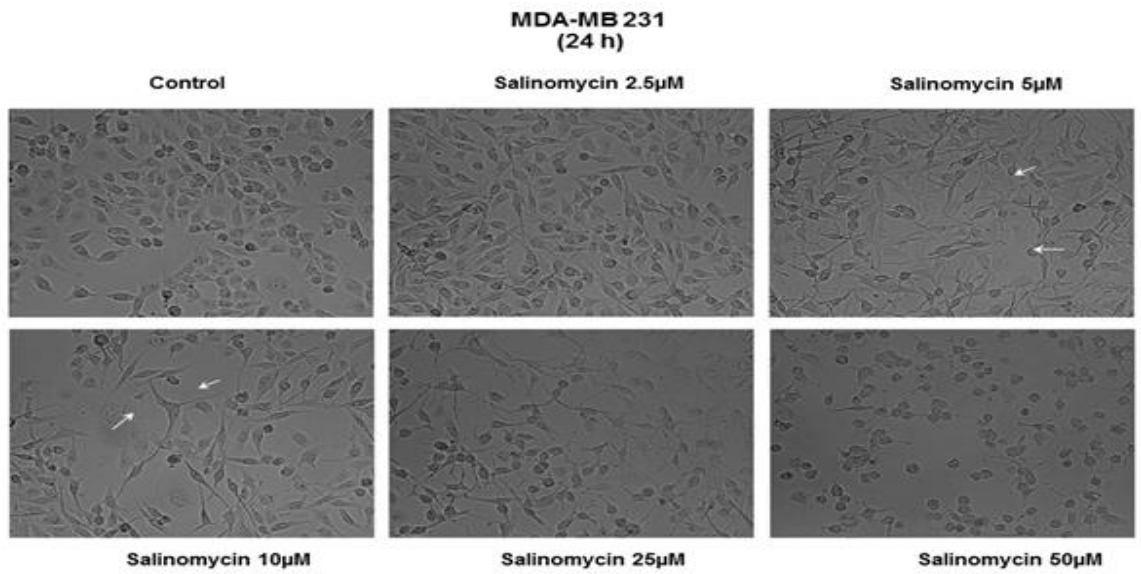


Figure 7. Morphological Changes Observed in the MDA-MB 231 Cells After 24 Hours of Treatment with Various Concentration of Salinomycin.

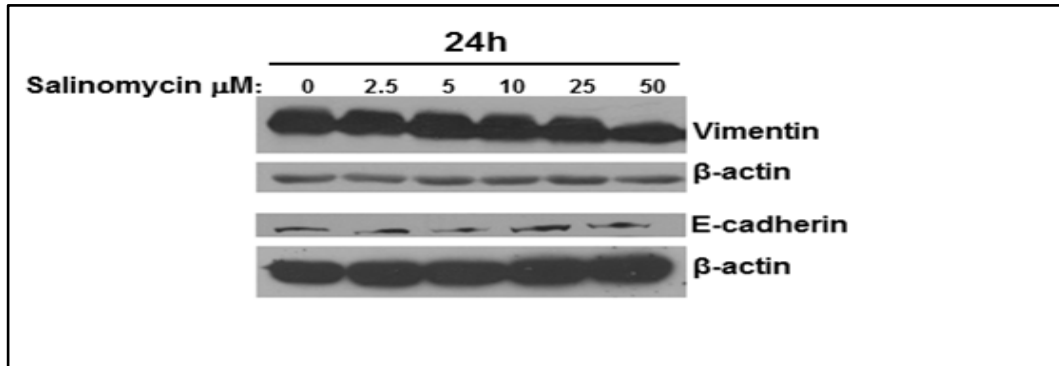


Figure 8. Western Blot Analysis of Vimentin and E-cadherin Expression in Salinomycin Treated MDA-MB-231 Cells.

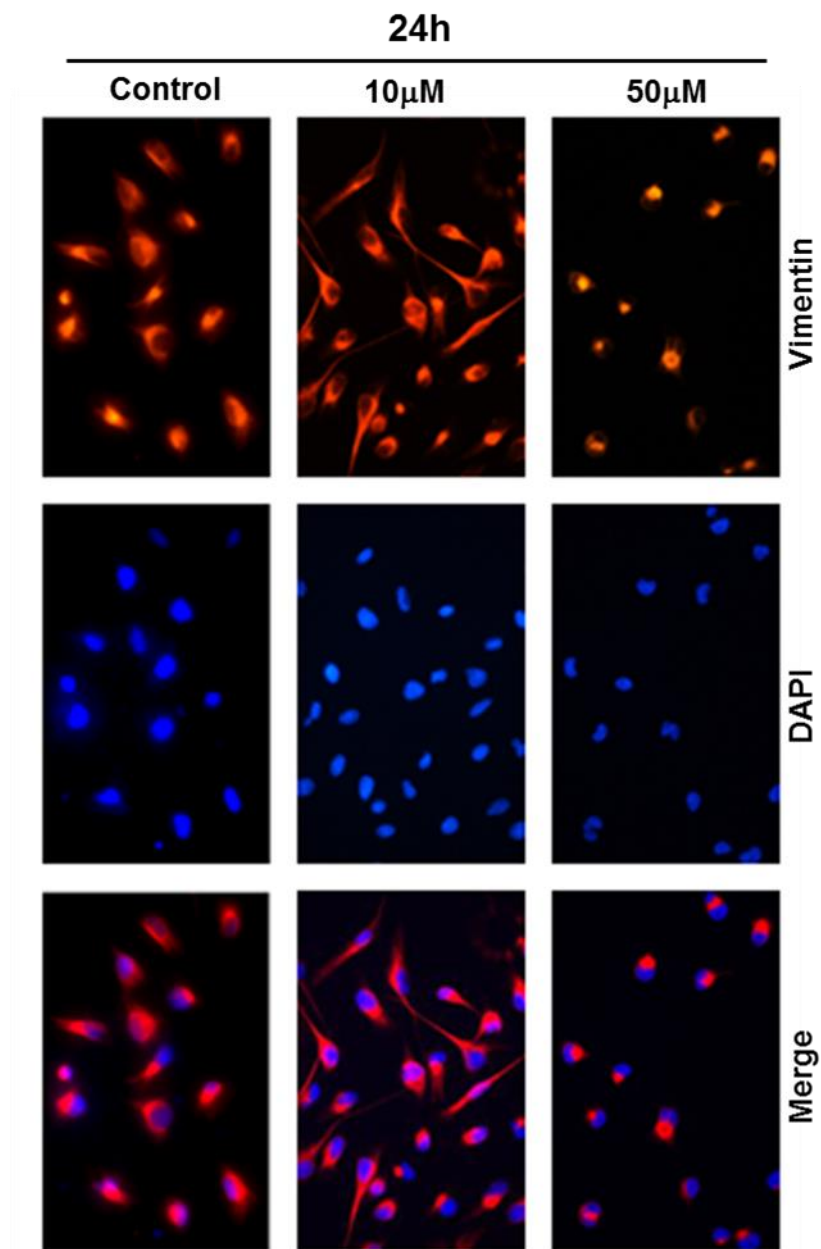


Figure 9. Immunofluorescence Staining for Vimentin in Salinomycin Treated MDA-MB-231 Cells.

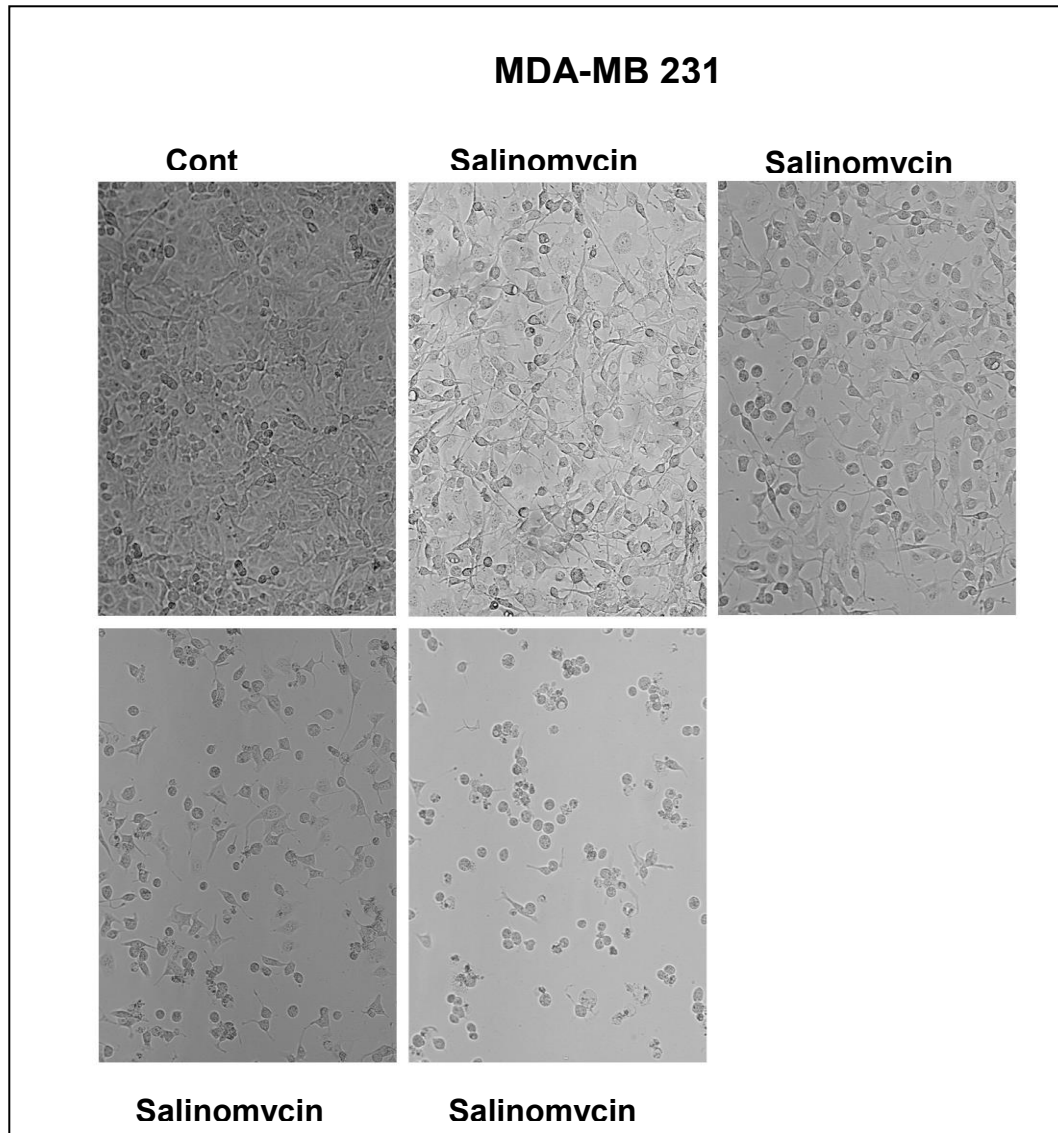


Figure 10. Morphological Changes Observed in the MDA-MB 231 Cells After 72 Hours of Treatment with Various Concentrations of Salinomycin.

### 3.3 Salinomycin Induces Apoptosis in MDA-MB-231 Cells

Salinomycin was reported to mediate apoptosis in many human cancer cells [115]. Therefore, we investigated whether the observed inhibition of cell viability upon Salinomycin treatment in the MDA-MB-231 cells was associated with the induction of apoptosis. Flow cytometry analysis of Annexin V and Propidium Iodide (PI) stain was used to determine the percentage of apoptotic cells induced by Salinomycin after 24 hours of treatment. Treatment with 5 and 10  $\mu\text{M}$  Salinomycin did not lead to a change in the early stage (Annexin V<sup>+</sup>/PI<sup>-</sup>) nor in the late stage apoptotic cells (Annexin V<sup>+</sup>/PI<sup>+</sup>)/necrotic cells suggesting the absence or minimal cell death in these populations (fig. 11). However, higher concentrations (25  $\mu\text{M}$ ) led to an increase in both early and late apoptotic/necrotic cell population.

Immunofluorescence microscopy was also used to confirm apoptosis in the Salinomycin-treated cells. Fluorescence staining of Annexin V was detected only in cells treated with 25  $\mu\text{M}$  of Salinomycin (fig. 3B, lower panel), while no Annexin V staining was detected at a concentration of 10  $\mu\text{M}$  (fig. 12, middle panel) or lower concentrations, further confirming the absence of apoptosis in these cells. Interestingly, the proportion of dead cells detected by Trypan Blue Exclusion Assay at 25  $\mu\text{M}$  was higher than the proportion of apoptotic cells detected by flow cytometry suggesting that apoptosis might account only partly for the cell death induced by high concentrations of Salinomycin.

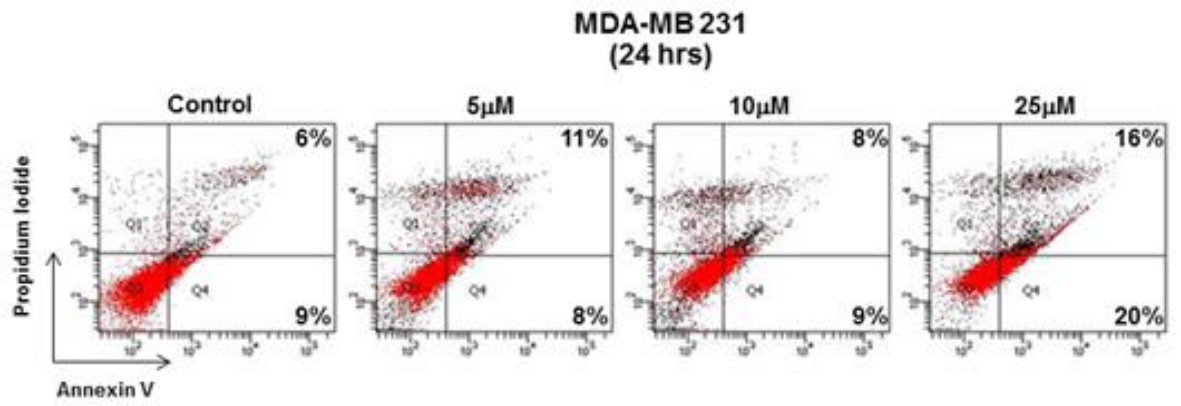


Figure 11. Salinomycin induced apoptosis in the MDA-MB-231 cells. Annexin V binding was carried out using Annexin V-FITC Detection Kit.

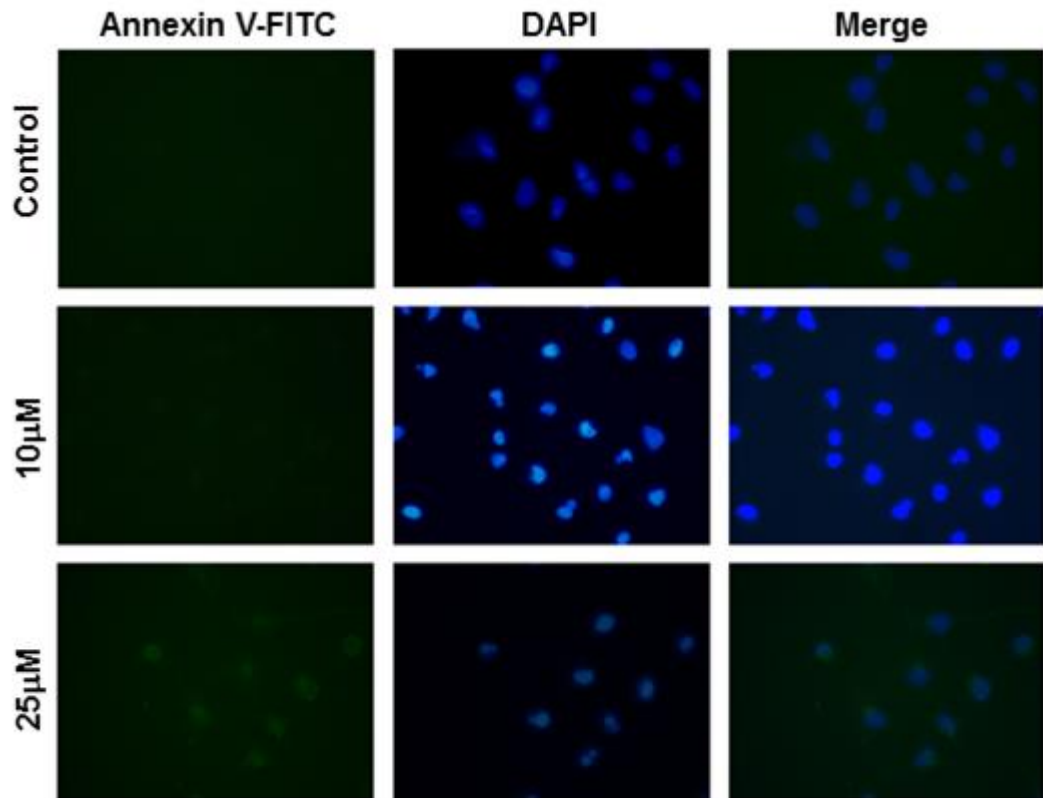


Figure 12. Immunofluorescence Staining for Annexin V-FITC in Salinomycin Treated MDA-MB-231 Cells.

Apoptosis was further examined by measuring Caspase 3/7 activation in MDA-MB-231 cells treated with low (10 $\mu$ M) or high concentrations (50 $\mu$ M) of Salinomycin after 24 and 48 hours of treatment. Consistent with Annexin V staining, Caspase 3/7 activation was detected in cells treated with 50 $\mu$ M but not in cells treated with 10 $\mu$ M (fig. 13). Furthermore, as figure 14 shows, PARP cleavage occurred only in cells treated with higher concentrations of Salinomycin (25 and 50 $\mu$ M), while no cleaved PARP is detectable at lower concentration of Salinomycin (5 and 10 $\mu$ M). The lack of Caspase 3/7 activation and cleavage of PARP in MDA-MB-231 suggest that the reduced cell viability observed in MDA-MB-231 cells treated with low concentrations of Salinomycin ( $\leq$ 10 $\mu$ M) resulted from an inhibition of cell proliferation and was not caused by cell death.

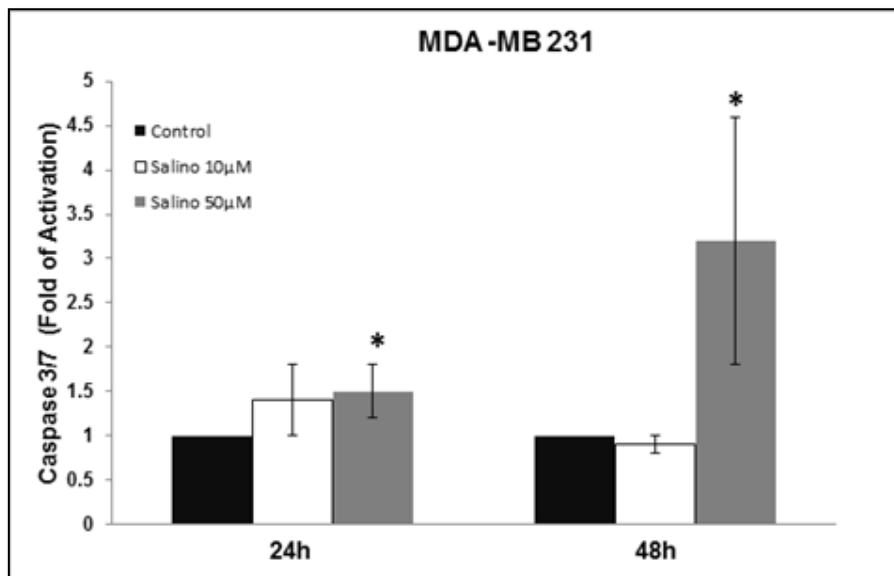


Figure 13. Stimulation of Caspase 3/7 Activity in MDA-MB-231 Cells After Exposure to Salinomycin (10 and 25  $\mu$ M) for 24 and 48 Hours.

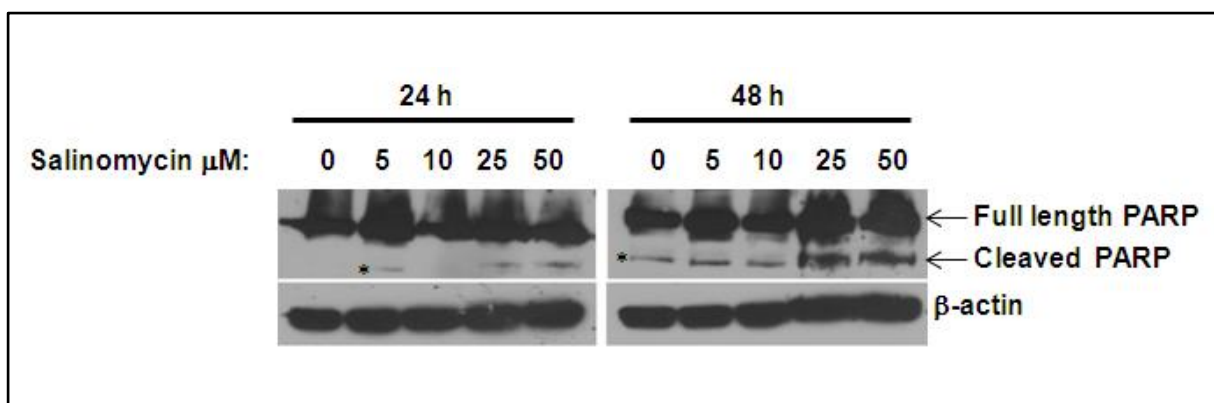


Figure 14. Western Blot Analysis Showing Dose- and Time-Dependent Induction of PARP Cleavage in Salinomycin Treated MDA-MB-231 Cells.

\* represents non-specific band

### 3.4 Salinomycin Induces Growth Arrest in MDA-MB-231 Cells and Inhibited Colony Growth

To confirm that low concentrations of Salinomycin induced growth inhibition of MDA-MB-231, cells were treated with DMSO or Salinomycin (2.5 and 5 μM) and kept in a culture for 6 days then cell viability was measured after 1, 3 and 6 days by counting viable cells using Trypan Blue Exclusion Assay. Figure 15 clearly shows that while DMSO treated MDA-MB-231 cells continued to proliferate, Salinomycin-treated cells exhibited a strong inhibition of proliferation. Moreover, the inhibition of cellular proliferation induced by low concentrations of Salinomycin persisted even upon removal of the drug further indicating that, a low concentration of Salinomycin induces a permanent cell cycle arrest of the MDA-MB-231 cells. These results along with the cell viability data strongly suggest that Salinomycin has a differential effect on the MDA-MB-231 cells depending on the concentration used. At low concentrations, Salinomycin inhibits

cellular proliferation without inducing cell death, while at high concentrations it exerts its effects by inducing apoptosis through activation of caspase 3/7 and PARP cleavage.

To further confirm the growth arrest potential of Salinomycin on MDA-MB-231 cells, we sought to determine if Salinomycin inhibits the growth of formed colonies. Figure 16 shows that the size of a control group of DMSO-treated colonies kept growing after three weeks compared to the size of the control colonies at two week; more large and medium size colonies are obtained in the three week plate, while fewer small colonies were counted, indicating that medium colonies became larger in size and smaller ones became medium sized colonies. Interestingly, the colony sizes counted in the three week Salinomycin-treated plates were indistinguishable from those in the two week control DMSO-treated plates, indicating that Salinomycin was able to completely block the growth of the MDA-MB-231 colonies. This data further confirms the growth inhibitory effect of low concentrations of Salinomycin on the proliferation of MDA-MB-231 cells.

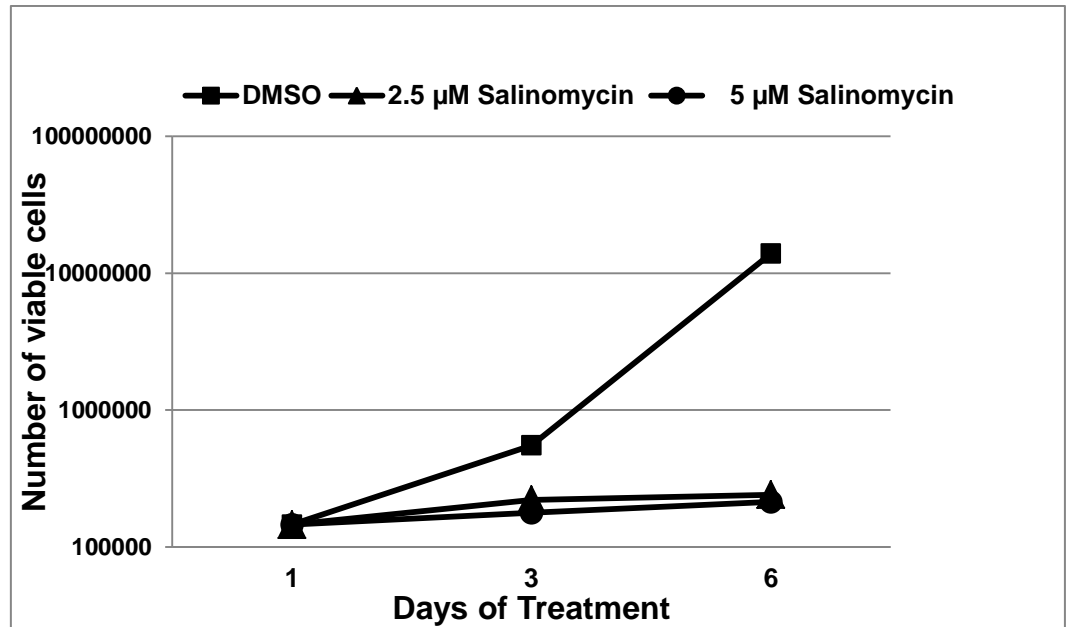


Figure 15. Inhibition of Proliferation by Salinomycin in MDA-MB-231 Cells.

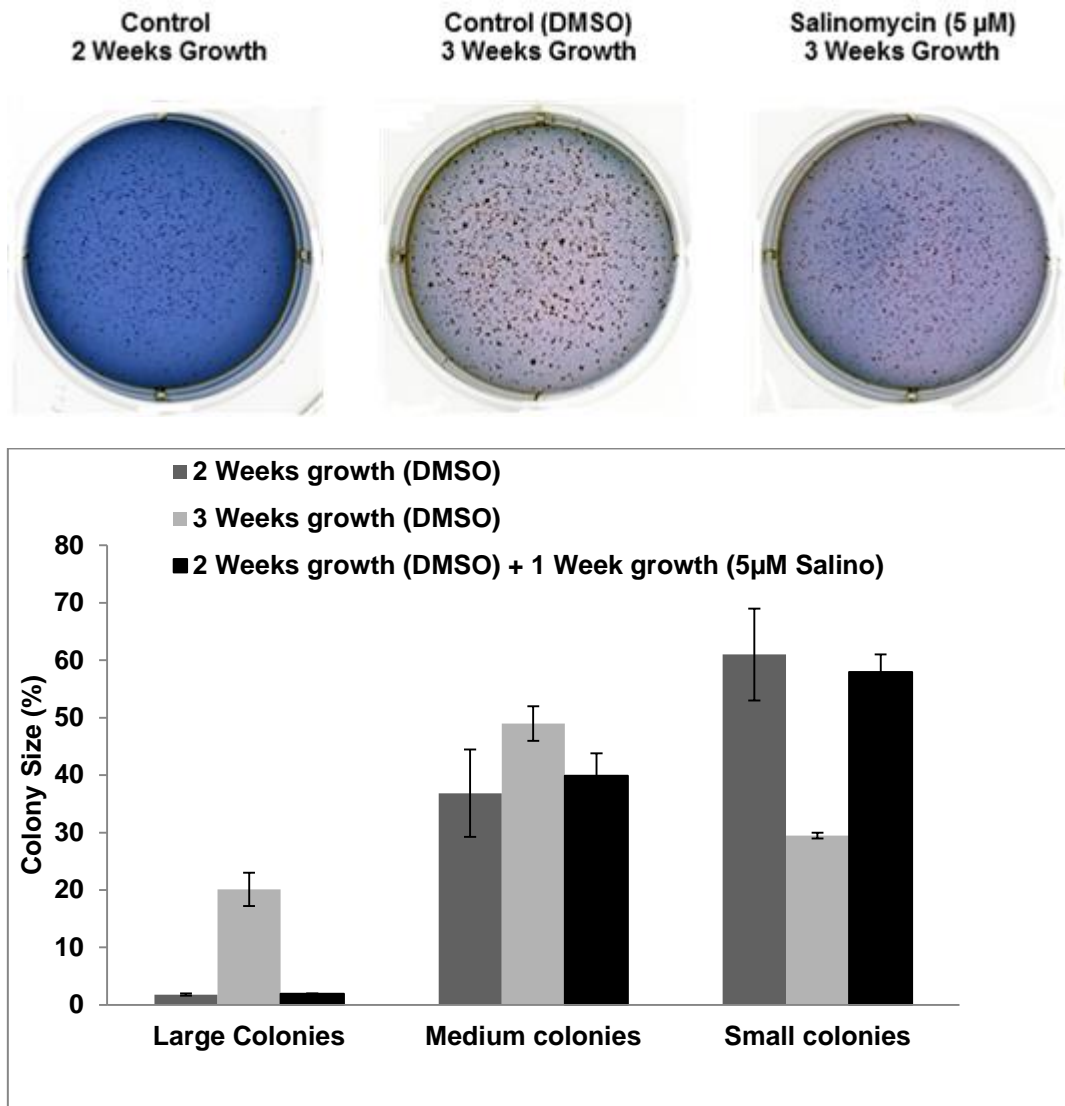


Figure 16. Induction of Growth Arrest by Salinomycin in MDA-MB-231 Cells.

### 3.5 Salinomycin Induced G2 Arrest and Senescence in MDA-MB-231 Cells

To examine the mechanism for Salinomycin-induced growth inhibition, cell cycle distribution was analyzed by flow cytometry. MDA-MB-231 cells were treated with the indicated concentrations of Salinomycin (5, 10 and 25  $\mu\text{M}$ ) for 24 and 48 h.

As shown in figure 17, the concentration of Salinomycin at 10 and 25  $\mu\text{M}$  caused an obvious G/2M arrest to the MDA-MB231 cells in a

concentration and time-dependent manner. The population of G2/M increased from 28% in DMSO-treated cells to 33 and 44% at 24 hours, respectively (fig. 17, upper panel). Similarly, the G2/M population increased from 22 to 43.6 and 49.67% at 48 hours, respectively (fig. 17, lower panel). Surprisingly, at lower concentration (2.5 and 5  $\mu$ M), Salinomycin was found to induce a transient cell cycle arrest in G1 and G2/M over time. In fact, Salinomycin induced an accumulation of cells in G1 phase at 24 hours and successive accumulation in the G2 phase at 48 hours post-treatment.

To determine whether Salinomycin induced cell cycle arrest specifically at mitosis or G2 phase, we examined the phosphorylation status of Histone H3 (Ser 10). Histone H3 is phosphorylated at serine 10 during mitosis by aurora kinase and the phosphorylation status of H3 is considered as a marker of mitosis [132]. We therefore, investigated the expression of p(ser10)H3 and found a time and dose-dependent decrease in the phosphorylation level of Histone H3 in response to the Salinomycin treatment (fig. 18, upper panel) . This result indicated that Salinomycin induced G2 arrest of MDA-MB231 cells. We also examined the expression of cyclin B1 in Salinomycin treated cells. An accumulation of cyclin B1 is well known to play an important role in G2/M transition. Knock-down of cyclin B1 with siRNA produces cell cycle arrest predominantly in the G2 phase [133], while an upregulation of cyclin B1 invokes mitotic arrest [134]. We found that Salinomycin also decreased cyclin B1 level in a time- and dose-dependent manner (fig. 18. middle panel), further confirming that Salinomycin induced a cell cycle arrest in the G2 phase in MDA-MB-

231 cells. However, a sensitive decrease of cyclin B1 began at higher concentrations of Salinomycin.

G1 arrest observed at 24 hours with low concentrations of Salinomycin prompted us to examine the expression levels of cyclin D1 protein involved in the control of the G1/S transition. It has been shown that overexpression of cyclin D1 shortens the G1 phase and occurs in many types of human cancers, whereas inhibition of cyclin D1 expression blocks G1-S transition [135-137]. As shown in Figure. 18 (lower panel), the level of cyclin D1 decreased upon treatment with Salinomycin in a time- and dose-dependent manner. Remarkably, no cyclin D1 protein was detected at 48 hours with a high concentration of Salinomycin.

MDA-MB-231 cells treated with low concentrations of Salinomycin exhibited the behavior of senescent cells characterized by cell viability; metabolically active and permanently growth arrested. Therefore, we next determined whether the growth arrested MDA-MB-231 cells did indeed undergo senescence. It is well known that senescent cells express a senescence-associated  $\beta$ -galactosidase (SA- $\beta$ -Gal), which is detected by incubating cells with X-gal at a pH of 6.0. Our results show that 30% of Salinomycin-treated cells expressed SA- $\beta$ -galactosidase (fig. 19), indicating that induction of senescence contributes to the inhibitory effect of Salinomycin on the proliferation of MDA-MB-231 cells.

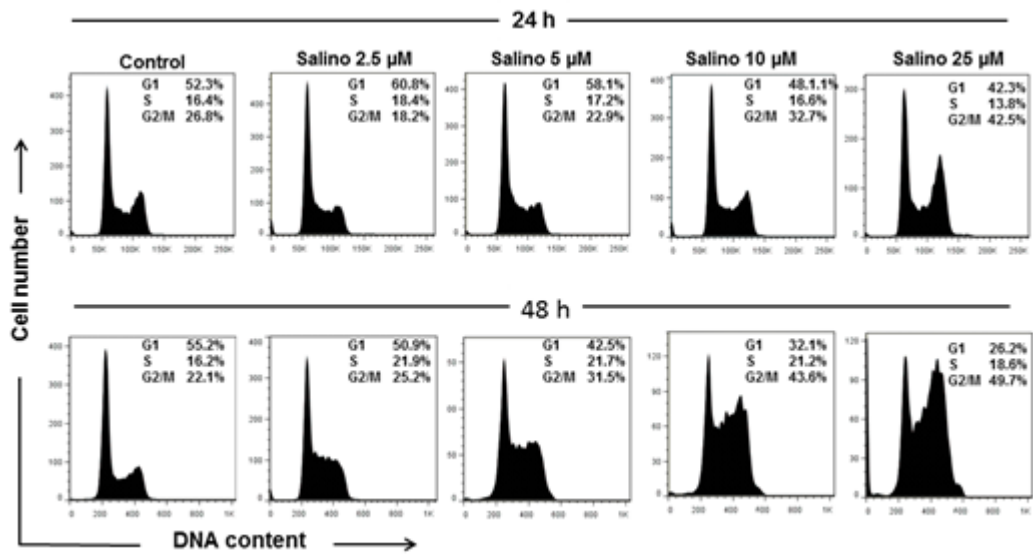


Figure 17. Flow Cytometry Analysis of Salinomycin-induced G2 Cell-Cycle Arrest in MDA-MB-231 Cells.

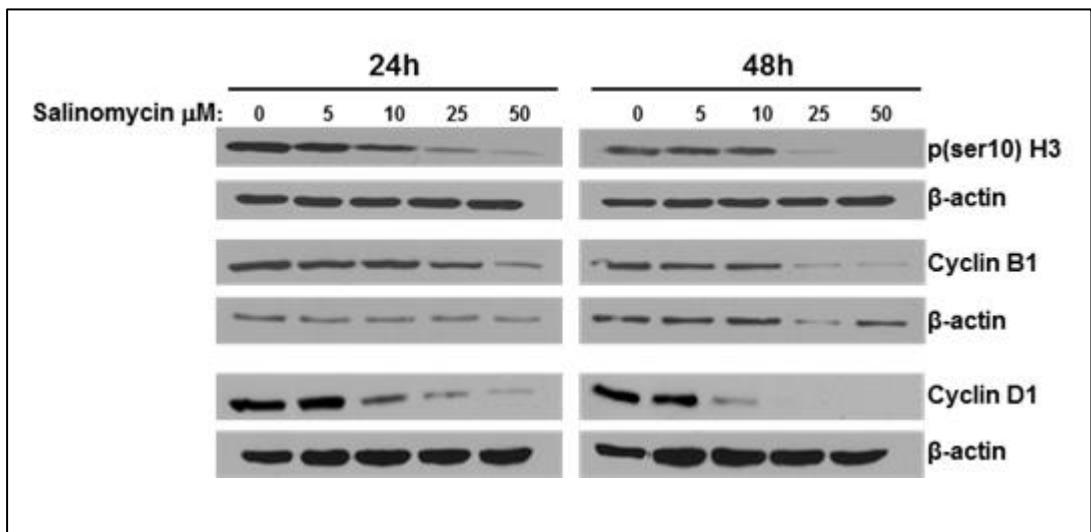


Figure 18. Western Blot Analysis of p(ser10) histone H3, cyclin B1 and cyclinD1 Expression in Salinomycin Treated MDA-MB-231.

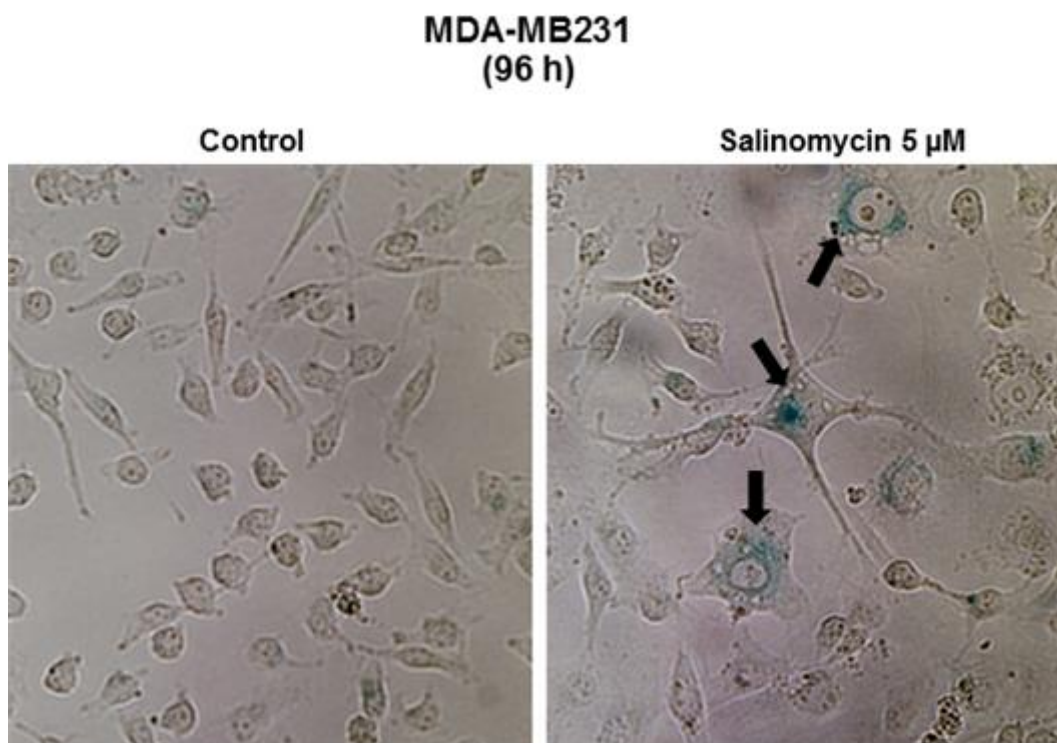


Figure 19. Salinomycin Induced Senescence in MDA-MB-231 Cells After Incubated with 5  $\mu$ M Salinomycin for 96 Hours and Stained for SA- $\beta$ -Galactosidase Activity.

### **3.6 Salinomycin Induced activation of $\gamma$ H2AX, a Marker of Double Strand Breaks, in MDA-MB 231 Cells**

Several studies showed that cells can undergo premature senescence in response to exposure to oxidative or genotoxic stresses that cause DNA damage. Interestingly, Salinomycin was shown to induce an elevation in the intracellular reactive oxygen species (ROS) levels and mitochondrial membrane depolarization [118]. Moreover, Salinomycin was also shown to induce DNA damage in MCF-7 and Hs578T human breast cancer cells [121, 122]. Therefore, we sought to investigate whether Salinomycin induced DNA damage in MDA-MB-231 cells as well. For this purpose, MDA-MB-231 cells were cultured for 6, 24 and 48 hours in

complete media containing either DMSO or an increasing concentration of Salinomycin (5-50  $\mu$ M). DNA damage was determined by measuring the levels of phosphorylated H2AX ( $\gamma$ H2AX) in non-treated and Salinomycin-treated cells. Western blot analysis revealed a concentration- and time-dependent increase in the levels of  $\gamma$ H2AX (fig. 20) in the MDA-MB-231 cells in response to the Salinomycin treatment, indicating an accumulation of double strand breaks in these cells. An increase in DNA damage was also assessed by immunofluorescence staining of  $\gamma$ H2AX in cells treated with 10 and 50 $\mu$ M Salinomycin for 24 hours. Figure 21 clearly shows a concentration-dependent increase of  $\gamma$ H2AX foci in response to Salinomycin. Since the activation of  $\gamma$ H2AX occurs even at concentrations of Salinomycin that do not lead to cell death (5 and 10 $\mu$ M), this rules out the possibility that the resulting DNA damage is a consequence of DNA fragmentation resulting from Caspase 3/7 activation and further confirming the potential of this drug to induce double strand DNA breaks in a concentration-dependent manner.

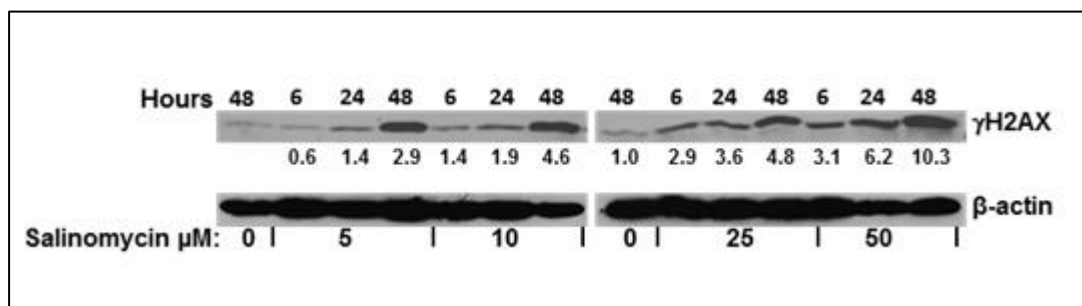


Figure 20. Western Blot Analysis of Phosphor-H2AX (Ser 139) in MDA-MB-231 Cells Treated for 6, 24 and 48 Hours with DMSO or Indicated Concentrations of Salinomycin.

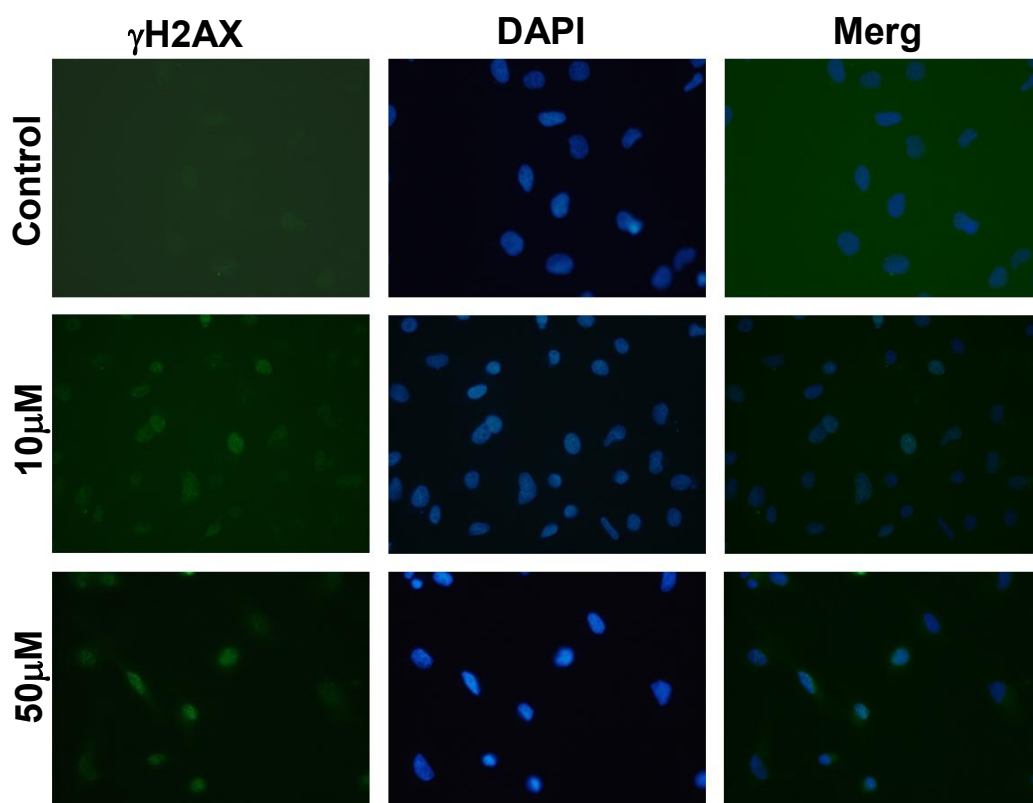


Figure 21. Immunofluorescence Staining for  $\gamma$ H2AX in Salinomycin Treated MDA-MB-231 cells.

### 3.7 Salinomycin Induced p53-Independent Upregulation of p21<sup>waf/cip</sup> in Growth Arrested MDA-MB-231 Cells

Because p21 protein has been reported to inhibit growth and apoptosis and mediate senescence, we investigated whether the growth inhibition and senescence mediated by Salinomycin was associated with an induction of p21. MDA-MB-231 cells were cultured in the presence of DMSO or an increasing concentration of Salinomycin for 6, 24 and 48 hours. Western blot analysis of p21 level in Salinomycin-treated cells with concentrations causing growth arrest and senescence showed an increase in the protein level detected starting from 6 hours of treatment (fig. 22). At the concentrations of Salinomycin causing cell death, we observed that while a concentration of 50  $\mu$ M caused a quick decrease of

p21 level detected as early as 6 hours, a concentration of 25  $\mu$ M, however, led to a transient increase of p21 at 6 hours followed by a decline in the protein level at 24 and 48 hours (fig. 22). These observations were further confirmed by immunofluorescence staining of p21 in cells treated with 10  $\mu$ M Salinomycin (fig. 23). As expected, no induction of mutant p53 in the MDA-MB-231 cells was observed, thus strongly suggesting that the induction of p21 by Salinomycin in MDA-MB-231 cells occurred independently of p53 function.

The levels of another CDK inhibitor, p27 was also determined at 24 and 48 hours post-treatment. As it is shown in figure 24, the level of p27 showed a concentration and time-dependent decrease in MDA-MB-231 cells.

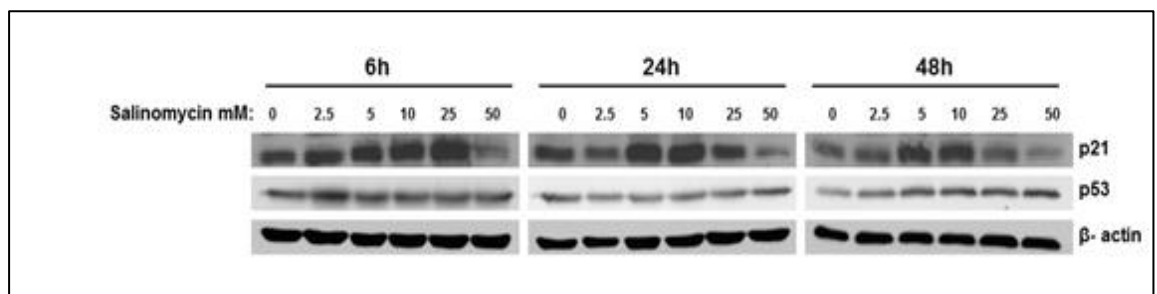


Figure 22. Western Blot Analysis of p21 Expression in Salinomycin Treated MD-MB 231 Cells.

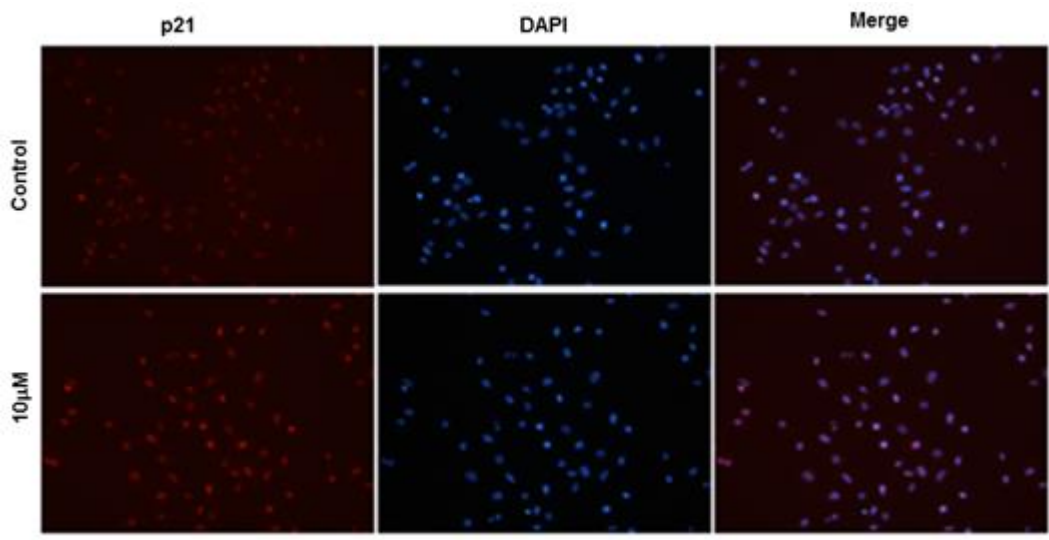


Figure 23. Immunofluorescence Staining for p21 in Salinomycin Treated MDA-MB-231 Cells. DAPI is used as a nuclear stain.

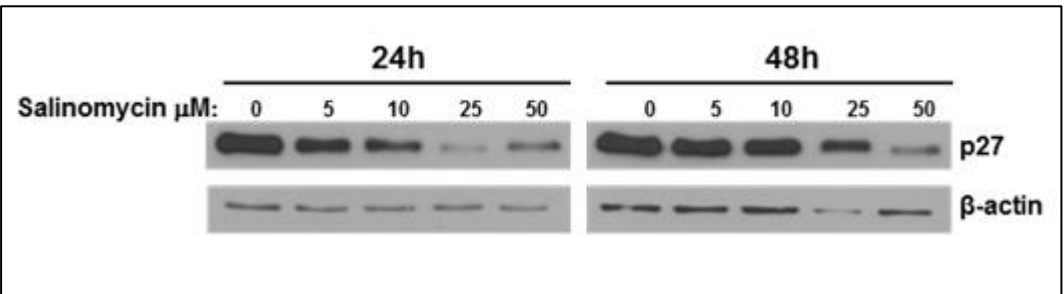


Figure 24. Western Blotting Analysis of p27 Expression in MDA-MB-231 Cells upon Salinomycin Treatment.

**3.8 Salinomycin Induced Downregulation of Survivin Expression in MDA-MB-231 Cells**

Survivin, a member of the inhibitor of apoptosis protein (IAP) family, plays an important role in both the regulation of cell cycle and the inhibition of apoptosis. However, a decrease in survivin levels has been shown to sensitize cells to apoptosis. Therefore, we examined the possible involvement of survivin in cell cycle arrest and apoptosis as triggered by Salinomycin. Toward this end, we analyzed, by Western

blotting, the expression of survivin in response to various concentrations of Salinomycin after 24 and 48 hours of treatment. As shown in figure 25, while low concentrations of Salinomycin led to no obvious change in survivin expression, higher concentrations (25 and 50  $\mu\text{M}$ ), caused a drastic decrease in survivin protein level at 24 and 48 hours, consequently sensitizing MD-MB-231 to cell death. The persistence of survivin expression at concentrations causing growth arrest and senescence could also account for the resistance to cell death of Salinomycin-treated cells.

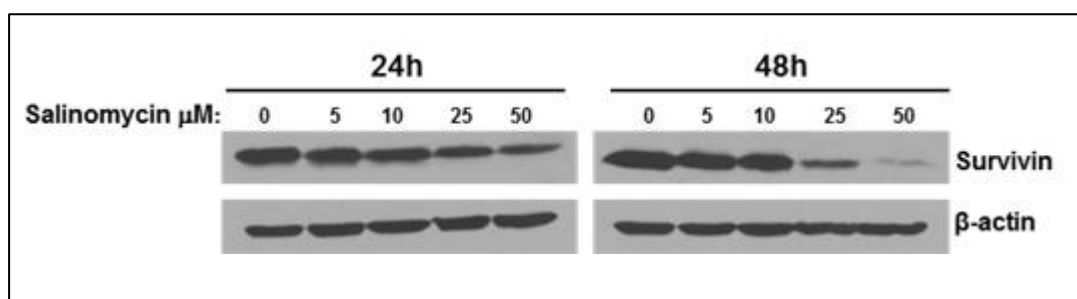


Figure 25. Western Blot Analysis of Survivin Expression in Salinomycin-Treated MDA-MB 231 Cells.

### 3.9 Salinomycin Induced Hyperacetylation of Histone H3 and H4 in the MDA-MB-231 Cells

The expression of p21 and increased histone hyperacetylation have been previously linked to apoptosis, growth arrest and cellular senescence. Therefore, we examined the acetylation profile of Histone H3 and H4 in MDA-MB-231 cells at 6, 24 and 48 hours with increasing concentrations of Salinomycin. In figure 26, time course analysis showed a gradual increase in acetylated Histones, H3 and H4. A marked overall increase in the acetylation status of histone H3 and H4 was also detected by immunofluorescence staining (fig. 27). Altogether, these results show that Salinomycin induces acetylation of Histone H3 and H4.

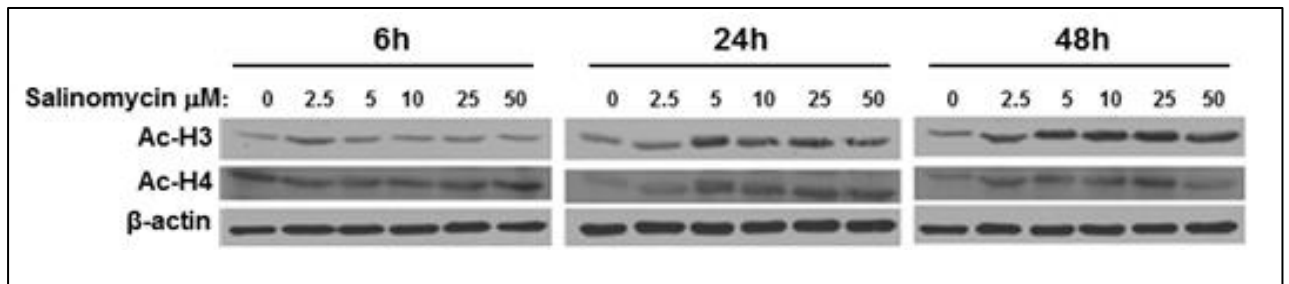


Figure 26. Western Blot Analysis of Ac-H3 and Ac-H4 Expression in Salinomycin Treated MDA-MB 231 Cells.  $\beta$ -actin was used as loading control.

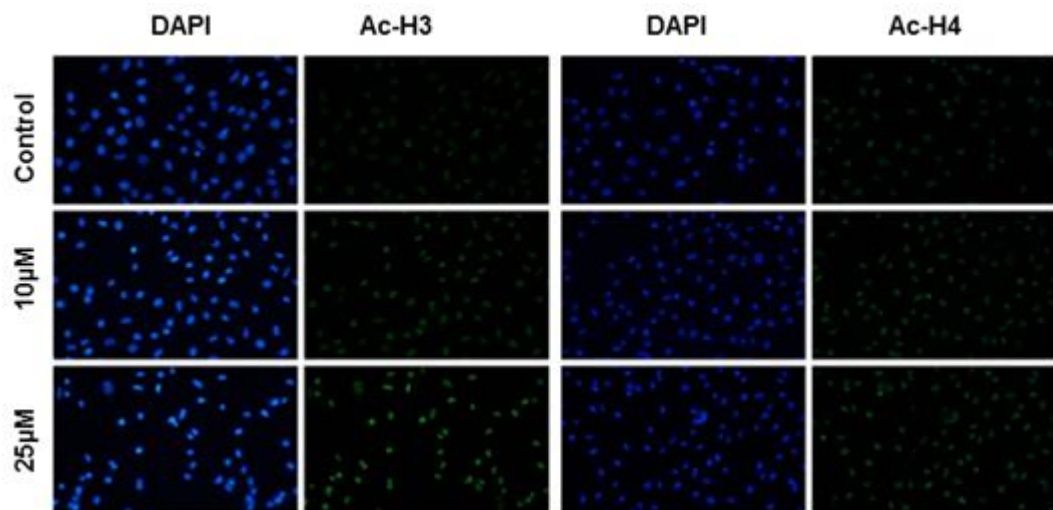


Figure 27. Immunofluorescence Staining of Ac-H3 and Ac-H4 in MDA-MB-231 Cells Treated with 10 and 25  $\mu$ M Salinomycin for 24 hours. DAPI was used as a nuclear stain.

### **3.10 Combination of Salinomycin with Frondoside A or with 4-Hydroxy-Tamoxifen Enhanced Cell Death and Activation of Caspase3/7**

Recently, frondoside A (Fr), a triterpenoid glycoside isolated from the sea cucumber, *Cucumaria frondosa*, has been shown to inhibit survival, migration, and invasion of MDA-MB-231 cells [138]. *In vivo*, frondoside A strongly decreased the growth of MDA-MB-231 tumor xenografts in athymic mice, without precipitating significant toxic side-effects. Although frondoside A is not used as an anti-cancer drug, we decided to investigate whether Salinomycin could sensitize MDA-MB-231 cells to this compound. We have chosen to use 1 $\mu$ M of frondoside A, a concentration that induces 30% inhibition of cellular viability. Remarkably, frondoside A potentiated the growth inhibitory effect of different concentrations of Salinomycin (fig. 28).

We next examined the efficacy of Salinomycin (2.5-50  $\mu$ M) in combination with 4-Hydroxy-Tamoxifen (20  $\mu$ M), the active metabolite of tamoxifen, the breast cancer drug, in MCF-7 cells. Combined treatment caused a significantly greater inhibition in cellular viability than treatment with either drug alone (fig. 29) after 48 hours of treatment. Moreover, a combination of Salinomycin with 4-Hydroxy-Tamoxifen significantly increased the activation of Caspase 3/7, suggesting that apoptosis is higher compared with treatment with either drug alone (fig. 30).

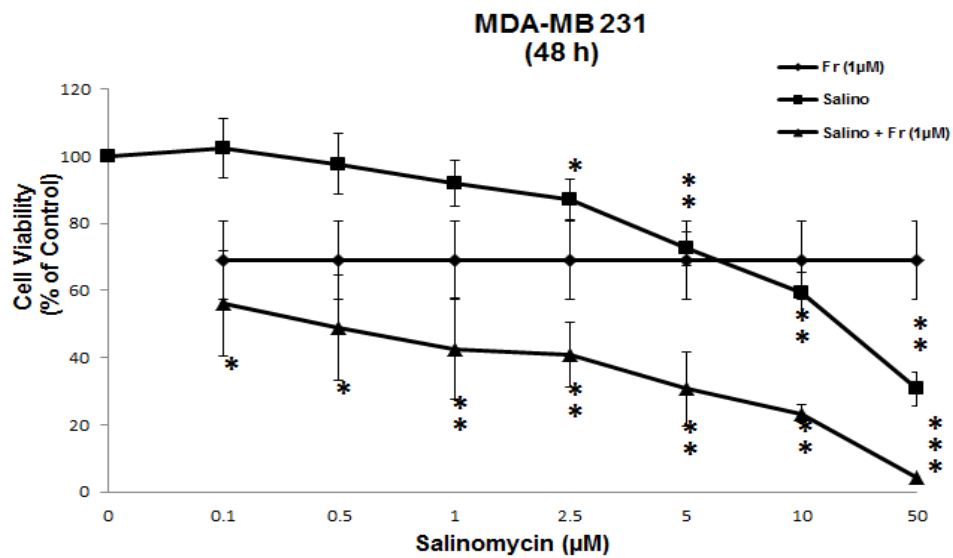


Figure 28. Salinomycin Enhanced Cell Death Induced by Frondoside A in MDA-MB-231 Cells.

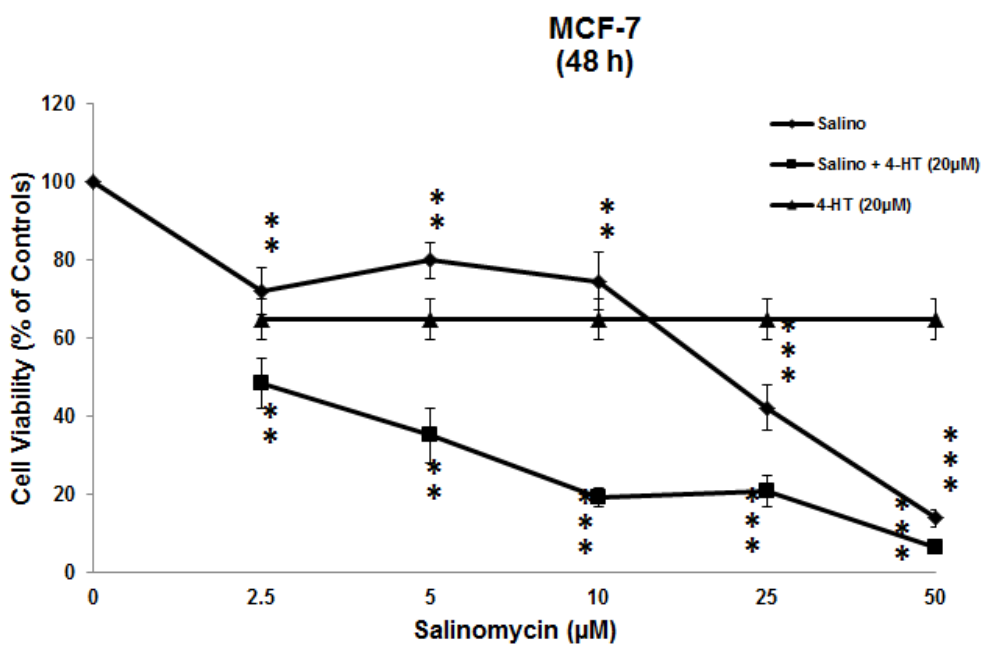


Figure 29. Salinomycin Enhanced Cell Death Induced by 4 Hydroxy-Tamoxifen in MCF-7 Cells.

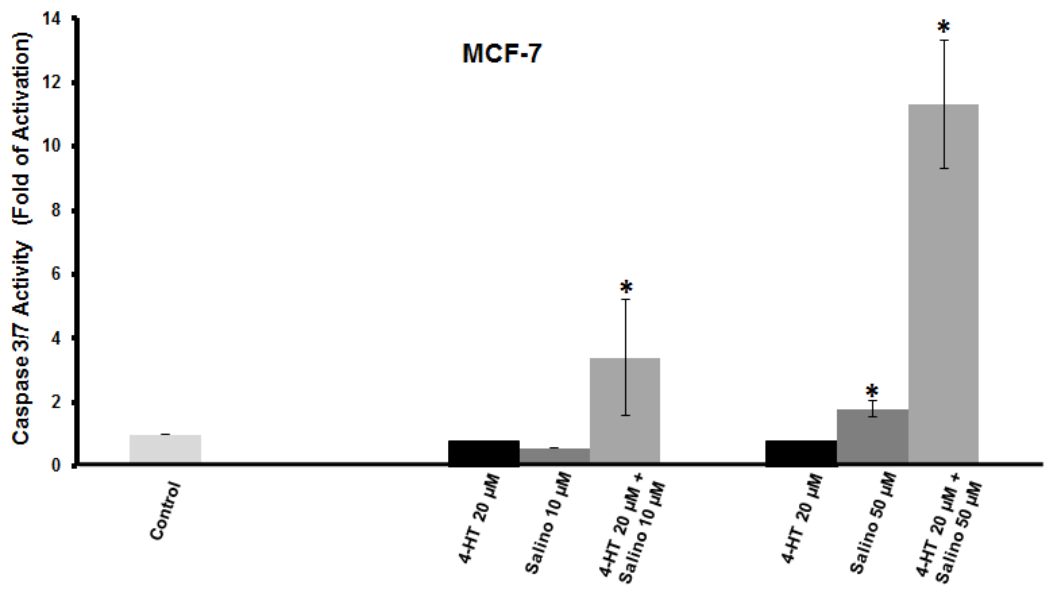


Figure 30. Salinomycin Induced Synergistic Apoptosis Against MCF-7 Cells. Fr represents frondoside A, Salino represents Salinomycin and 4-HT represents 4-Hydroxy-Tamoxifen.

## DISCUSSION

Common cancer treatment drugs aim at inducing cell death and apoptosis, which are considered prerequisites for preventing malignant cell growth. Several studies have demonstrated that cellular senescence can occur *in vivo* and may provide a critical barrier for cancer development and cancer progression [139]. In fact, treatment of cancer cell lines with different chemotherapeutic drugs induces irreversible growth arrest associated with senescence like-phenotype [140, 141]. Indeed, induced-senescence appears to be a promising alternative strategy for cancer treatment.

Our present work shows that (1) Salinomycin significantly decreased viability of the wild-type p53 MCF-7 and T47D as well as mutant p53 MDA-MB-231 human breast cancer cell lines in concentration and time-dependent manners, and that (2) MDA-MB-231 cells respond differently to low and high concentrations of Salinomycin. Our results demonstrate that high concentrations of Salinomycin (25 and 50  $\mu\text{M}$ ) induce G2 arrest, downregulation of survivin and activation of the apoptotic signaling pathway resulting in the activation of Caspase 3/7 and PARP cleavage. This finding is in agreement with previous reports demonstrating that the anti-cancer effect of Salinomycin on different cancer cell lines was due to its apoptosis-inducing activity [115, 118, 123, 142]. Interestingly, our results show for the first time that low concentrations of Salinomycin ( $\leq 10\mu\text{M}$ ) induce senescence in MDA-MB-231 cells. We found that Salinomycin-treated MDA-MB-231 cells exhibited markers of senescence including SA- $\beta$ -galactosidase activity, changes in

morphology, cell cycle arrest, Histone H3 and H4 hyperacetylation and elevated expression of the cyclin-dependent kinase inhibitor, p21. We also report that Salinomycin enhanced the killing of the MCF-7 and MDA-MB-231 cells by chemotherapeutic agents, 4-Hydroxy-Tamoxifen and frondoside A, respectively.

We showed that data on the cell viability of MDA-MB-231 determined by CellTiter-Glo and Trypan Blue Exclusion were not superimposable even though they follow the same pattern i.e. growth inhibition at lower concentrations and cell death at higher concentrations. CellTiter-Glo Assay which is based on quantification of the ATP present showed less effect on the viability of the MDA-MB-231 compared to the Trypan Blue Exclusion Assay when the same concentration was used. Interestingly, it has been reported that DNA-damaging agents such as etoposide and temozolomide induce an ATP surge in cancer cells [143], which explains the differences observed between CellTiter-Glo and Trypan Blue Exclusion Assay in Salinomycin-treated MDA-MBA-231 cells.

In our study, we observed that at a concentration of 2.5 and 5  $\mu\text{M}$ , Salinomycin induced a G1 arrest at 24 hours and G2 arrest at 48 hours post-treatment. Earlier reports have shown that low concentrations of 2.5 and 5  $\mu\text{M}$  of Salinomycin also induced a G1 arrest in the MCF-7 and Hs578T breast cancer cells after 24 hours of treatment [122, 123] which is in agreement with our data on the MDA-MB-231 cells. However, no further concentrations or time points were tested. Cyclin D1, a cyclin required for G1 to S transition, was found to be reduced upon Salinomycin treatment and could be the main cause for the G1 block. Our data also suggested

that cell cycle arrest at the G2 phase might be mediated by the reduction of cyclin B1. Moreover, the level of cyclin B1 at 5  $\mu$ M Salinomycin seemed to decrease at later times than cyclin D1 decreased. Interestingly, Curcumin was also shown to induce a successive G1/S arrest at earlier times and G2/M phase arrest at later time point in HOS cells [144]. The exact mechanism by which cells undergo a transient G1 arrest followed by a G2 arrest remains unclear. Our data also showed, for the first time, that Salinomycin at higher concentration induced a robust G2 arrest confirmed by cyclin B1 decrease and p(ser10) Histone H3. The cell cycle arrest data is in agreement with the growth inhibition data shown by cell viability (fig 1, 5,6, 15) and colony growth assay (fig. 16). Interestingly, we found that the CDK inhibitor p27, also a marker of G1 arrest, was downregulated during the transient G1 arrest observed at 5  $\mu$ M. This is not surprising as a report by Yongxian and Miskimins showed that G1 arrest in MDA-MB-231 breast cancer cells treated with metformin involves down regulation of cyclin D1 and requires p27 or p21 [145].

Inhibitor of Apoptosis Proteins (IAPs), which includes survivin, represents a family of anti-apoptotic proteins that bind and inactivate Caspase 3, 7 and 9 [146-148] and can modulate cell division and cell cycle progression [149]. Survivin has been shown to be highly expressed in most cancers, where it functions as an inhibitor of apoptosis. In breast cancer, overexpressed survivin was shown to protect cells against apoptosis induced by chemotherapeutic agents, such as Etoposide [150]. In consideration of the role of survivin as a custodian of cancer cell survival, our results suggest that Salinomycin at high concentration might

exert its cytotoxic anti-cancer effects at least partly via the down-regulation of survivin.

Senescent cells are known to remain viable and metabolically active, but are permanently growth arrested [151]. Growth arrest is achieved and maintained in either G1 or G2/M stage of cell cycle, at least through overexpression of specific cyclin-dependent kinase inhibitors such as p16, p21 and p27 [139] [152-154]. Schwarze et al have previously shown that p21 is more important in cell cycle arrest that is associated with early senescence, while p16 appears to be important for maintaining the senescence phenotype [152]. Senescence is triggered by DNA damage to cells which respond via the induction of a group of genes responsible for the development of the senescence phenotype [155]. The decision of the cell to undergo either apoptosis or senescence is dependent, at least in part, upon the magnitude of DNA damage caused to cancer cells. Low levels of DNA damage may induce senescence without activating the apoptotic pathway. Several studies reported that many senescence inducing drugs generate DNA damage. In fact, treatment of prostate cancer cells with high doses of doxorubicin, a DNA-damage inducing chemotherapeutic drug, leads to apoptosis, while a lower dose of doxorubicin induces senescence [156]. Furthermore, doxorubicin was shown to induce senescence in numerous cancer cell lines, including those lacking p53 [157]. The same observation was made when cisplatin [158], hydroxyurea [159] or bromodeoxy uridine [160] were used.

The expression of the cyclin-dependent kinase inhibitor p21 has been implicated in chemotherapy induced cell cycle arrest in various human cancers [152, 153, 161-163]. The contribution of p21 to cellular senescence has been demonstrated by numerous studies [152-154]. In fact, p21 has been found to be upregulated in senescent cells. Moreover, forced overexpression of p21 was shown to be sufficient to induce cell cycle arrest, and premature senescence in wild-type and mutant p53 cells [155]. In line with this data, we reported that Salinomycin at concentrations of  $\leq 10 \mu\text{M}$  is able to induce maintained upregulation of p21 expression in the MDA-MB-231 cells. Based on these data, we propose that induction of senescence in Salinomycin-treated MDA-MB-231 breast cancer cells is mediated, at least, partly through a p53-independent upregulation of p21 protein and does not involve p27 since, its expression decreased in a time- and dose dependent manner (fig. 24).

It has also been reported that cellular senescence is associated with modifications in chromatin structure [156, 157]. Histone hyperacetylation has been directly linked to the upregulation of p21 and this activation can also occur independently of p53 [39]. Our data showed that Salinomycin induced Histone H3 and H4 hyperacetylation. We have also found that histone hyperacetylation correlated with a p53-independent upregulation of p21 expression and growth inhibition in the MDA-MB-231 cells. Our data suggest that Histone H3 and H4 hyperacetylation could be one of the mechanisms through which Salinomycin exerts its anti-cancer activity, at least, in breast cancer.

Recent studies reported that Salinomycin potentiates the anti-cancer activity of several DNA damage-inducing chemotherapeutic drugs [121] as well as sensitizes cancer cells to radiation [122]. Salinomycin was also shown to sensitize cancer cells to inhibitors of DNA replication [120] and to antimetabolic drugs [123]. Consistent with these reports, our results show that Salinomycin indeed potentiates the anti-cancer activity of two other drugs, namely frondoside A and the anti-estrogen 4-Hydroxy-Tamoxifen in MDA-MB-231 and MCF-7 respectively.

In summary, our study is consistent with the model shown in figure 31, in which treatment with Salinomycin induces double strand breaks, revealed by an accumulation of  $\gamma$ H2AX. The magnitude of DNA damage, which depends on the concentration of Salinomycin, determines the response of the cells to this damage. We propose that the presence of large amounts of DNA damage induced by high concentrations of Salinomycin, MDA-MB-231 cells respond by triggering the apoptotic signaling pathway through activation of Caspase 3/7 and cleavage of PARP. In contrast, limited DNA damage caused by low concentrations of Salinomycin triggers a rapid program of senescence which is mediated, at least partly, through hyperacetylation of Histone H3 and H4 which subsequently results in the upregulation of p21 expression.

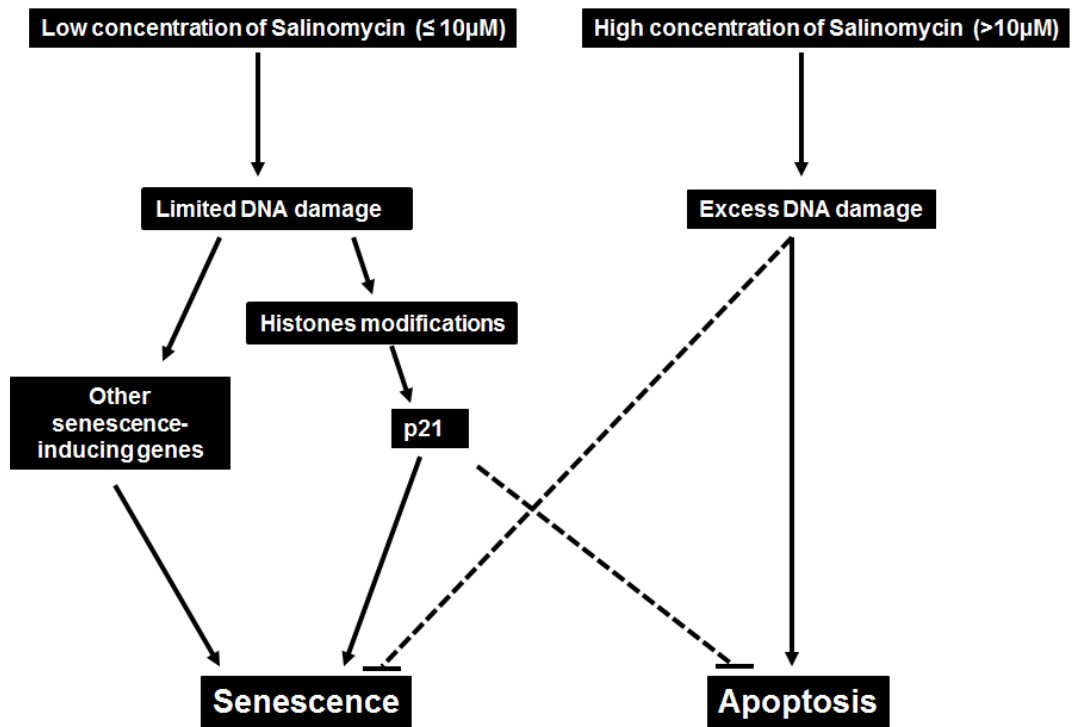


Figure 31. Hypothetic Model for the Differential Effect of Salinomycin in MDA-MB-231 Breast Cancer Cells.

## CHAPTER 3: RESULTS AND DISCUSSION

### Part II. Anti-Tumor Growth and Anti-Metastatic Activity of *Origanum majorana* Extract on the Triple Negative Breast Cancer

#### 3.12 *O. majorana* Extract Inhibited the Viability of the MDA-MB-231 Breast Cancer Cells

To examine the anticancer activity of *Origanum majorana* extract (OME) on breast cancer cells, we first measured the effect of various concentrations of the extract (0, 50, 150, 300, 450 and 600 µg/mL) on the proliferation of the MDA-MB-231 breast cancer cell line (fig. 32). Our results show that exposure of the MDA-MB-231 to OME decreased cellular viability in a concentration- and a time-dependent manner. The IC<sub>50</sub> (producing half-maximal inhibition) was approximately 350 µg/mL at 24 hours and 400 µg/mL at 48 hours treatment. Observation of the OME-treated MDA-MB231 cells under light microscopy also revealed that the number of cells decreased when the concentration increased. Furthermore, as shown in figure 33, light microscopy observation of MDA-MB231 cells treated with concentrations of 150, 300 and 450 and 600 µg/mL OME, underwent morphological changes characterized by a loss of their epithelial morphology visible after 24 hours of treatment. Echinoid spikes and cellular rounding, characteristics of apoptotic cells were also observed.

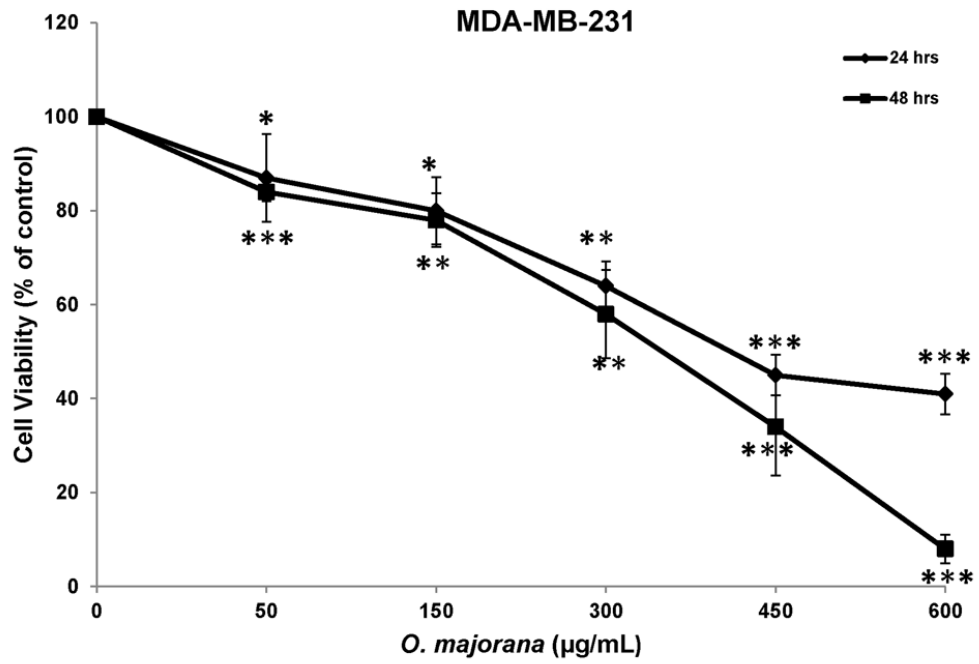


Figure 32. Inhibition of Cell Viability of MDA-MB-231 Cells by *O. majorana* Extract.

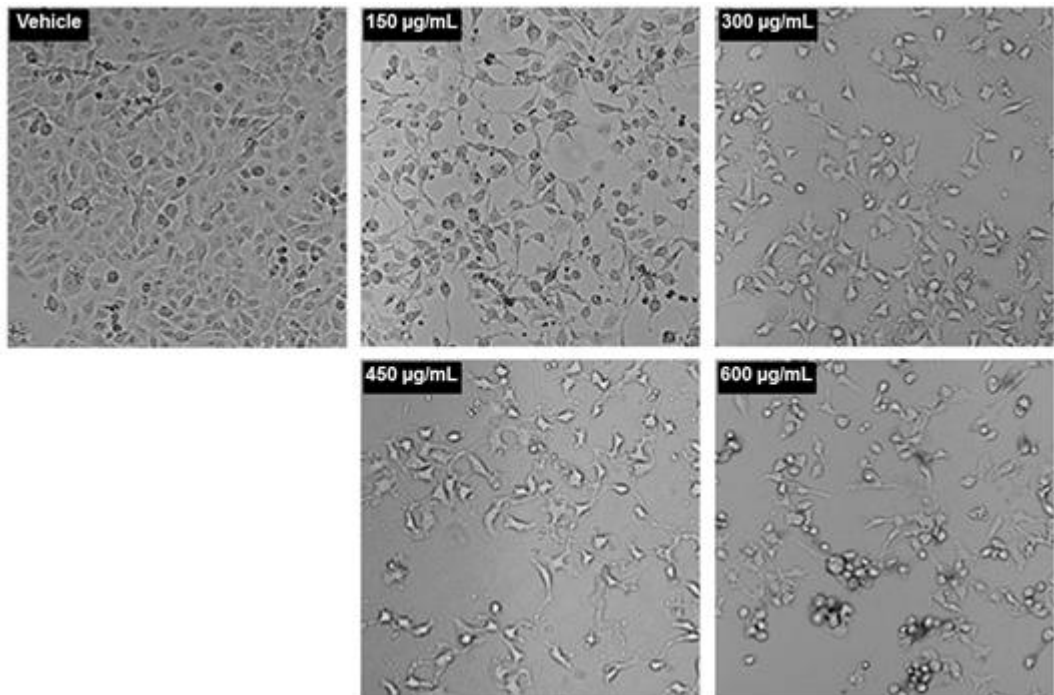


Figure 33 . Micrograph of MDA-MB-231 Cells After 24 Hours Incubation with Various Concentrations of OME.

### **3.13 *O. majorana* Extract Lead to Mitotic Arrest and Apoptosis in MDA-MB-231 Cells**

The ability of an anticancer drug to affect cell cycle distribution can provide information regarding its cytotoxic mechanism(s) of action. For this reason, we investigated the effect of OME on cell cycle distribution using flow cytometry. MDA-MB 231 cells were treated with the indicated concentration of *O. majorana* for 24 hours and subjected to cell cycle analysis. At a concentration of 150 µg/mL, OME caused an obvious G2/M arrest of these cells (fig. 34). Indeed, the population of G2/M increased significantly from 23 to 51.7% as the concentration of the OME increased to 150 µg/mL, indicating that OME-treated MDA-MB-231 cells were arrested in the G2/M phase. A slight increase in the sub-G1 population (6.2%) was also observed by these concentrations indicating that a small population of OME-treated MDA-MB-231 cells is undergoing cell death. Interestingly, at higher concentrations of OME, flow cytometry analysis revealed a dramatic increase in the apoptotic population (sub-G1 peak) rising from 0.9% in the control group to 48.4% and 56.7% in cells treated with 600 and 450 µg/mL, respectively (fg. 34).

To determine whether OME specifically induced cell cycle arrest at mitosis or the G2 phase, we examined the phosphorylation status of Histone H3 (Ser 10). Histone H3 is phosphorylated at serine 10 during mitosis by aurora kinase and the phosphorylation status of H3 is considered a marker of mitosis [132]. We therefore, investigated the expression of p(ser10)H3 and found that treatments 150 and 300 µg/mL of *O. majorana* significantly increased the phosphorylation level of Histone

H3 (fig. 35, upper panel). This result indicates that OME induces mitotic arrest of MDA-MB231 cells. Next, we investigated the mechanism of OME-induced mitotic arrest. Accumulation of cyclin B1 is well known to play an important role in G2/M transition. Knock-down of cyclin B1 with siRNA produces cell cycle arrest predominantly in the G2 phase [133], while an upregulation of cyclin B1 invokes mitotic arrest [134]. We, therefore, investigated the protein level of cyclin B1 in OME-treated MDA-MB-231 cells. We found that treatment with these concentrations of OME leading to mitotic arrest, caused also an increase of cyclin B1 protein in MDA-MB-231 cells (fig. 35, lower panel), suggesting that cyclin B1 accumulation might play a crucial role in OM triggered mitotic arrest. Taken together, our findings reveal a differential concentration effect of OME on cell cycle progression of MDA-MB 231 cells. Whereas, lower concentrations of OME (150 and 300  $\mu\text{g}/\text{mL}$ ) induced a major mitotic arrest with a slight increase in the apoptotic population, higher concentrations (450 and 600  $\mu\text{g}/\text{mL}$ ) induced massive cell death by apoptosis. The reduced cell viability observed in MDA-MB231 cells treated with low concentrations of OME, is possibly due to a large extent to an inhibition of cell proliferation rather than to cell death.

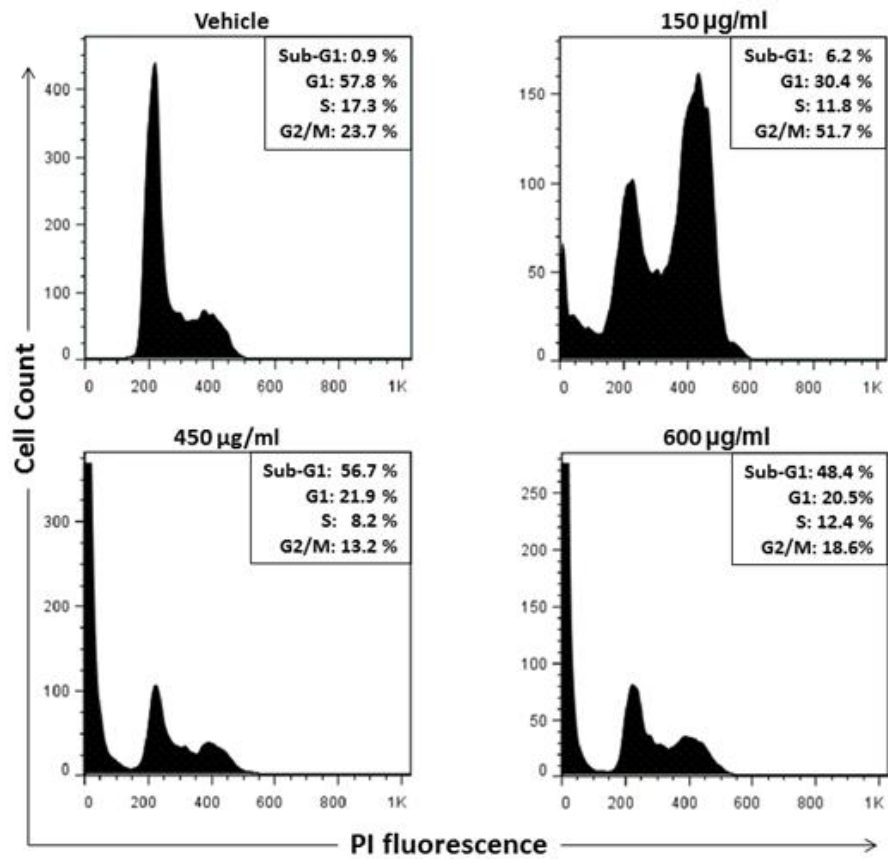


Figure 34. Flow Cytometry Analysis Showing a G2/M Cell Cycle Arrest Induced by *O. majorana* Extract in MDA-MB-231 Cells.

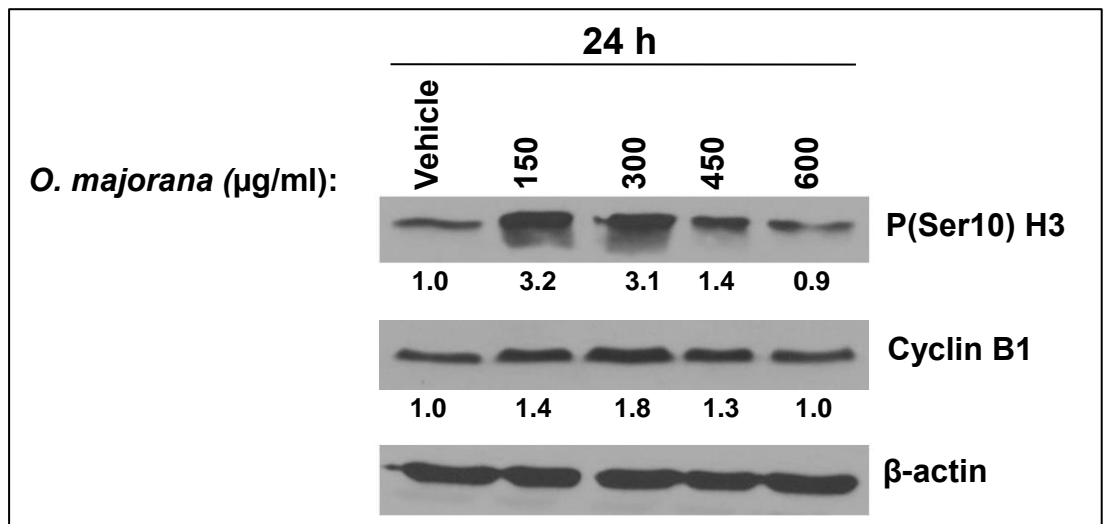


Figure 35 . 75Western Blot Analysis of Phosphor(ser10)-H3, and Cyclin B1 in OME Treated MDA-MB231 Cells.

Apoptosis in OME-treated MDA-MB-231 cells was further examined by measuring Caspase 3/7 activation in MDA-MB 231 cells treated with various concentrations (300, 450 and 600  $\mu\text{g}/\text{mL}$ ) of OME after 24 hours of treatment. A concentration- and time-dependent activation of caspase 3/7 was detected in treated cells (fig 36). Interestingly, cleavage of the poly(ADP-ribose) polymerase (PARP) occurred only in cells treated with higher (450 and 600  $\mu\text{g}/\text{mL}$ ), but not at lower concentrations (150 and 300  $\mu\text{g}/\text{mL}$ ) of OME (fig. 37). It is worth mentioning that at these lower concentrations of OME, only a low apoptotic induction rate was observed despite the detection of Caspase 3/7 activation.

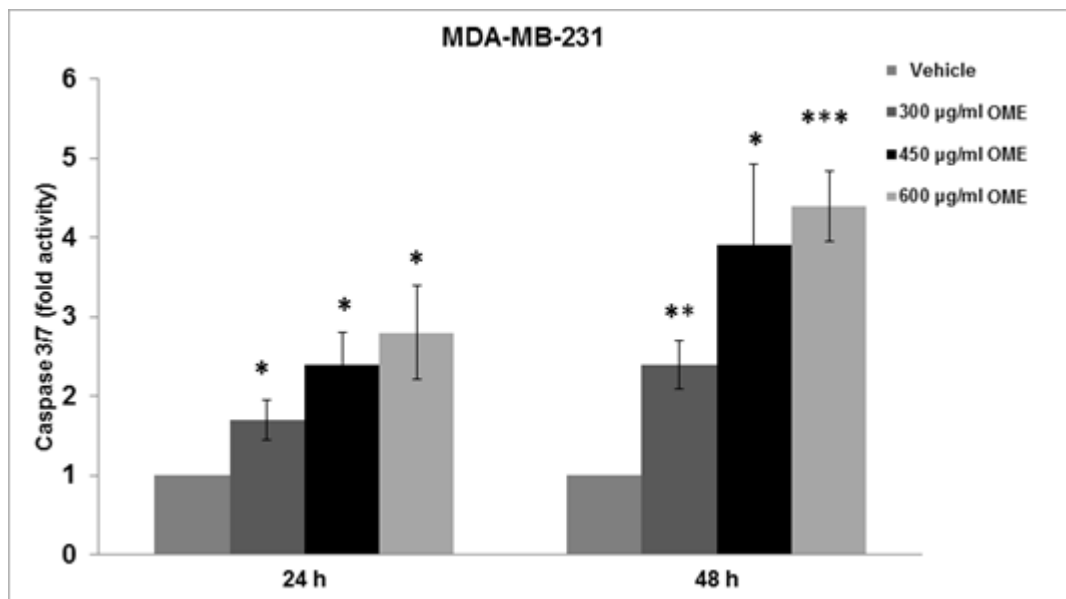


Figure 36. Stimulation of Caspase 3/7 Activity in OME Treated in MDA-MB-231 Cells.

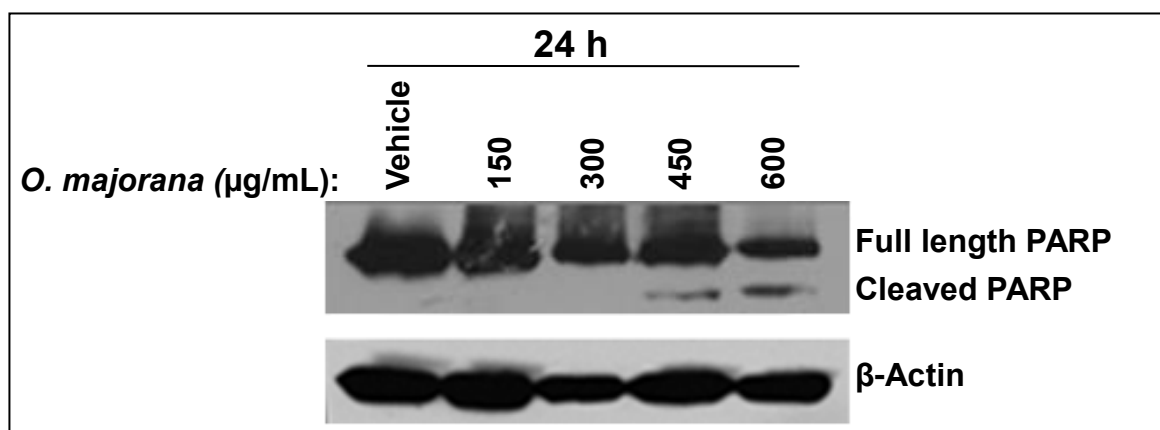


Figure 37. Concentration-Dependent Induction of PARP Cleavage in OME Treated MDA-MB231 Cells.

### 3.14 Concentration-Dependent Regulation of Survivin Expression by *O. majorana* Extract

Survivin, a member of the inhibitor of apoptosis protein (IAP) family, plays an important role in both the regulation of cell cycle and the inhibition of apoptosis. Survivin levels increase in the G2/M phase conferring resistance to apoptosis to the G2/M arrested cells. However, a decrease in survivin levels sensitizes the cells to apoptosis. Several studies have reported that survivin exerts its negative effect on apoptosis by inhibiting the activity of Caspase 3, 7 and 9. Therefore, we examined the possible involvement of survivin in cell cycle arrest and apoptosis triggered by OME. We analyzed, by Western blotting, the expression of survivin in response to various concentrations of OME after 24 hours of treatment. Interestingly, we observed a differential concentration-effect of OME on survivin expression in the MDA-MB-231 cells (fig. 38). We found that low concentrations of OME led to a substantial increase in the level of survivin, while higher concentrations caused a drastic decrease of survivin

(99%). Based on these results, we concluded that OME exerts a concentration-dependent effect on MDA-MB-231 cells. Low concentrations of OME induced a mitotically arrested cells accompanied by survivin upregulation which, in turn, conferred resistance to cell death to this population of cells, probably by inhibiting the activity of Caspase 3/7 which was monitored by the absence of PARP cleavage at these concentrations. Treatment of MDA-MB-231 cells with higher concentrations of OME caused a dramatic decrease in survivin expression and consequently sensitized MD-MB-231 cells to apoptosis.

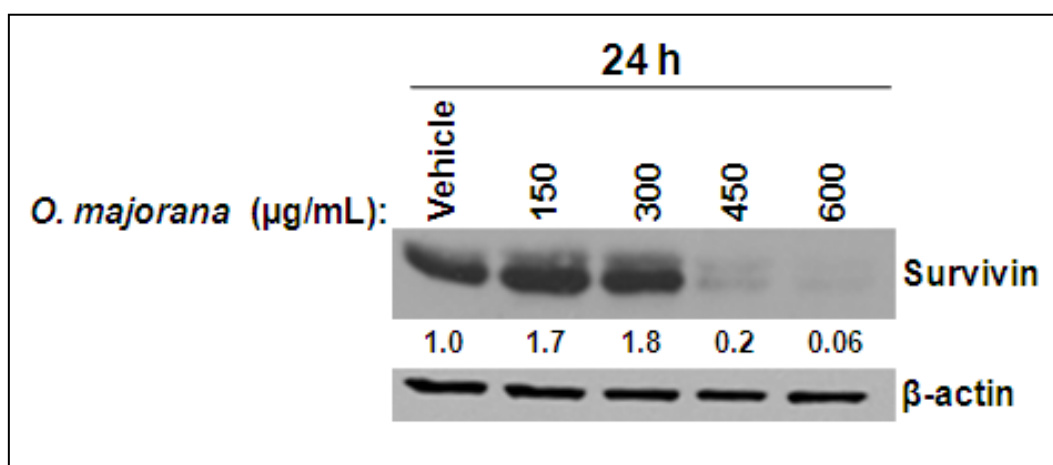


Figure 38. Western Blot Analysis Showing A differential Effect on Survivin Expression by Different Concentrations of OME in MDA-MB-231 Cells.

### 3.15 *O. majorana* Extract Activates the Extrinsic Pathway for Apoptosis via an Upregulation of TNF- $\alpha$ and Activation of Caspase 8

Having shown that OME induces the activation of the effector Caspases 3/7, we looked at the activity of the initiator caspases of the extrinsic and intrinsic cell death pathway, namely Caspase 8 and Caspase 9, respectively. Surprisingly, no Caspase 9 activation was detected in

response to various concentrations of OME after 24 hours of treatment (fig 39). On the other hand, caspase 8 activity increased in a concentration-dependent manner in response to OME treatment (fig 39). This result demonstrates that the apoptotic effect of the extract on MDA-MB-231 is dependent on caspase 8 activity, which implicates only the extrinsic cell death pathway since no caspase 9 activation was observed. After showing that the extrinsic cell death pathway is implicated in OME-dependent apoptosis, we were then interested in determining how this pathway is activated by OME. We determined the changes in the expression level of the Tumor Necrosis Factor Alpha (TNF- $\alpha$ ) in response to OME after 24 hours of treatment. Western blot analysis revealed a clear increase in the level of TNF $\alpha$  in MDA-MB-231 cells in response to OME treatment (fig. 40). The upregulation of TNF- $\alpha$  was further confirmed by immunofluorescence assay (fig 41). Even though we have shown that OME exerts its effect via the activation of the extrinsic pathway of cell death, we cannot rule out, at this stage, the possibility of OME-dependent apoptosis could also be triggered by another mechanism.

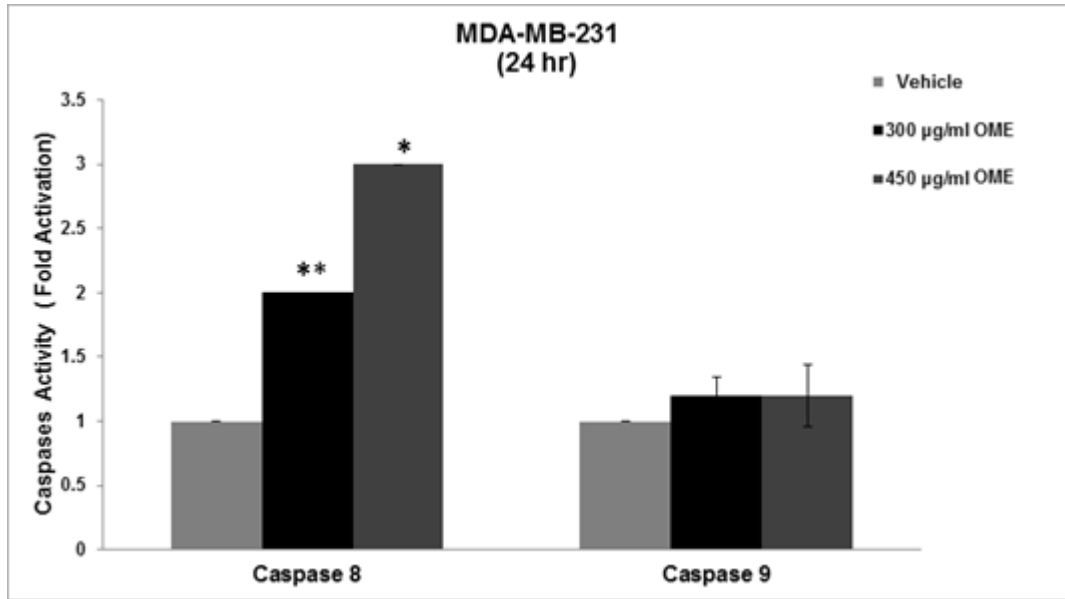


Figure 39. *O. majorana* Induced Apoptosis by Activation of Caspase 8 and but not Caspase 9 in MDA-MB-231 Cells.

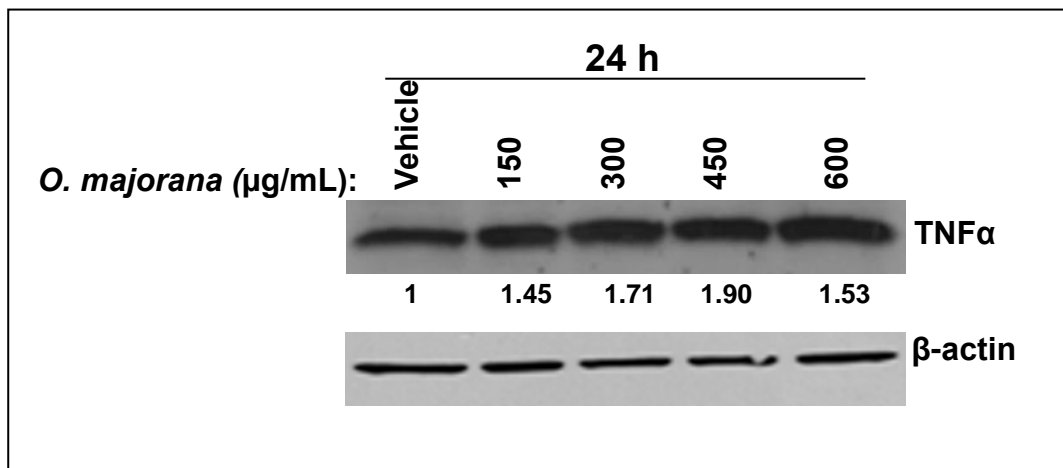


Figure 40. Western Blot Analysis Showing An increase in Cellular TNF- $\alpha$  Protein in the MDA-MB-231 Cells Treated with OME.

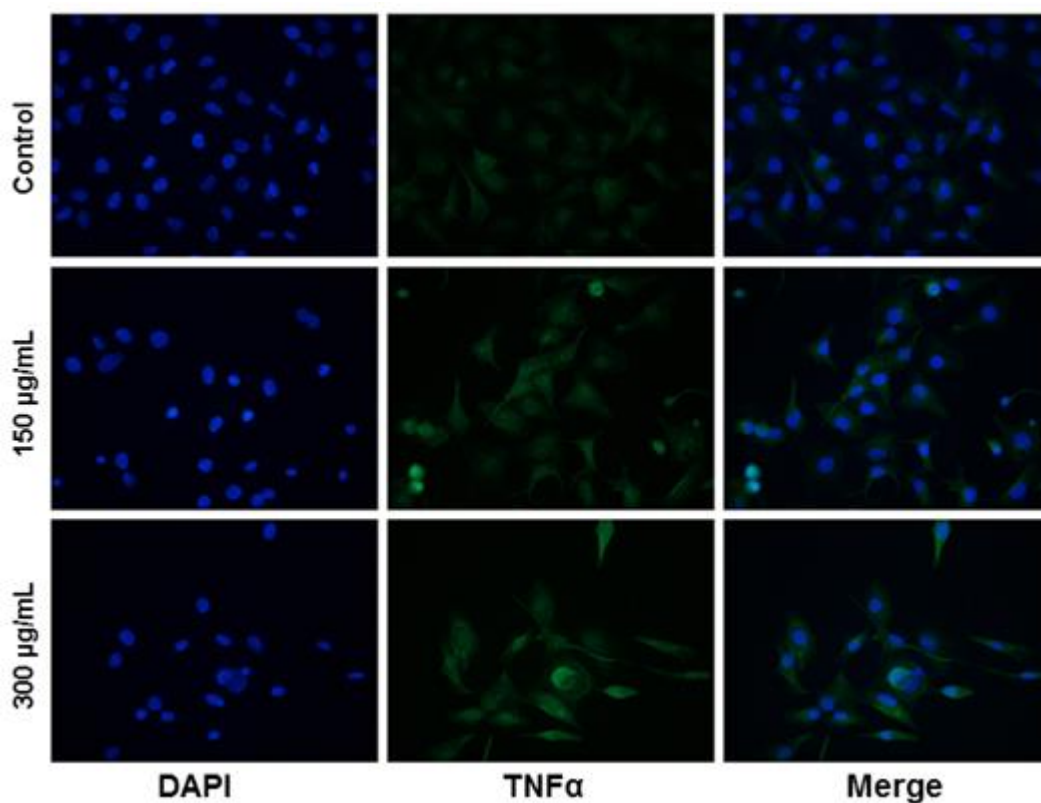


Figure 41. Immunofluorescence Staining for TNF- $\alpha$  in OME Treated MDA-MB- 231 Cells.

### **3.16 *O. majorana* Lead to Depletion of Mutant p53 in MDA-MB-231 and Upregulation of p21<sup>WAF1/CIP1</sup>**

Next, we tested the effect of OME on the expression of the tumor suppressor p53 in MDA-MB-231. Toward this aim, cells were treated with various concentrations of OME and the protein level of the mutant p53 was determined. We found that low concentrations of 150 and 300  $\mu\text{g}/\text{mL}$  of OME led to a slight increase in the protein level of mutant p53 (fig. 42, upper panel). Most importantly, Western blotting analysis revealed apoptotic concentrations (450 and 600  $\mu\text{g}/\text{mL}$  of OME) lead to almost complete depletion of mutant p53 in MDA-MB-231 cells. This result is a potentially important finding because of the role of mutant p53 protein in human cancers. Because mutant p53 renders cancer cells more resistant

to anti-cancer drugs, abolishing mutant p53 may therefore offer a promising approach for cancer prevention and therapy.

Because p21 protein has been reported to inhibit growth and apoptosis, we investigated whether the growth inhibition mediated by low concentrations (150 and 300  $\mu\text{g}/\text{mL}$  of OME) was also associated with an induction of p21. Western blotting showed an upregulation of p21 protein with at least 2.5 fold increases in cells treated with low concentrations of OME, while little or no effect on p21 expression was observed with higher concentrations of OME (fig. 42, lower panel). Based on that, we can postulate that p21 upregulation contributes, at least partially, to the cell cycle arrest observed with lower concentrations, while it has little or no role in cell death occurring at higher concentrations of OME.

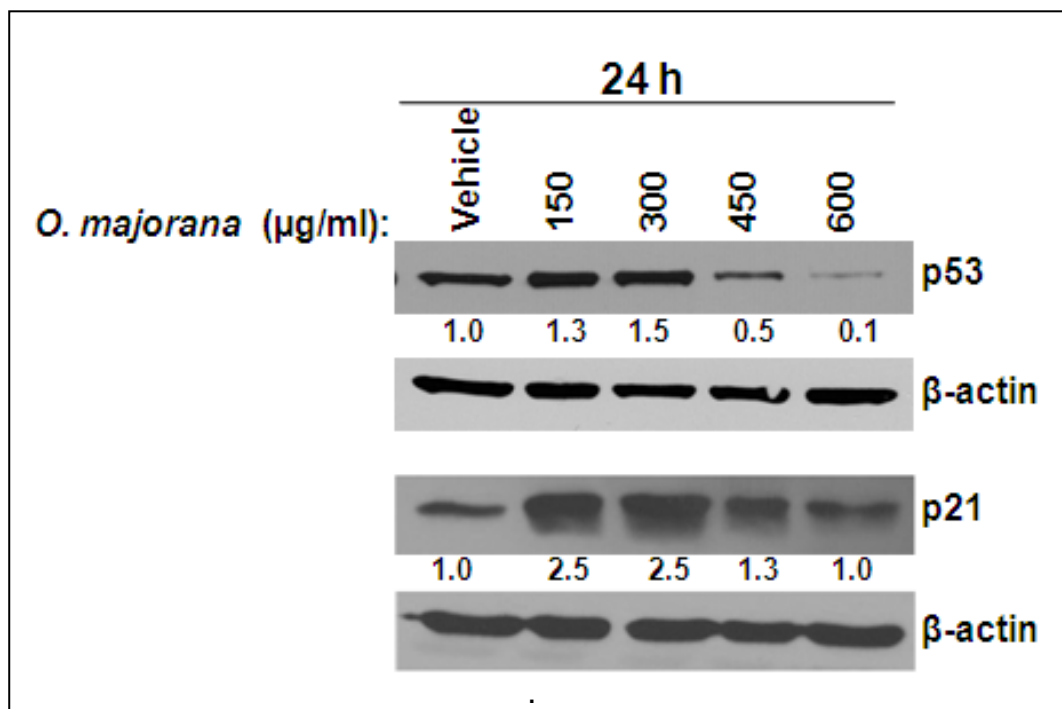


Figure 42. Western Blot Analysis Showing Expression Levels of Mutant p53 and p21 in *O. majorana* Treated MDA-MB-231 Cells.

### 3.17 *O. majorana* Extract Induced Hyperacetylation of Histone H3 and H4 in the MDA-MB 231 Cells

Previously, expression of p21 and increased histone hyperacetylation has been linked to apoptosis and to growth arrest. Therefore, we examined the acetylation profile of histone H3 and H4 in MDA-MB-231 in response to treatment for 24 hours to increasing concentrations of OME. As shown in figure 43, the time course analysis showed a gradual increase in acetylated histones, H3 and H4. A marked overall increase in the acetylation status of Histone H3 and H4 was also detected by immunofluorescence staining (fig 44). Altogether, these results showed that OME induced hyperacetylation of Histone H3 and H4.

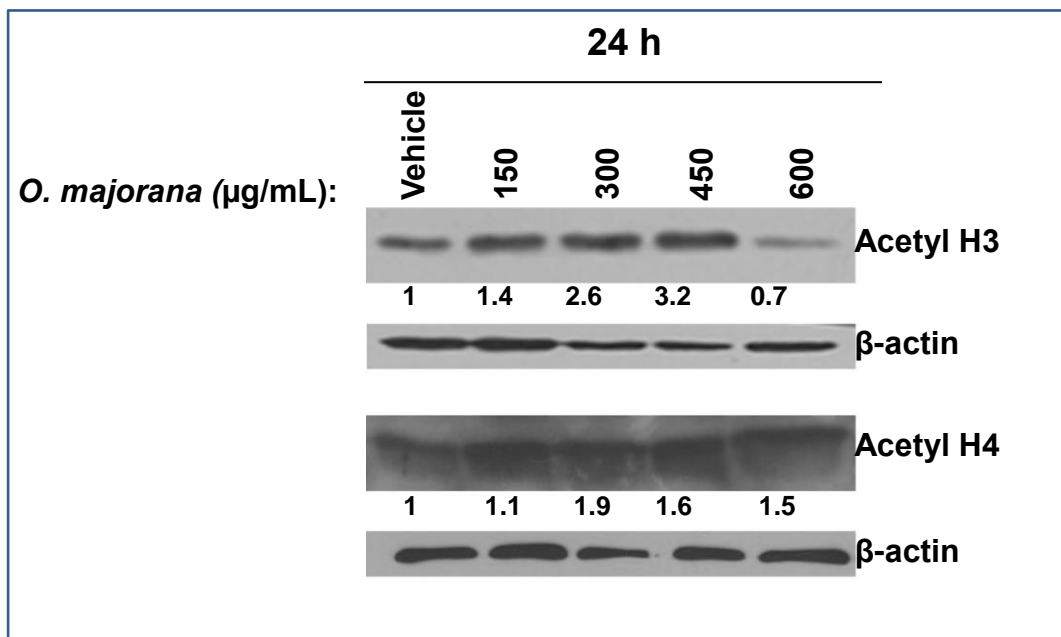


Figure 43. Western Blot Analysis Showing Protein Levels of Ac-H3 and Ac-H4, Extracted from OME Treated Cells. β-actin was used as loading control.

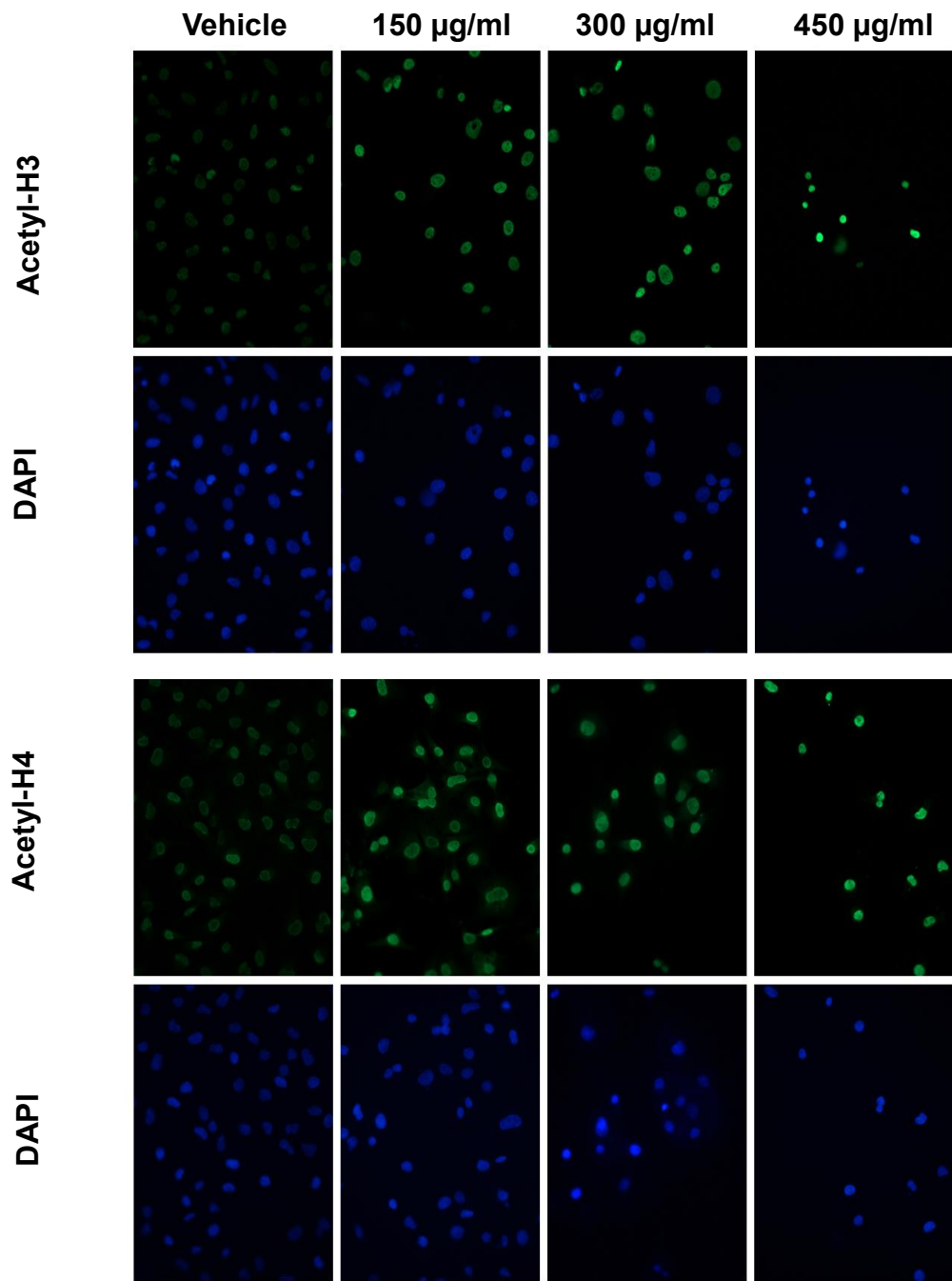


Figure 44. Immunofluorescence Staining of Ac-H3 and Ac-H4 in MDA-MB231 Cells Treated with OME for 24 Hours. DAPI was used as a nuclear stain.

### **3.18 *O. majorana* Induced Activation of $\gamma$ H2AX, a Marker of Double Strand Breaks, in MDA-MB-231 Cells**

We sought to investigate whether OME induced DNA damage in MDA-MB-231 cells. For this purpose, MDA-MB 231 cells were cultured for 6 and 24 hours in a complete media containing either ethanol (control) or increasing concentrations of OME (75, 150, 300, 450 and 600  $\mu$ g/mL). DNA damage was determined by measuring the levels of phosphorylated H2AX ( $\gamma$ H2AX) after 6 and 24 hours of treatment of the MDA-MB-231 cells with OME. Western blot analysis revealed a time-and a concentration-dependent increase in the levels of  $\gamma$ H2AX in response to OME treatment (fig 45), indicating an accumulation of double strand breaks in these cells. The increase in DNA damage was also assessed by immunofluorescence staining of  $\gamma$ H2AX in cells treated with 150, 300 and 450  $\mu$ g/mL OME for 24 hours. Figure 47 clearly shows a concentration-dependent increase of  $\gamma$ H2AX foci in response to OME. Since the activation of  $\gamma$ H2AX occurred as early as 6 hours, a time in which no cell death or Caspase 3/7 activation was observed (fig. 46), this rules out the possibility that the resulting DNA damage is a consequence of DNA fragmentation resulting from caspases' activities and further confirms the potential of this OME extract to induce double strand DNA breaks in a concentration-dependent manner.

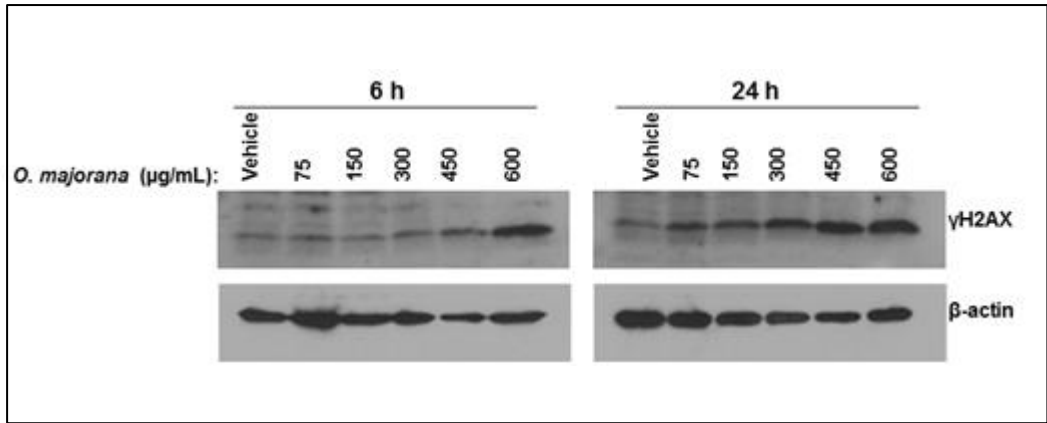


Figure 45. Western Blot Analysis of Phosphor-H2AX (Ser 139) in MDA-MB231 Cells Exposed to OME.

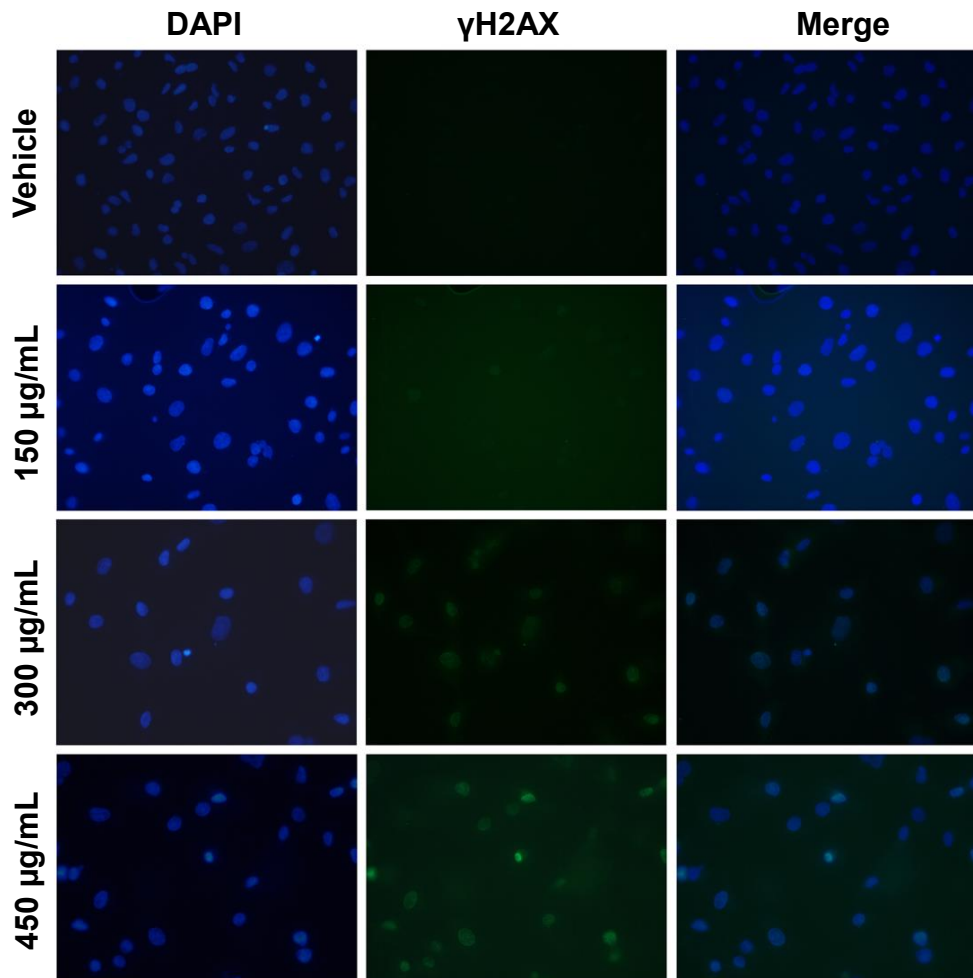


Figure 46. Immunofluorescence Staining for γH2AX in OME Treated MDA-MB 231 Cells.

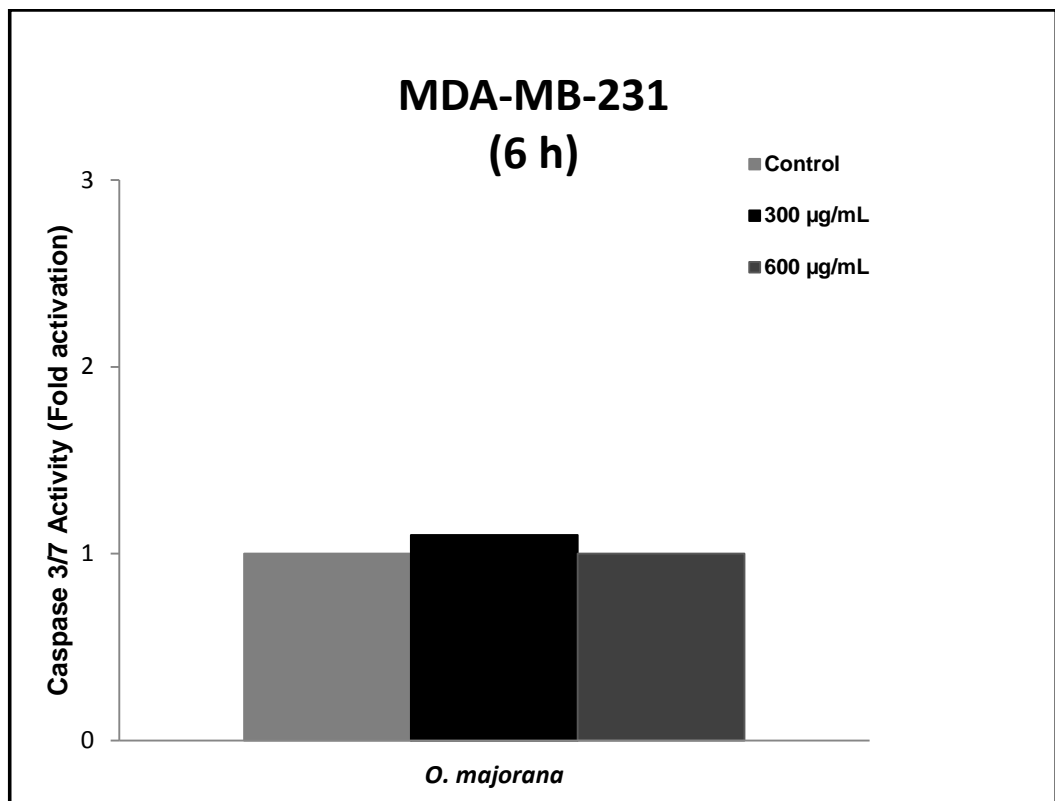
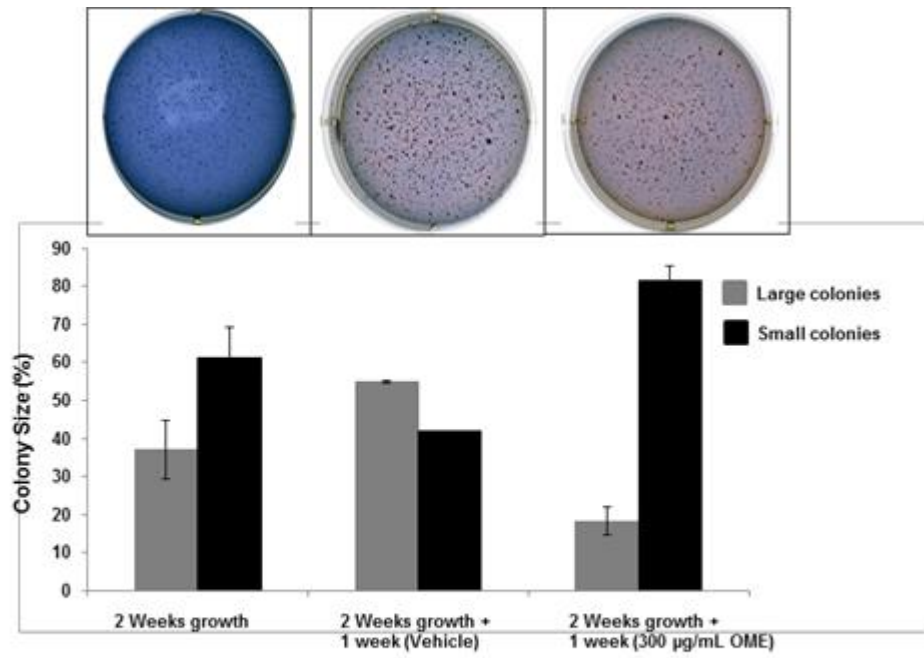


Figure 47. Caspase 3/7 Activation in OME Treated MDA-MB-231 Cells After 6 Hours.

### **3.19 *O. majorana* Inhibited Colony Growth of MDA-MB-231**

To further confirm the inhibitory potential of *O. majorana* on MDA-MB 231 cells, we sought to determine if OME could inhibit the further growth of already formed MDA-MB-231 colonies. For this purpose, MDA-MB-231 cells were first allowed to grow and form visible colonies in the absence of treatment. After 14 days of growth, colonies were incubated with ethanol as a control, and with OME, and allowed to grow for one more week. Figure 48 shows that the size of the ethanol-treated (control) colonies kept growing compared to the size of the two week colonies; more large colonies were obtained in the three week plate, while fewer small colonies were counted, indicating that small colonies became larger in size. Interestingly, OM treated colonies showed regression in colony size compared to the two week colonies. In OM-treated plates, the number of large size colonies counted was fewer than that obtained in the two week plate, while the number of small colonies was significantly greater, suggesting size regression in the large colony induced by OME. This result along with the viability and flow cytometry data confirm the anti-cancer effect of OME on triple negative mutant p53 MDA-MB-231 breast cancer cells.



	2 weeks	3 weeks (vehicle)	3 weeks (300 µg/mL OME)
% Large size colonies	38 ± 7.65	58 ± 0.3	18.2 ± 3.65
% Small size colonies	61.3 ± 7.85	41.8 ± 0.1	81.5 ± 3.77

Figure 48. Inhibition of Colony Growth by *O. majorana* Extract.

### **3.20 *O. majorana* Attenuated the Migration Ability of the MDA-MB-231 Breast Cancer Cells**

As cell migration plays a crucial role in tumor metastasis, we sought to investigate whether OME affects the migration behavior of MDA-MB-231 cells. We first measured the migration ability of these cells by using a wound-healing migration assay. For this purpose, we performed the test with concentrations of OME and periods of treatment that were previously shown to be non-cytotoxic to the MDA-MB-231. As shown in figure 49, OME treatment significantly inhibited wound healing cellular migration of MDA-MB-231 cells in a concentration-dependent manner. The ability of OME to inhibit the migration of MDA-MB-231 cells was also measured by using the Boyden Chamber Transwell Assay. For this purpose, MDA-MB-231 cells were seeded in the upper wells with or without 300 µg/mL OME. As shown in Figure 51 and 52, the number of OME-treated cells that migrated to the lower chamber, after 6 hours of treatment, was significantly reduced approximately three fold compared to the number of control cells. Cell viability of the OME-treated cells at the concentrations and time tested was not affected (fig. 50) thus confirming that the inhibitory effect on the MDA-MB-231 cells motility was not due to the cytotoxic effect of OME. Taken together this confirms the inhibitory effect of OME on the migration potential of MDA-MB-231 cells.

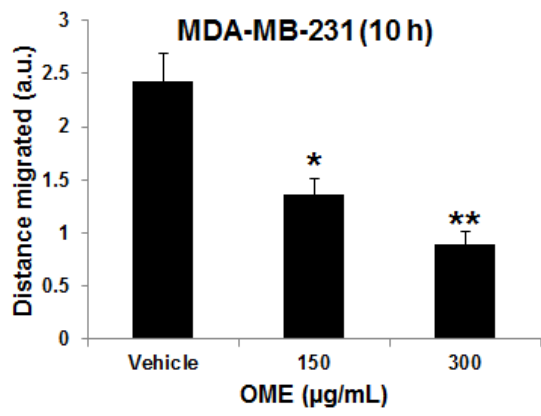
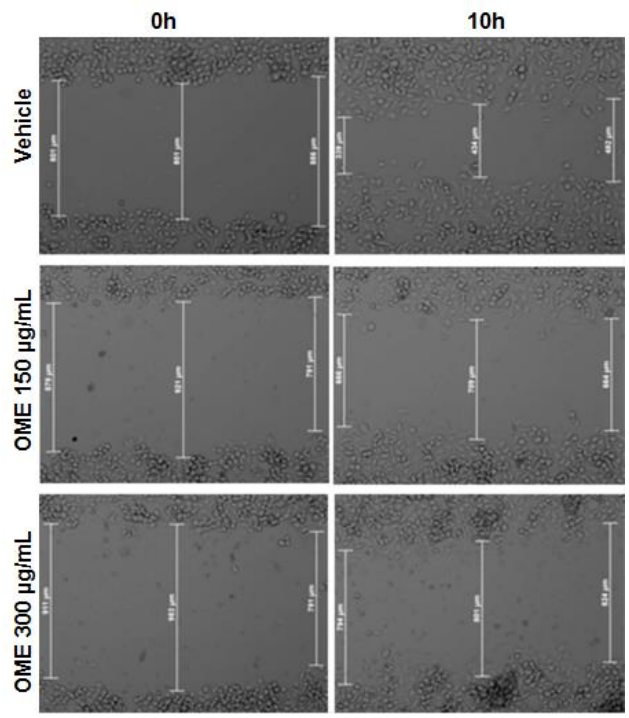


Figure 49. Wound Healing Assay Showing that OME Inhibited the Migration of MDA-MB-231 Breast Cancer Cells in Dose-Dependent Manner.

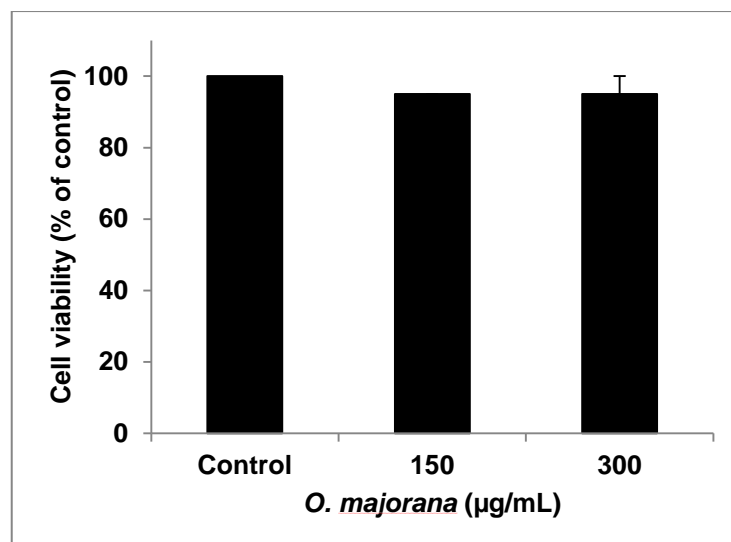


Figure 50. Cell Viability After Incubation of MDA-MB-231 Cells with OME For 10 Hours.

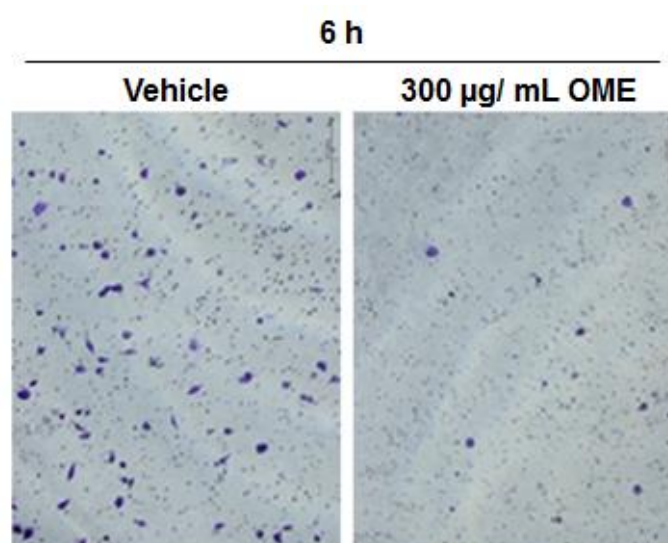


Figure 51. Boyden Chamber Transwell Assay Indicating that OME inhibited the Migration of MDA-MB-231 Cells.

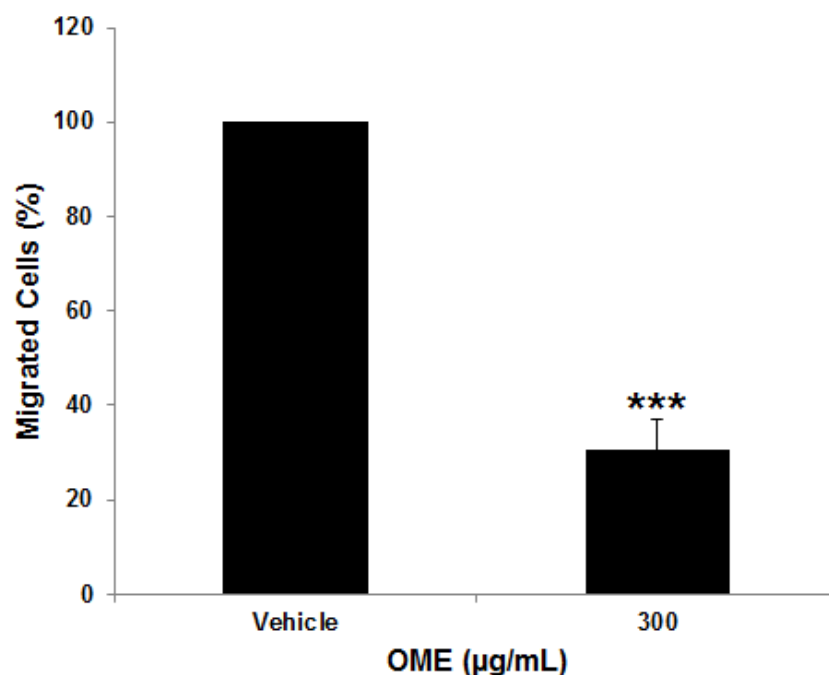


Figure 52. Quantification of Migrated MDA-MB-231 Cells.

### 3.21 *O. majorana* Promoted Cell-Cell Aggregation and Induced E-Cadherin Upregulation in MDA-MB-231 Cells

Lost capacity for homotypic adherence is also associated with cancer cell metastasis. To determine whether OME would affect the cell-cell adherence behavior of MDA-MB 231, cell aggregation assay was conducted on a control and OME-treated cells. We found that OME significantly increased the ability of MDA-MB-231 cells to form cell aggregates visible and as early as 30 minutes post-treatment (fig. 53). It is known that loss of E-cadherin expression promotes tumor progression and metastasis while its overexpression prevents the invasion of tumor cells. We therefore sought to examine the expression of E-cadherin in MDA-MB-231 cells in response to OME exposure. We first examined the protein level of E-cadherin in MDA-MB-231 cells treated with and without

OME. As shown in figure 54, OME induced a significant increase of E-cadherin protein in a concentration-dependent manner. This increase in E-cadherin expression was further confirmed by immunofluorescence staining (fig. 55). The expression of E-cadherin was mostly detected at cells junctions.

Next we determined whether the effect of OME on E-cadherin expression was mediated through transcriptional regulation. Toward this, transcription activity was measured in cells transfected with a Luciferase Reporter gene containing E-cadherin promoter and treated with and without OME. As shown in figure 56, OME induced a concentration-dependent increase in the luciferase activity, thus indicating that OME positively regulates the expression of E-cadherin at the transcriptional level. Taken together, the data clearly show that E-cadherin is upregulated by OME and further suggests that the expression of this protein could account for the inhibition of cellular migration and invasion.

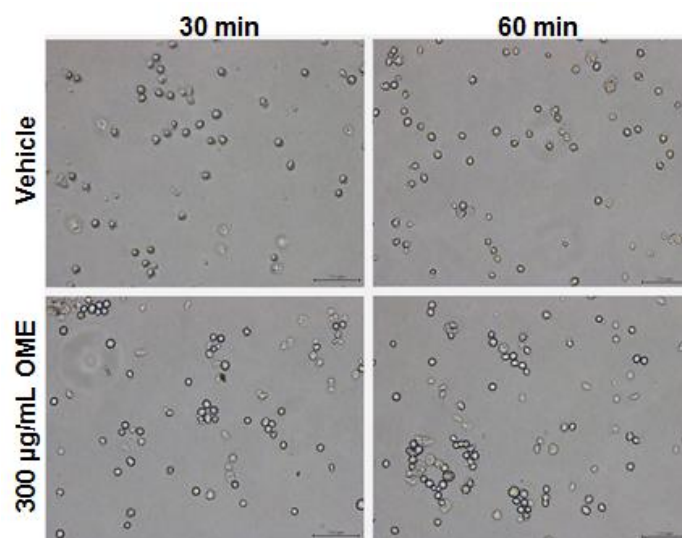


Figure 53. Photograph Under Phase-Contrast Microscope (x100 Magnification) Showing Aggregated Cells After OME Treatment.

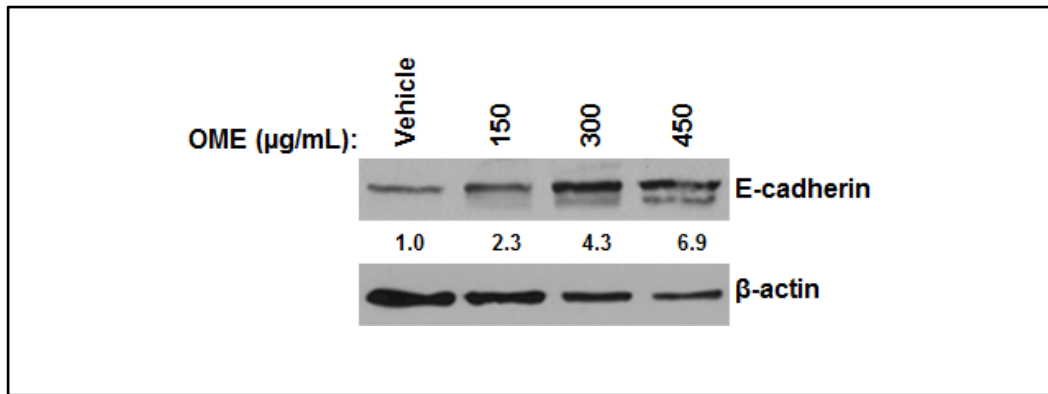


Figure 54. Western Blot Analysis of E-cadherin Expression in OME Treated MD-MB-231 Cells.

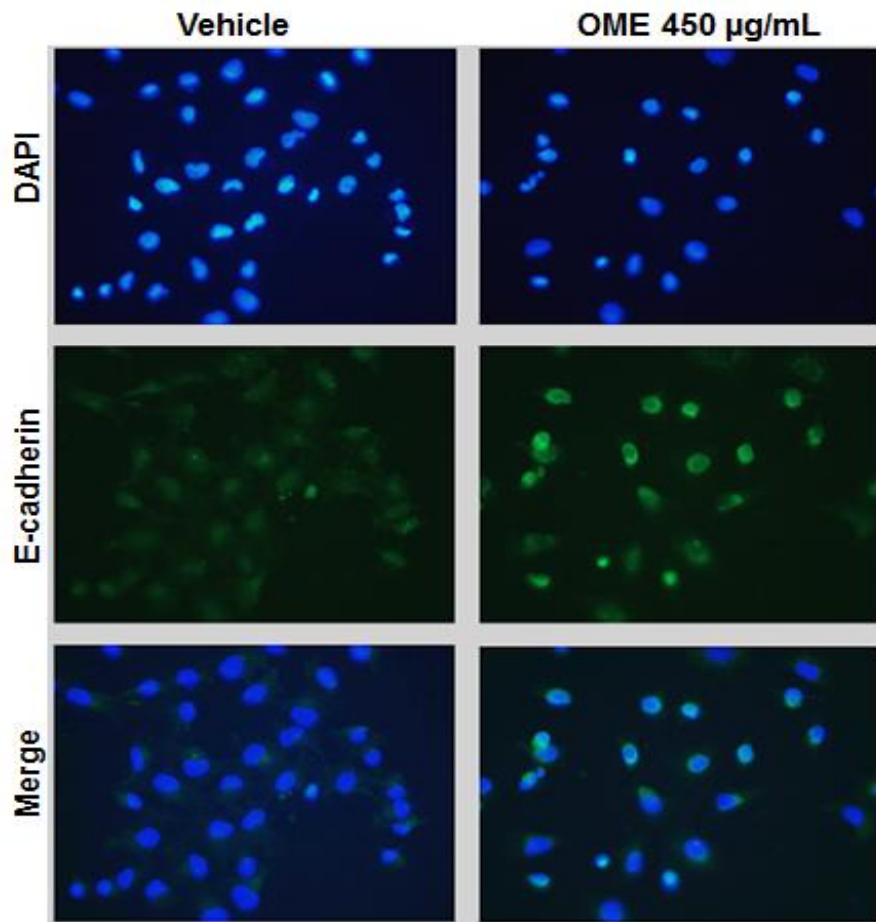


Figure 55. Immunofluorescence Staining for E.cadherin in OME Treated MDA-MB 231Cells. DAPI was used as a nuclear stain.

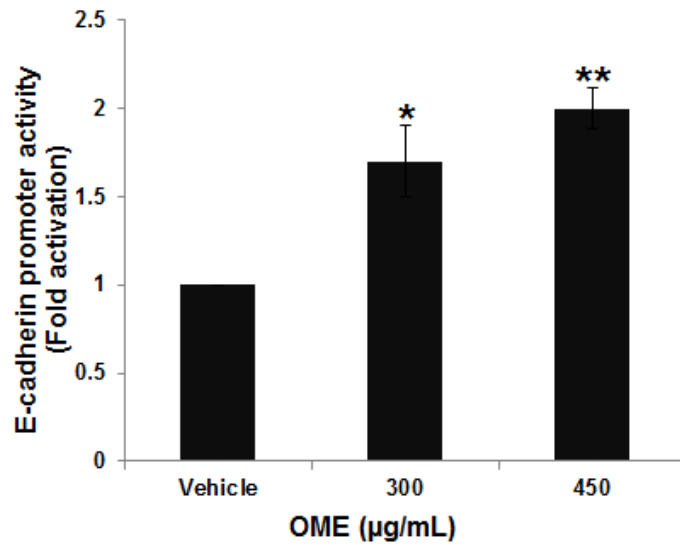


Figure 56. E. cadherin Promoter Activity Following Transfection with A Luciferase Reporter Gene Containing E-cadherin Promoter in MDA-MB-231 Cells.

### 3.22 *O. majorana* Inhibited Invasive Capacity of MDA-MB-231 Cells

Next, we examined the invasive potential of MDA-MB-231 cells in the Matrigel-coated Boyden Chamber in the absence, or presence, of 150 µg/mL OME. The number of OME-treated cells that has passed through the Matrigel coated membrane was markedly reduced by 55% (fig. 57, and 58), indicating that OME can inhibit the invasive ability of the MDA-MB-231 cells.

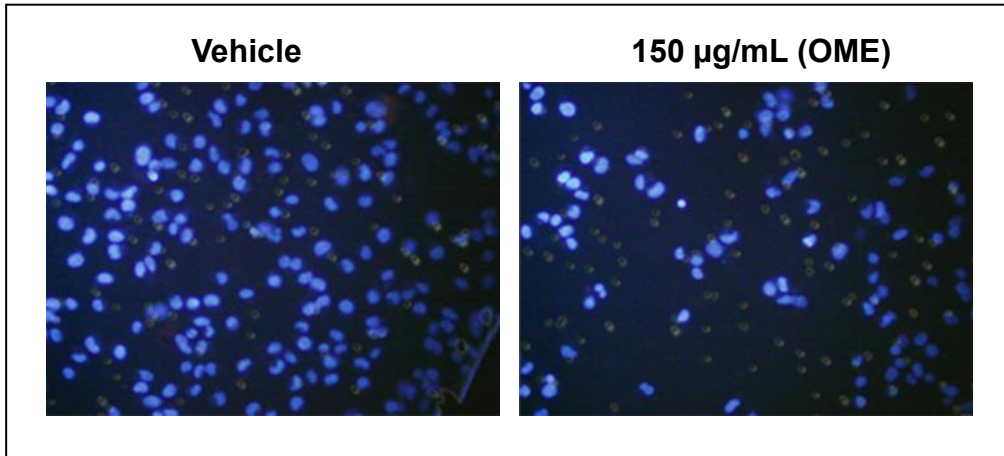


Figure 57. *O. majorana* Inhibited the Invasive Activity of MDA-MB-231 Cells.

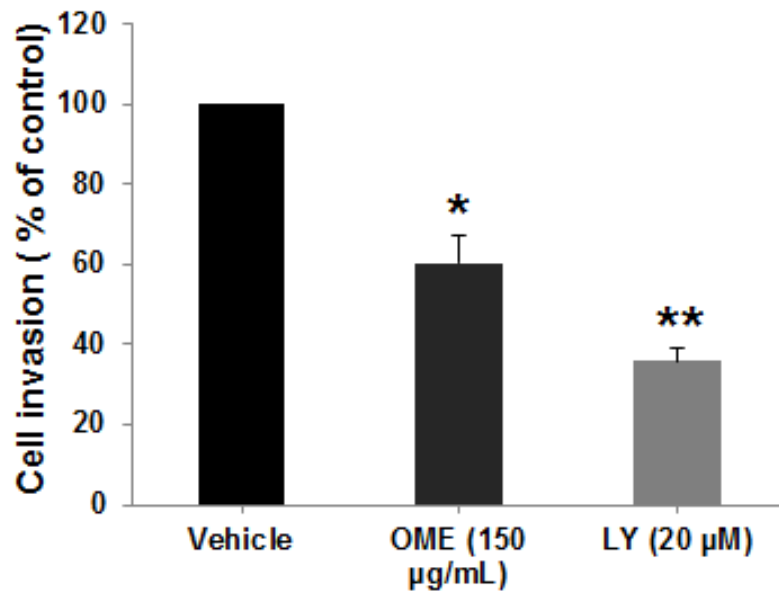


Figure 58. Quantification of Invaded MDA-MB-231 into the Matrigel.

### 3.23 *O. majorana* Suppressed the Expression and the Activity of MMP-2 and MMP-9 and downregulated uPAR in MDA-MB-231 Cells

Matrix metalloproteinases (MMP) -2 and -9, among other MMPs, are known to play an important role in breast cancer cell invasion and metastasis. To test whether *O. majorana* inhibits breast cancer cell invasion by affecting the expression of MMP-2 and MMP-9, we decided to examine the expression levels of MMP-2 and MMP-9 proteins in a conditioned medium using OME-treated MDA-MB-231 cells. The protein level of MMP-2 and MMP-9 (fig. 59) were found to be significantly reduced in response to OME treatment. RT-PCR analysis also revealed that the MMP-2 and MMP-9 mRNA level was reduced in MDA-MB-231 cells upon treatment with OME (fig. 60) indicating that OME can inhibit the transcription of MMP-2 and MMP-9 genes in these cells.

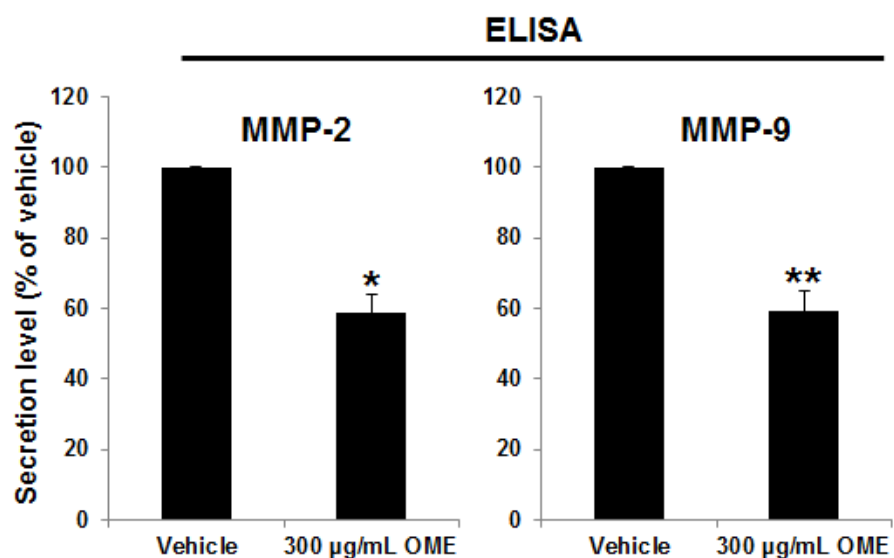


Figure 59. Effects of OME on the Secretions of MMP-2 and MMP-9 in the Collected Conditioned Medium of OME Treated MDA-MB-231 Cells.

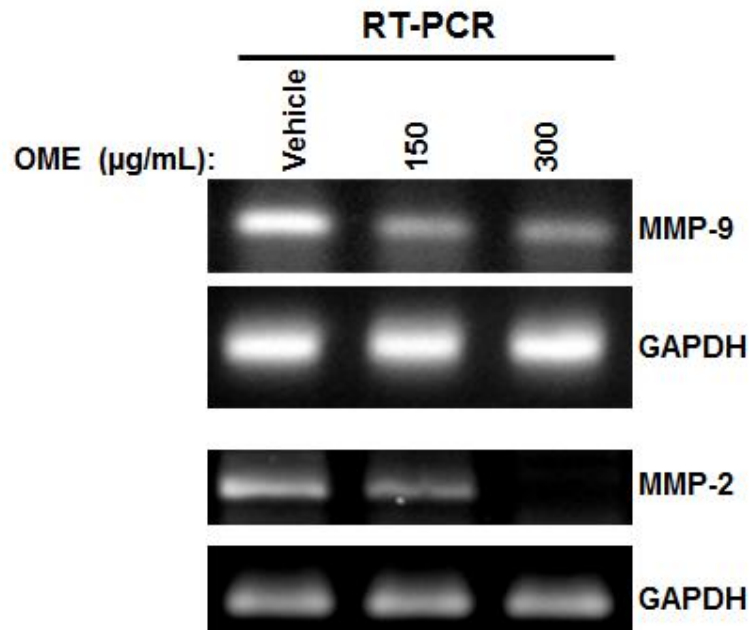


Figure 60. RT-PCR Analysis of the mRNA Levels of MMP-2 and MMP-9 in MDA-MB-231 Cells Treated with OME for 24 Hours. GAPDH was used as an internal control.

Then, we decided to examine the effect of OME on the activity of MMP-2 and MMP-9. MDA-MB-231 cells were treated with 150 and 300 µg/mL OME for 24 hours in serum free DMEM, the media was collected, concentrated and tested for MMP2 and MMP-9 activity by using gelatin zymography. As shown in figure 61, MMP-2 and MMP-9 activities were significantly reduced in response to OME treatment. Altogether, our results showed that OME significantly inhibits both, the expression and the activities of MMP-2 and MMP-9.

The Urokinase Plasminogen Activator (uPA) and its receptor (uPAR) were also shown to play a crucial role in breast cancer cell invasion and metastasis. Therefore, we examined whether OME also alters the expression of uPAR. Western blot analysis clearly shows that

the expression level of uPAR decreased markedly in OME-treated MDA-MB-231 cells (fig. 62).

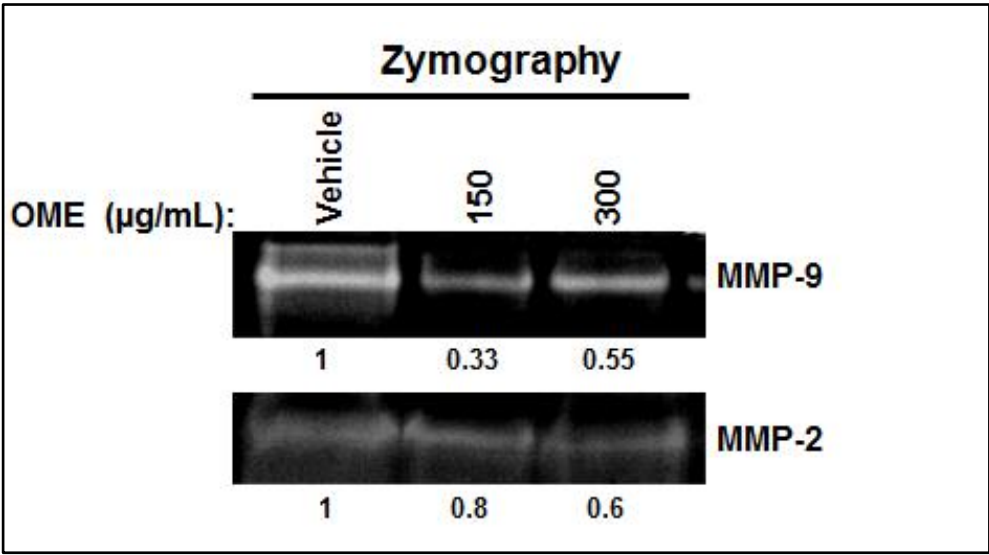


Figure 61. Activities of MMP-2 and MMP-9 in OME Treated MDA-MB 231 Cells.

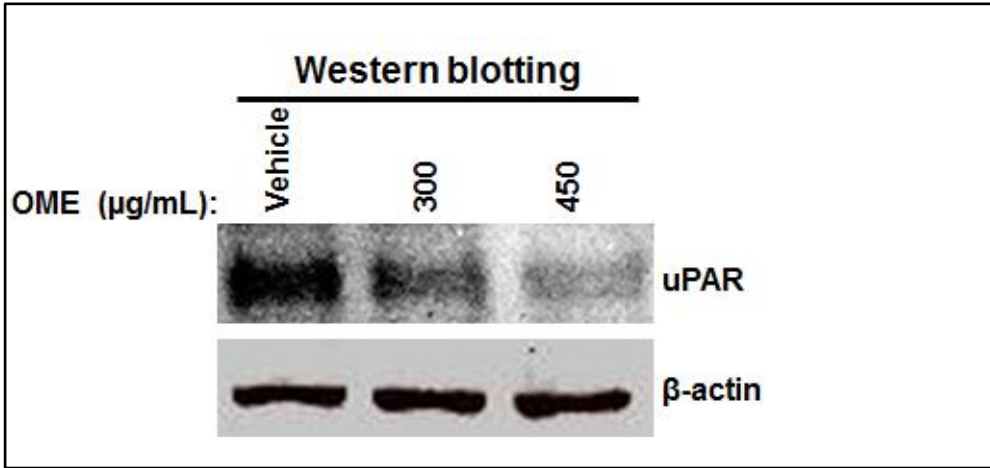


Figure 62. Western Blot Analysis of uPAR Expression in OME Treated MD-MB-231 Cells. β-actin is used as loading control.

### **3.24 *O. majorana* Decreased Adhesion of MDA-MB-231 to HUVEC and downregulated the Expression of ICAM-1 in Breast Cancer Cells**

The attachment of tumor cells to endothelial blood vessels is also a crucial event in the process of metastasis. The effect of OME on MDA-MB-231 cell adhesion to TNF- $\alpha$  stimulated HUVECs was then investigated by co-incubating both cell types for 1 hour with, and without various concentrations of OME. Figure 24A shows that OME significantly inhibited the adhesion of MDA-MB-231 cells to HUVECs in a concentration-dependent manner.

Also, because the intercellular adhesion molecule (ICAM)-1, has been shown to play an important role in the adhesion of cancer cells to endothelial cells and therefore in metastasis, we sought to examine whether OME affects the expression of this adhesion molecule in MDA-MB-231 cells. Toward this aim, cells were treated with various concentrations of OME and the protein level of the ICAM-1 was determined by Western blotting. As it is shown in figure 64, the level of ICAM-1 protein decreased in a concentration-dependent manner in OME-treated MDA-MB-231 cells. Taken together, our results suggest that OME exerts an inhibitory effect on the adhesion of MDA-MB-231 cells to HUVEC and that this effect is associated with downregulation of ICAM-1 protein.

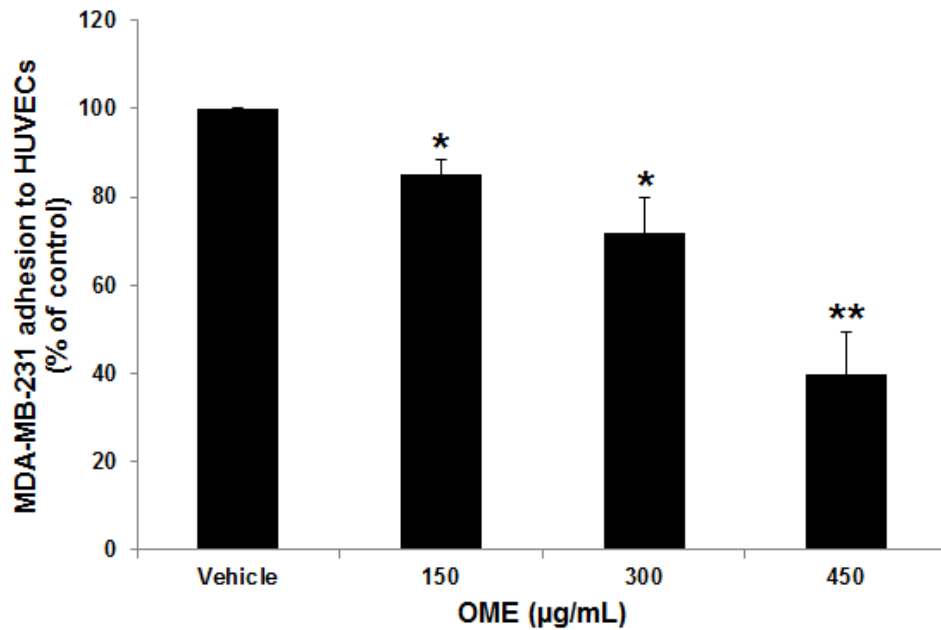


Figure 63. Inhibition of Adhesion of MDA-MB-231 Cells to HUVEC by *O. majorana*.

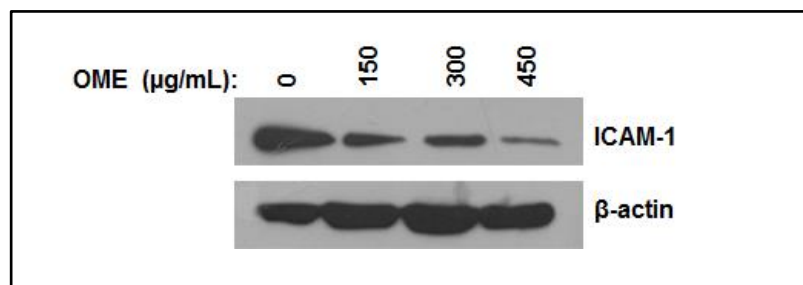


Figure 64. Western Blot Analysis of ICAM-1 Expression in OME Treated MD-MB-231 Cells. β-actin is used as loading control.

### 3.25 *O. majorana* Inhibited Transendothelial Migration of MDA-MB-231 Through TNF-α-Stimulated HUVECs

Since the migration of tumor cells through the vascular endothelium is another crucial event in the metastasis process, we used the Transendothelial Migration Assay to investigate the effect of OME on the ability of MDA-MB-231 cells to migrate across a monolayer of endothelial (HUVEC) cells. As seen in figure 65, the transendothelial migration of

OME treatment through the monolayer of HUVEC was significantly reduced by the treatment with OME in a concentration-dependent manner.

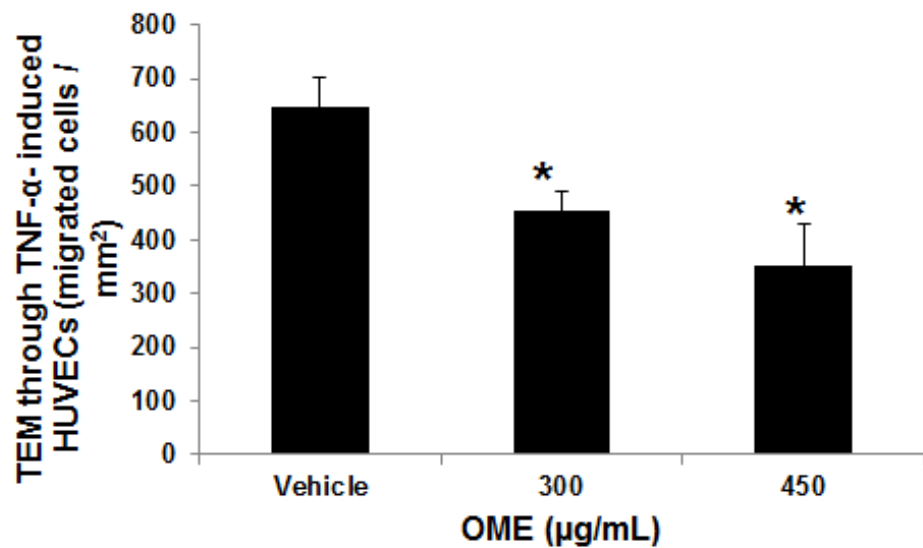


Figure 65. *O. majorana* Inhibited Migration of MDA-MB-231 Cells A cross Monolayer of TNF-  $\alpha$  Activated HUVECs.

### 3.26 *O. majorana* Suppressed VEGF Production in HUVECs and MDA-MB-231 Cells

Tumor growth and metastasis critically depend on angiogenesis. VEGF, a pro-angiogenic growth factor, has been shown to play an important role in this process. Thus, we investigated the effect of OME on the production of VEGF by both the MDA-MB-231 and endothelial cells (HUVEC) with, and without, the presence of TNF- $\alpha$ . We first examined the effect of OME on basal expression levels of VEGF in MDA-MB-231 cells. Cells were grown with various concentrations of OME, the conditioned medium was collected and the level of VEGF measured by ELISA. Data shown in Figure 66 revealed that treatment with 300 and 450  $\mu$ g/mL OME for 24 hours markedly reduced the secretion of VEGF by MDA-MB-231

cells. VEGF levels dropped from 1300 pg/mL in the control to 800 and 400 pg/mL respectively. To further confirm the inhibition of VEGF production in breast cancer cells, we measured the level of VEGF in MDA-MB-231 cells that were first treated with various concentration of OME and then stimulated with TNF- $\alpha$ . As shown in figure 67, the production of VEGF was enhanced in TNF- $\alpha$  - stimulated (2600 pg/mL) compared to vehicle-treated (1500 pg/mL) MDA-MB-231 cells. However, VEGF production was significantly reduced in a concentration-dependent manner by OME (fig. 67). Next, we examined VEGF production in HUVECs. As expected, a HUVEC cultured in the absence of TNF- $\alpha$  produced low level of VEGF (20 pg/mL), while in the presence of TNF- $\alpha$ , VEGF production increased to approximately 120 pg/mL (fig. 68). Exposure of HUVEC to OME also led to a concentration-dependent suppression of VEGF production (fig. 68).

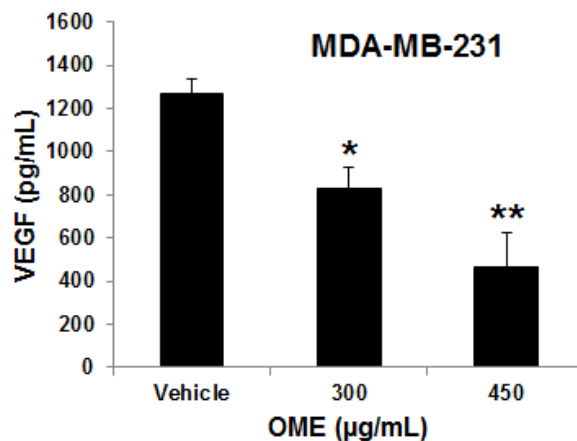


Figure 66. Quantification of Basal Level of VEGF Secretion in Conditioned Medium from Vehicle or OME Treated MDA-MB-231 Cells.

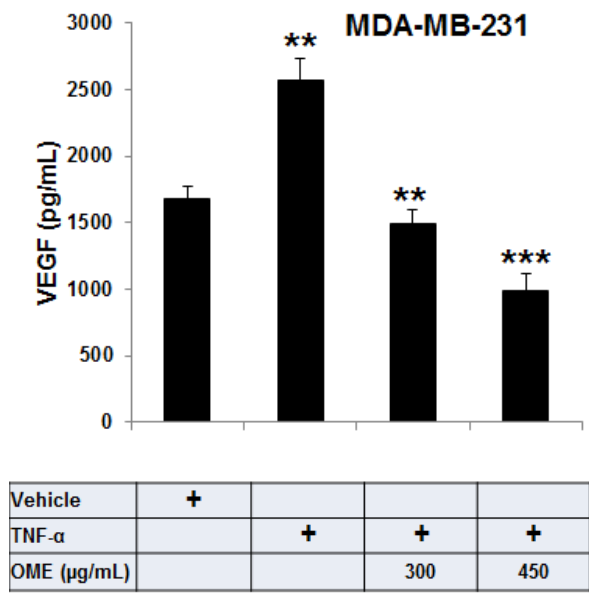


Figure 67. Quantification of VEGF Secretion in TNF- $\alpha$  Induced MDA-MB-231 Cells Cultured in Presence of Vehicle or Indicated Concentrations of OME.

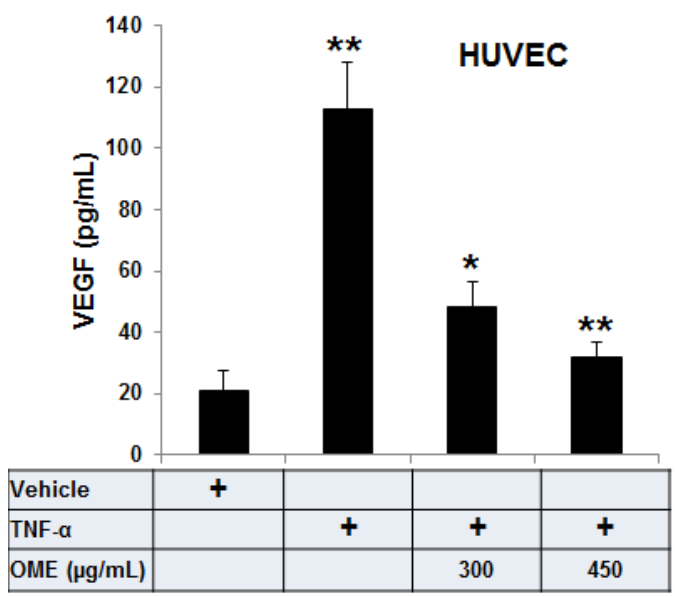


Figure 68. Quantification of VEGF Secretion in TNF- $\alpha$  Induced HUVECs Cultured in Presence of Vehicle or Indicated Concentrations of OME.

### 3.27 *O. majorana* Inhibited Phosphorylation of I $\kappa$ B; Downregulated Nuclear Level of NF $\kappa$ B

The NF $\kappa$ B signaling pathway is known to regulate the expression of various genes involved in tumor cell invasion. To investigate the effect of OME on the activation of the NF $\kappa$ B signaling pathway, we first examined, by Western blotting, the phosphorylation status of I $\kappa$ B in OME-treated MDA-MB-231 cells. We found that OME drastically inhibited the phosphorylation of I $\kappa$ B (fig. 69). Moreover, we found that OME reduced the level of nuclear NF $\kappa$ B remarkably (fig. 70). Taken together, the data clearly indicates the OME exerts its effect at least partly through an inhibition of the NF $\kappa$ B signaling pathway.

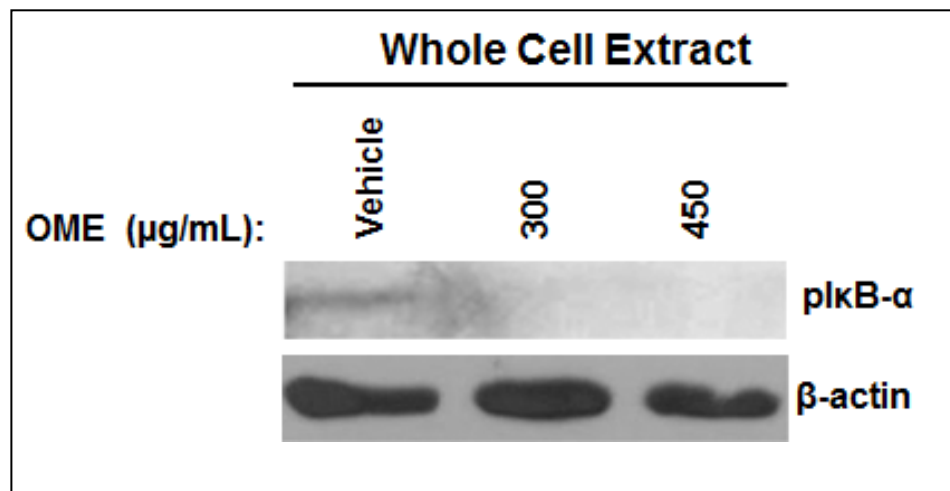


Figure 69. Western Blot Analysis of the Phosphorylation Status of I $\kappa$ B $\alpha$ .

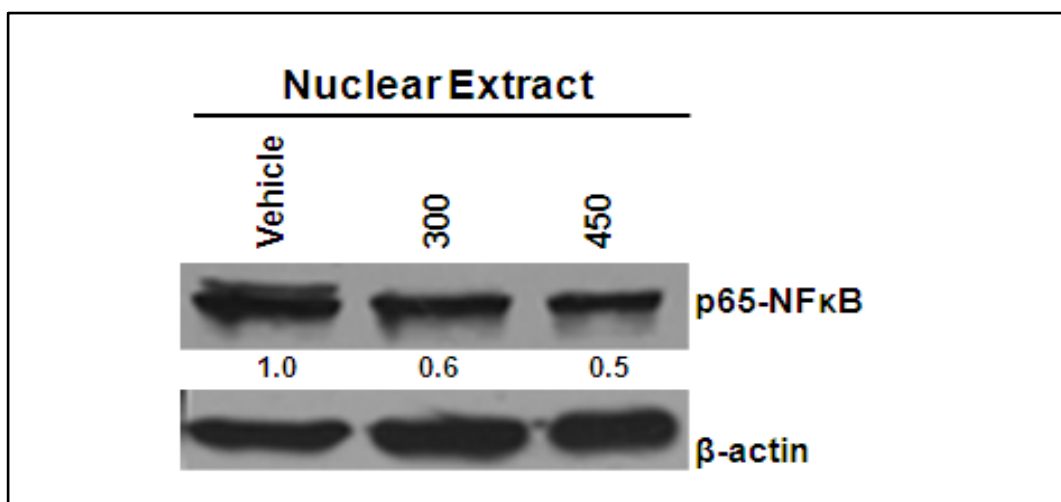


Figure 70. Western Blot Analysis of the Nuclear p65 (NFκB). β-actin (loading control) proteins.

### 3.28 *O. majorana* Reduced Nitric Oxide (NO) production in MDA-MB-231 Cells

Nitric oxide (NO) signaling has also been shown to promote breast tumor growth and metastasis by altering the expression of genes implicated in cellular migration, invasion and angiogenesis [164-166]. To test whether OME could affect the level of NO, the amount of nitrate/nitrite production was determined by ELISA in vehicle and OME-treated MDA-MB-231 cells. Results shown in figure 71 clearly show that OME decreased NO production in a concentration-dependent manner in MDA-MB-231 cells, thus suggesting that OME could also exert its anti-metastatic effect by modulating the level of NO in breast cancer cells.

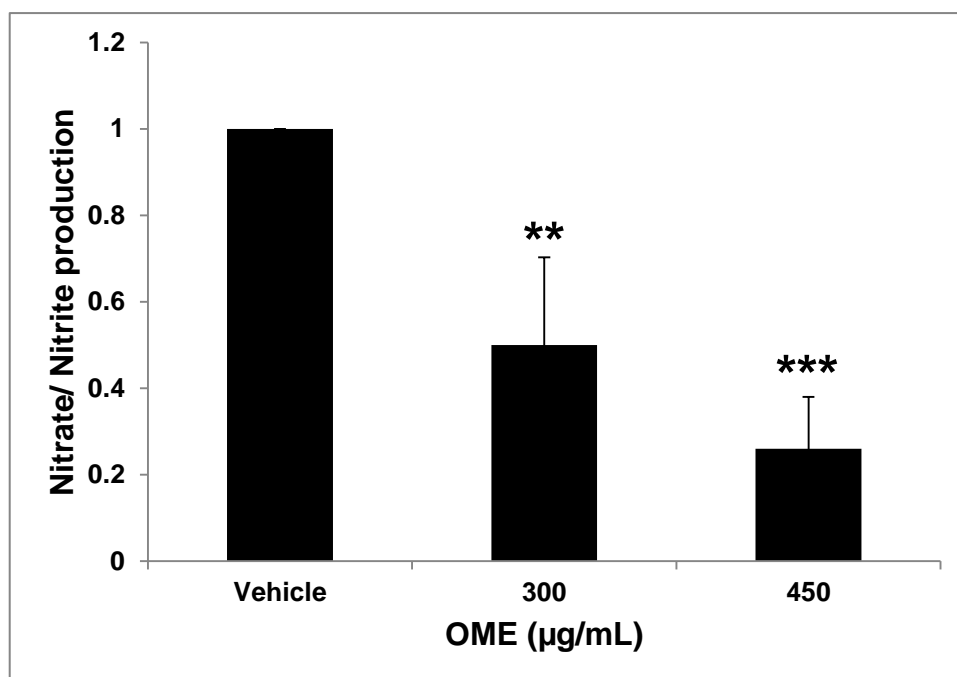


Figure 71. Quantification of NO Levels in OME Treated MDA-MB-231 Cells.

### 3.29 *O. majorana* Inhibited Tumor Growth and Metastasis in Chick Embryo Tumor Growth and Metastasis Assay

To further confirm the *in vitro* anti-breast cancer activities of *O. majorana*, we decided to investigate its effect on tumor growth *in vivo* by using the chick embryo model. MDA-MB-231 cells were grafted on the chorioallantoic membrane (CAM) and formed tumors were treated every 48 hours with vehicle, colchicine (2 μM) or increased concentrations of OME (300 and 450 μg/mL). At E19, tumors were recovered from the upper CAM and weighed. As it is shown in figure 72 and 73, OME significantly inhibited tumor growth compared with the control treatment. In fact, concentrations of 300 and 450 μg/mL OME led to reduced tumor growth by 55 and 60% respectively. A similar effect (65% inhibition) was obtained with 2 μM colchicine. Toxicity was evaluated by comparing the

number of dead embryos in OME-treated and control (vehicle-and colchicine-treated) embryos. We found that OME showed no toxicity to the embryo (data not shown).

We next assessed for the ability of OME to inhibit metastasis by counting the number of nodules in the lower CAM in vehicle, colchicine and OME treated tumors. An average of 6.6 nodules were counted in the lower CAM of vehicle-treated chick embryo, while an average of only 1.1 nodules were counted in 300 and 450  $\mu\text{g}/\text{mL}$  OME-treated embryos (fig. 74). The data clearly demonstrates that OME could efficiently inhibit breast tumor growth and metastasis *in vivo*.

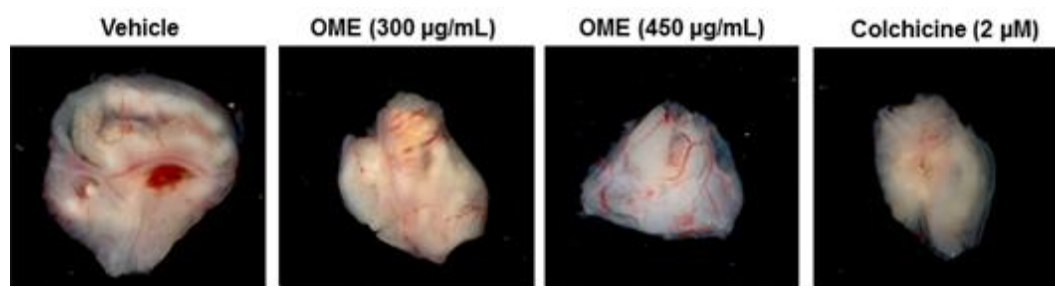


Figure 72. Anti-tumor Growth of *O. majorana* on Breast Tumor in a Chick Embryo Chorioallantoic Membrane Model System.

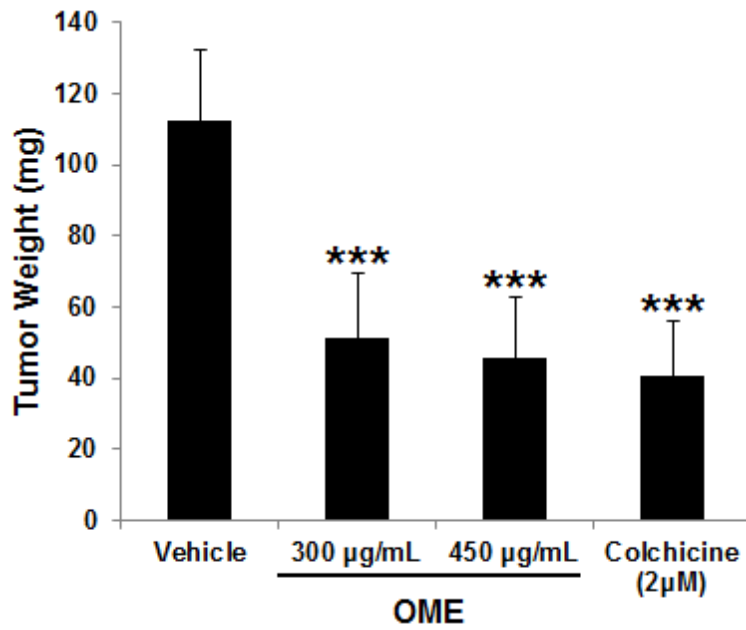


Figure 73. Quantification of Tumor Weight in Vehicle, Colchicine and Indicated Concentrations of OME Treated Chick Embryo.

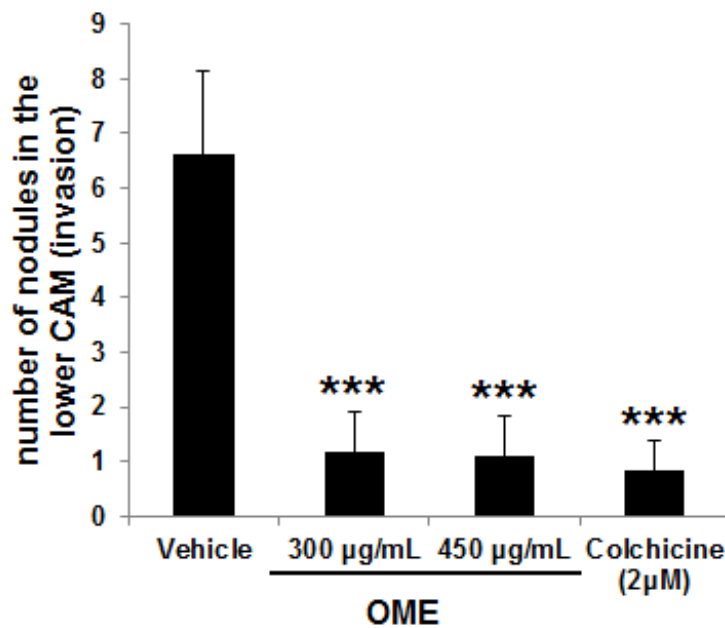


Figure 74. Anti-Metastatic Effect of *O. majorana*. Quantification of Nodules Observed in the Lower CAM of Chick Embryo Treated with Vehicle, Colchicine or OME.

## DISCUSSION

Common cancer treatment drugs aim at inhibiting cell cycle progression and at inducing cell death and apoptosis. Cancer chemoprevention through these two events (cell cycle arrest and apoptosis) has been reported for several natural compounds [21, 167-70].

In the present study, we have shown that extract of an ethanolic fraction of *Origanum majorana* inhibited the proliferation of mutant p53 triple negative breast cancer (TNBC) cell line, MDA-MB-231. We have also demonstrated that OME induces a differential concentration-dependent effect on these cells. OME induces a cell cycle arrest at the G2/M phase and more precisely a mitotic arrest at low concentrations. This finding is supported by a body of evidence: (i) an increase in the level of p(ser10)H3, a mitotic marker, and (ii) an increase of cyclin B1 protein level, whose upregulation was reported in several mitotically arrested cells. We have also shown that cell cycle arrest correlates with an upregulation of the CDK inhibitor p21 and the anti-apoptotic protein, survivin. At high concentrations, however, OME induced a massive apoptosis demonstrated by a dramatic increase in the sub-G1 population. We have demonstrated that OME exerts its apoptotic effect by activating the cell death extrinsic pathway, at least partially, via the activation of TNF- $\alpha$ . We have also shown that OME-induced apoptosis is mediated by an increase in DNA damage, revealed by an upregulation of  $\gamma$ H2AX, severe depletion of the mutant p53 and survivin proteins from the treated cells.

The process of apoptosis can be induced either by the extrinsic pathway which involves signaling from death receptors at the cell surface or by the intrinsic mitochondria-mediated pathway [171]. Activation of the death receptor-mediated apoptosis requires the interaction of ligands such as TNF- $\alpha$  and Fas with their transmembrane receptors [172]. The ligand-receptor interaction leads to the activation of the effector Caspase 8, which in turn activates the effector Caspase 3 directly and/or through mitochondria [173]. The mitochondria-mediated apoptosis pathway is associated with permeabilization of the mitochondria outer membrane, reduced mitochondrial membrane potential ( $\Delta\psi_m$ ), change in expression of the anti-apoptotic Bcl2 family members, such as Bcl2 and Bcl-XL and the pro-apoptotic members such as Bax and Bak lead to the formation of apoptosome, activation of Caspase 9 and consequently activation of caspase 3 [174]. Intrinsic- and extrinsic-pathways activated Caspase 3, cleave PARP, thus resulting in apoptosis [175]. In the present study, we showed that OME induced a TNF- $\alpha$ -mediated extrinsic apoptotic pathway. A TNF- $\alpha$  receptor was activated at 24 hours and induced downstream signaling such as Caspase 8, caspase 3, and PARP cleavage. On the other hand, OME did not induce mitochondria-mediated apoptotic pathway since no change in the BAX/Bcl2 ratio or activation of Caspase 9 were detected. We suggest that OME induces apoptosis solely through a TNF- $\alpha$  activated signal pathway in MDA-MB-231 cells.

Studies have reported that DNA damage is one of the molecular events associated with cell cycle arrest and apoptosis. Indeed, many anti-cancer drugs have been shown to induce DNA damage [176] [177].

Moreover, cancer cells are reported to be more susceptible than normal cells to DNA damaging agents [178], therefore there is a growing interest in dietary phytochemicals that possess DNA-damaging activity. In the present study we showed that OME elicited DNA damage measured by an increase in a concentration-dependent manner of the marker of DNA damage,  $\gamma$ -H2AX, after treatment with OME for 6 or 24 hours. The differential response to the different concentrations of OME (G2/M arrest and/or apoptosis), may be partially mediated by the extent of DNA damage that occurs within the genome. Low levels of DNA damage may trigger recruitment of DNA repair complexes, expression of anti-apoptotic and survival proteins leading to arrested cell cycle until the genotoxic lesions are repaired. In this case, survival proteins such as survivin get activated in order to maintain the viability of G2/M arrested cells. On the other hand, when genomes are overwhelmed by DNA damage, cells are eliminated by apoptosis [179, 180]. In this study, we have found that high concentrations of OME triggered high level of DNA damage to the genome, causing cell to enter apoptosis. Our data suggest that *Origanum majorana* possess a genotoxic effect on MDA-MB-231 cells. At this stage, the mechanism(s) by which OME induces DNA damage remain(s) unknown, and certainly deserves further study.

Inhibitor of apoptosis proteins (IAPs), which includes survivin, represents a family of anti-apoptotic proteins that bind and inactivate active Caspase 3/7 [146, 147] and Caspase 9 [148] and can modulate cell division and cell cycle progression [149].

Interestingly, survivin has no effect on Caspase 8 activity. Survivin has been shown to be highly expressed in most cancers, where it functions as an inhibitor of apoptosis. In breast cancer, overexpressed survivin was shown to protect cells against apoptosis induced by chemotherapeutic agents, such as etoposide [146]. Based on these reports, survivin proteins represents an attractive target of particular importance in cancer therapy at large and in breast cancer therapy in particular. In consideration of the recognized role for survivin as a custodian of cancer cell survival, our results suggest that OME might exert its cytotoxic anti-cancer effects, at least partly via the downregulation of survivin. In our study, we have shown that survivin expression is differentially regulated in a concentration-dependent manner by OME. Lower concentrations of OME induced an upregulation of survivin which causes cells to arrest the cell division and to resist apoptosis by inhibiting the cell death program. In fact, we showed that in these arrested cells, PARP cleavage was not detected despite the activation of Caspase 3/7. This effect might be mediated by the inhibition of active 3/7 by the upregulated survivin. Survivn function could also account for the mitotic arrest induced by OME. In fact, survivin, has also been shown to be required for mitotic arrest of HeLa cells induced by the anti-cancer drug UCN-01 [181].

The tumor suppressor protein, p53 is found to be mutated in about 50% of human cancers [150]. Mutant p53 is reported to play a key role in cancer cells resistance to certain anti-cancer drugs and thus is considered as a potential cancer-specific target for pharmacologic interventions [182], [183]. Studies have shown that inhibition of mutant p53 by RNA

interference sensitizes cancer cell to cell death by chemotherapeutic agents [184]. Wang et al. 2011, showed that the naturally occurring isothiocyanate (ITC) phenethyl isothiocyanate (PEITC), derived from the watercress plant, and the synthetic ITC, 2,2-di phenethyl isothiocyanate selectively deplete mutant, but not the wild-type p53, and induce apoptosis in many cancer cells, including MDA-MB-231 breast cancer cells [185]. Here, we showed that OME led to a dramatic decrease in the mutant p53 level in MDA-MB-231 cells. As such, mutant p53 depletion may be an important target for chemoprevention and therapy by *O. majorana* for TNBC.

Increase in the expression of the cyclin-dependent kinase inhibitor, p21 has been shown to augment G2/M arrest via a p53-independent mechanism in human breast cancer [186]. In most cases, growth arrest was found to be associated with apoptosis. In this study, we showed that low concentrations of OME treatment led to G2/M arrest without significant increase in cell death after 24 hours treatment. Histone hyperacetylation has been demonstrated to be directly linked to the upregulation of p21 and this activation can also occur independently of p53 [187]. Moreover, histone hyperacetylation was also shown to be associated with growth suppression and apoptosis. Our data showed that OME induced histone H3 and H4 hyperacetylation in MDA-MB-231 cells, suggesting that the anti-breast cancer effects of OME were at least partly mediated by Histone H3 and H4 hyperacetylation by regulating the expression of the genes controlling these two events. The mechanism by which OME induces histone hyperacetylation might involve a Histone Deacetylase

Inhibitor (HDI) activity. Interestingly, the plant, *O. majorana*, contains luteolin, a dietary flavonoid with HDI activity [98]. In fact, luteolin was able to decrease the viability of lung, colon, liver and breast cancer cells and induce hyperacetylation of histone H3 and H4 [188]. In light of this, we conclude that the Histone hyperacetylation induced by OME is involved with the HDI activity of luteolin. We are currently undertaking further investigations to better understand the mechanism(s) by which OME induces Histone hyperacetylation.

In conclusion, our data is consistent with the model shown in figure 75 which shows the concentration-dependent differential effect of *O. majorana* extract on mutant p53, triple negative MDA-MB-231 cells. At low concentrations, OME induced a mitotic arrest associated with low level of DNA damage (75, thin arrow), upregulation of the CDK inhibitor p21 and the inhibitor of apoptosis, survivin. We believe that these events along with other yet to be identified events contribute to the cell cycle arrest. In addition we also propose that, at these concentrations, survivin is also implicated in the blockage of the TNF-mediated apoptosis pathway, by directly inhibiting the activity of the active Caspase 3. On the other hand, high concentrations, OME induce massive apoptosis via the activation of the TNF- $\alpha$  extrinsic pathway which is associated with high level of DNA damage (fig. 75, thick arrow) and almost complete depletion of the mutant p53 and surviving proteins from these cells. Our findings provide the first instance of a potential role for OME as an anti-breast cancer agent *in vitro* which certainly deserves more attention and further exploration to identify novel compounds for breast cancer.

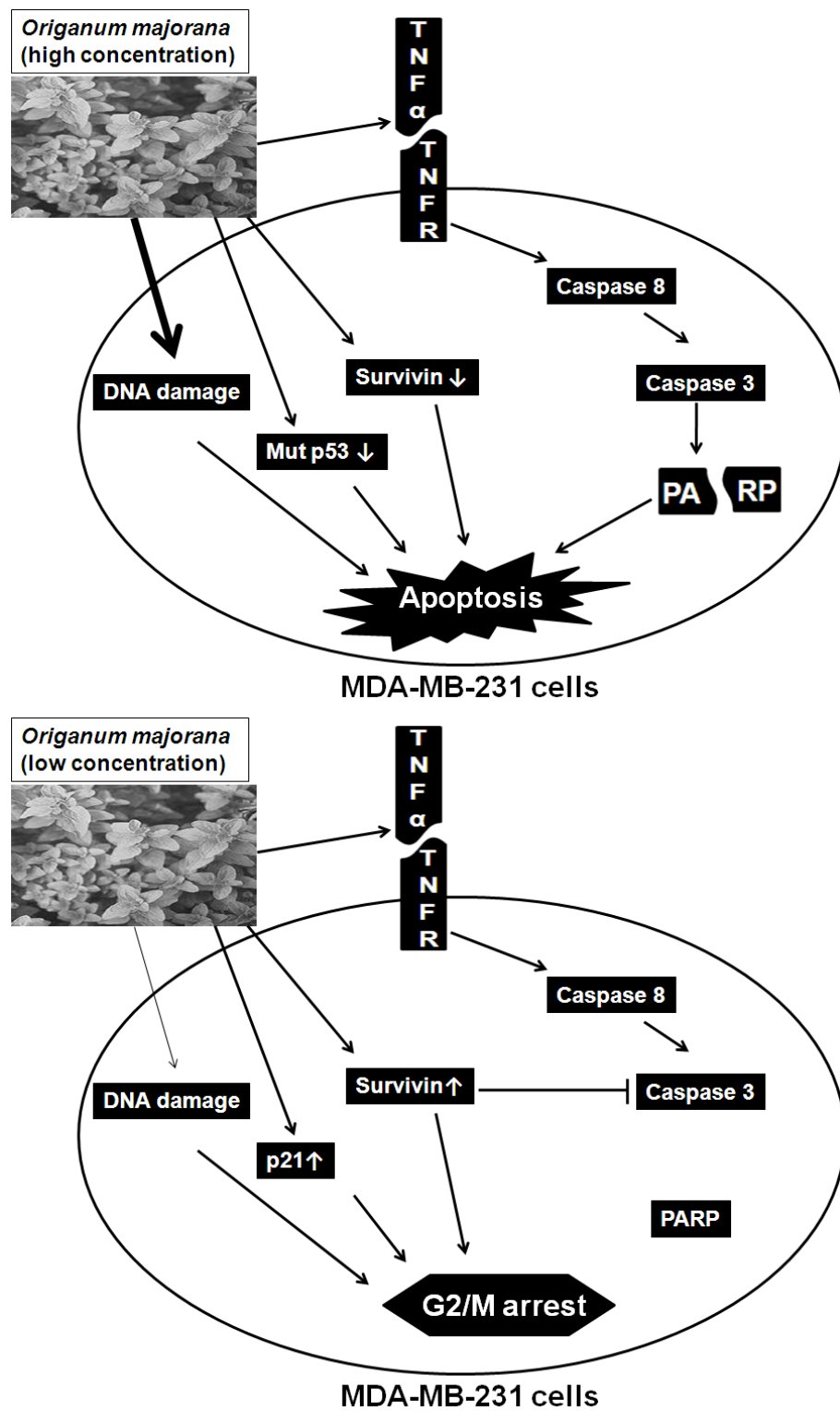


Figure 75. Proposed Mechanisms of Action of *O. majorana* on MDA-MB-231 Cells.

Tumor invasion and metastasis is a multistep process involving cell adhesion, proteolytic degradation and migration through the ECM and angiogenesis. Common cancer treatment drugs aim at blocking cell cycle progression, inducing cell death and/or inhibiting tumor migration and invasion. Cancer chemoprevention through these events has been reported for several natural compounds [21] [167-170]. Nowadays, there is a growing interest in combination therapy using multiple anti-cancer drugs affecting several targets/pathways. Herein, we demonstrate for the first time that *O. majorana*, at non-cytotoxic concentrations, possesses potent anti-metastatic properties against the highly invasive triple negative breast cancer cell line, MDA-MB-231. In fact, *O. majorana* efficiently inhibited the migratory abilities and induced homotypic aggregation of MDA-MB-231 cells, associated with an upregulation of E-cadherin expression. We also showed that *O. majorana* not only decreased the adhesion of MDA-MB-231 to HUVECs as well as their transendothelial migration, but also inhibited the secretion of the pro-angiogenic factor VEGF from both endothelial and breast cancer cells. In addition we demonstrate that *O. majorana* suppressed the expression and the activities of MMP-2 and MMP-9 and downregulated the expression of uPAR and ICAM-1. *O. majorana* also blocked I $\kappa$ B- $\alpha$ /NF $\kappa$ B and reduced Nitric Oxide (NO) production, both signaling events involved in cancer cell invasion. Moreover, we demonstrated that *O. majorana* significantly inhibited tumor growth and metastasis *in vivo* in a chick tumor growth assay.

It is well known that disruption of cell-cell adhesion during cancer progression is the initial stage required for the acquisition of invasive properties. Decreased cell-cell adhesion in cancer cells is often characterized by diminished expression of E-cadherin. Indeed, E-cadherin, a calcium-dependent, cell adhesion molecule, is considered as a tumor suppressor in breast cancer [189]. A decrease in E-cadherin expression is a critical and necessary event required in the disruption of cell-cell adhesion and thus for the acquisition of invasive phenotype of various tumors including breast cancer. In fact, downregulation or loss of E-cadherin during cancer progression is associated with aggressive behavior by the tumor and a poor prognosis for the patient [190]. Conversely, expression of E-cadherin can lead to a reduced progression and invasion of breast cancer cells [191]. In the present study, we demonstrated that *O. majorana* inhibited cell migration and promoted homotypic cell-cell aggregation and induced overexpression of E-cadherin in the MDA-MB-231 cells. We postulate that *O. majorana* exerts its anti-migratory effect on breast cancer cells, at least partly, through reactivation of the expression of E-cadherin gene. In fact we showed that OME was able to induce transactivation of E-cadherin promoter in transfected cells (Fig. 3D). Induction of E-cadherin expression promotes then homotypic aggregation of OME-treated MDA-MB-231 cells. Thus, E-cadherin overexpression is one of possible mechanism by which *O. majorana* exerts its anti-invasive effect on the MDA-MB-231 cells.

Recent studies showed that treatment with histone deacetylase inhibitors such as SAHA and trichostatin A strongly inhibited the migration

and invasion of breast and prostate cancer cells and caused an upregulation of E-cadherin [192, 193]. Histone Deacetylase (HDAC) Inhibitors, promising anticancer agents, have been shown to mediate their effects by activating the transcription of specific genes through histone hyperacetylation. Interestingly, we have recently shown that *O. majorana* induces hyperacetylation of Histone H3 and H4 at non-cytotoxic concentrations. Moreover, *O. majorana* has been shown to contain luteolin [98], a dietary flavonoid with Histone Deacetylase Inhibitor activity, which was also shown to inhibit the invasive potential of MDA-MB-231 cells [188].

Based on these findings, we can suggest that one possible mechanism by which *O. majorana* exerts its anti-migratory and anti-metastatic effects on MDA-MB-231 involves an upregulation of E-cadherin gene expression through Histone hyperacetylation. However, at this stage, we cannot rule out the involvement of other mechanism(s) being involved in this regulation. Further investigation will be needed to decipher the exact mechanism by which *O. majorana* exert its effect on E-cadherin expression.

The dissemination of cancer cells from the primary tumor is another crucial event in the process of cancer invasion and metastasis, which involves the degradation of the ECM and the components of the basement membrane through proteases. Of these proteases, MMPs such as MMP-2, MMP-9 and the uPA are thought to play a key role in cancer cell invasion and metastasis [194, 195]. It has been shown that increasing expression of MMPs in breast cancer cells correlates with increasing

aggressiveness of breast cancer cell growth and metastatic potential [196]. Therefore, inhibiting the activity or the expression of these proteases can be considered as a potential therapeutic target against breast cancer. Interestingly, here we clearly demonstrate that *O. majorana* exerts its anti-invasive effect against MDA-MB-231 cells by significantly downregulating the expression of uPAR, MMP-2 and MMP-9 and decreasing the activity of these two proteases and consequently reducing ECM degradation.

The ability of tumor cells to metastasize also largely depends on their ability to adhere and transmigrate through endothelial cells. Cancer cell-endothelial cell interaction is mediated by various adhesive molecules such as intracellular adhesion molecule-1 (ICAM-1), vascular cell adhesion molecule-1 (VCAM-1) and E-selectin [197]. Studies have shown that the level of ICAM-1 protein expression on the cell surface positively correlated with metastatic potential of several breast cancer cell lines [16]. Moreover, down regulation of ICAM-1 at the protein and mRNA levels strongly inhibited human breast cancer cell invasion [16]. Tanshinone I, a natural compound derived from medicinal plant, *Salvia miltiorrhiza*, efficiently inhibited the adhesion of MDA-MB-231 cells to HUVECs by down regulating the expression of ICAM-1 and VCAM-1 [198]. Recent studies have revealed that ICAM-1 expression is associated with a more aggressive breast tumor phenotype [199]. Based on these findings, ICAM-1 represents a potential target in breast cancer treatment. Our study revealed that *O. majorana* was able to reduce the expression levels of ICAM-1 proteins in MDA-MB-231 cells and blocked their adhesion to the

human vascular endothelial cells (HUVECs). Hence, we propose that downregulation of ICAM-1 expression could be one mechanism by which *O. majorana* blocks MDA-MB-231 cells capability to adhere to HUVECs and consequently prevents their metastasis.

Angiogenesis, a process by which new blood vessels form, is crucial for tumor growth and metastasis. Blockade of angiogenesis can inhibit both tumor growth and metastasis [200]. Thus inhibition of angiogenesis can be considered as a promising strategy in cancer therapy [201, 202]. One possible way to block angiogenesis is to target pro-angiogenic factors secreted by tumor cells. VEGF is the major pro-angiogenic protein expressed in 60% of breast cancer patients at the time of first diagnosis [203]. Interestingly, we found that *O. majorana* significantly reduced the production of VEGF in both HUVECs and MDA-MB-231 cells, suggesting that OME not only inhibits breast cancer cell invasion, but could also block angiogenesis.

The NF $\kappa$ B signaling pathway is known to regulate the expression of various genes involved in the process of tumor metastasis. Elevated levels of NF $\kappa$ B are frequently detected in breast cancer cells. Studies showed that inhibition of NF $\kappa$ B activity could suppress metastasis in breast cancer cells. In fact, studies showed that inactivation of NF $\kappa$ B in MDA-MB-231 breast cancer cells inhibit the expression of many downstream target genes involved in tumor metastasis such as MMP-2 [196], MMP-9 [26, 204, 205], VEGF [205], ICAM-1 [26] and uPAR [26]. The phosphorylation of I $\kappa$ B, by the IKK $\beta$  subunit of the IKK serine kinase complex, is a crucial step in the activation of NF $\kappa$ B.

In fact, phosphorylation of I $\kappa$ B triggers its polyubiquitination and proteasome-mediated degradation with consequent NF $\kappa$ B nuclear localization [206]. Nuclear NF $\kappa$ B can then upregulate the transcription of its target genes. Therefore, one way to inactivate the activated NF $\kappa$ B signaling in cancer cells is to block the phosphorylation of I $\kappa$ B by inactivating the IKK complex. Interestingly, in the present work, we demonstrated that *O. majorana* inhibited the phosphorylation of I $\kappa$ B and reduced the protein level of nuclear NF $\kappa$ B suggesting that *O. majorana* may negatively regulate the activity of NF $\kappa$ B possibly by affecting the activity of the IKK complex. It is worth mentioning that *O. majorana* significantly reduced the expression of several NF $\kappa$ B downstream target genes (MMP-2, MMP-9, uPAR, ICAM-1 and VEGF) involved in tumor metastasis. It appears that the inhibitory effect on NF $\kappa$ B could account for the anti-metastatic effects of *O. majorana*.

Nitric Oxide (NO), synthesized by several nitric oxide synthases (NOSs), nNOS/NOS-1, iNOS/NOS2 and eNOS/NOS3 is a signaling molecule that regulates several physiological responses such as vasodilatation, cell migration, immune reactions and apoptosis [198]. Interestingly, various studies have shown that NO can both promote and inhibit tumor progression and metastasis. The pro- or anti-tumorigenic activities of NO have been related to the p53 status [166, 207]. It has been shown that NO-mediated apoptosis in leukemia cells requires wild-type p53 [208]. On the other hand, it has been shown that iNOS/NOS2 expressing carcinoma cells with mutant p53 have accelerated tumor growth and increased VEGF production [209]. NO was shown to promote

cancer progression through the activation of oncogenic signaling pathways including the extracellular signal-regulated kinases (ERK)1/2, phosphoinositide 3-kinases (PI3K)/AKT, and c-Myc [124]. Recent studies showed that increased iNOS/NOS2 and consequently NO production, predicted poor survival in women with estrogen receptor  $\alpha$ -negative (ER-negative) breast tumors. Moreover, exposure to NO enhanced cell motility and invasion of Estrogen Receptor negative ER(-) cells [209]. It appears then that discovery of inhibitors targeting NO production may be particularly efficacious against ER(-), mutant p53 breast cancer patients. In the present study we showed that *O. majorana* efficiently reduced the level of NO production in the MDA-MB-231 in a concentration dependent manner, suggesting that *O. majorana* might exert its anti-metastatic effect, at least partly, by modulating the NO production in MDA-MB-231 cells. As such, NO production may be an important target for chemoprevention and therapy by *O. majorana* for the ER(-), mutant p53 MDA-MB-231 cells.

In summary, this study clearly demonstrated, for the first time, that *O. majorana* possesses anti-invasive and anti-metastatic effects against highly proliferative and highly invasive human MDA-MB-231 breast cancer cell line by modulating the activity and/or the expression of proteins regulating the process of cellular migration, adhesion invasion and angiogenesis such as E-cadherin, ICAM-1, MMP-2, MMP-9, uPAR and VEGF, at least partly, through inhibition of the NF $\kappa$ B and NO signaling pathways. Our results also showed that *O. majorana* inhibited tumor growth and metastasis in an *in vivo* tumor growth assay. Thus, our current study identifies *Origanum majorana* as a promising chemopreventive and

therapeutic candidate that inhibits breast cancer growth and metastasis by modulating the expression and activities of several targets. Nowadays, there is a growing interest in combination therapy using multiple anti-cancer drugs affecting several targets/pathways, thus *O. majorana* certainly merits a lot of attention and further exploration to identify novel compounds for breast cancer therapy.

## GENERAL CONCLUSION

In conclusion, our study has focused on natural products such as plant extracts and natural compounds found in nature and in our diets as potential anti-breast cancer agents. We demonstrated that Salinomycin induces apoptosis and senescence in breast cancer through upregulation of p21, downregulation of survivin and Histone H3 and H4 hyperacetylation. Further, we provided evidence that *Origanum majorana* attenuates breast cancer cell invasion, migration and tumor growth *in vivo*, at least in part, through inhibiting the NF $\kappa$ B activation cascade and reduction of Nitric Oxide production. In recent years, an increasing number of natural products possessing anti-cancer properties have been uncovered. Coupled with the elucidation of their anti-cancer mechanisms, the exploitation of their use in clinical chemotherapeutic strategies is promising. A potential advantage of phytochemicals and other compounds derived from natural products is that they may act through multiple cell signaling pathways and reduce the development of resistance by cancer cells. Thus, natural products and naturally occurring phytochemicals are indeed worthy of further development as anti-cancer and anti-metastatic agents for clinical use.

## REFERENCES

- [1] Siegel, R. , Ma, Zou Z, and Jemal, A. (2014). Cancer statistics, *Cancer J Clin*, 64, 9-29.
- [2] Rakha, E. A. , Chan, S. (2011). Metastatic triple-negative breast cancer. *Clin Oncol (R Coll Radiol)*, 23(9), 587-600.
- [3] Kurebayashi, J. (2009). Possible treatment strategies for triple-negative breast cancer on the basis of molecular characteristics. *Breast Cancer*, 16(4), 275-80.
- [4] Dawood, S. (2010). Triple-negative breast cancer: epidemiology and management options. *Drugs*, 70(17), 2247-58.
- [5] Caroenuto, P. , Roma, C. , Rachiglio, A. M. , Bott, G. , D'Alessio, A. , Normanno, N. (2010). Triple negative breast cancer: from molecular portrait to therapeutic intervention. *Crit Rev Eukaryot Gene Expr*, 20(1),17-34.
- [6] Rodrigo, O. B. , & Tang, S. (2010). Triple-Negative Breast Cancer: Unique Biology and Its Management. *Cancer Investigation*, 28(8), 878-883. doi:10.3109/07357907.2010.483507.
- [7] Carey, L. , Winer, E. , Viale, G. , Cameron, D. , Gianni, L. (2010). Triple-negative breast cancer: disease entity or title of convenience? *Nat Rev Clin Oncol*, 7(12), 683-92.
- [8] Hudis, C. A. , & Gianni, L. (2011). Triple-negative breast cancer: an unmet medical need. *Oncologist*, 16(1), 1-11.
- [9] Anders, C. , & Carey, L. A. (2008). Understanding and Treating Triple Negative Breast Cancer. *Oncology (Williston Park)*, 22(11), 1233–1243.
- [10] Reis-Filho, J. S. , & Tutt, A. N. J. (2008). Triple negative tumours: a critical review. *Histopathology*, 52, 108–118.
- [11] Li, F. , Li, C. , Zhang, H. , Lu, Z. , Li, Z. et al. (2012). VI-14, a novel flavonoid derivative, inhibits migration and invasion of human breast cancer cells. *Toxicology and Applied Pharmacology*, 261, 217-226.
- [12] Yachida, S. , Jones, S. , Bozic, I. , Antal, T. , Leary, R. et al. (2010). Distant metastasis occurs late during the genetic evolution of pancreatic cancer. *Nature*, 467, 1114–1117.

- [13] Baranwal, S. , & Alahari, S. K. (2009). Molecular mechanisms controlling E-cadherin expression in breast cancer. *Biochem Biophys Res Commun*, 384(1), 6–11. doi: 10.1016/j.bbrc.2009.04.051.
- [14] Corn, P. G. , Smith, B. D. , Ruckdeschel, E. S. , et al. (2000). E-Cadherin Expression Is Silenced by 5' CpG Island Methylation in Acute Leukemia. *Clin Cancer Res*, 6, 4243-4248.
- [15] Park, J. S. , Kim, K. M. , Kim, M. H. , Chang, H. J. , Baek, M. K. , et al. (2009). Resveratrol inhibits tumor cell adhesion to endothelial cells by blocking ICAM-1 expression. *Anticancer Res*, 29, 355–362.
- [16] Rosette, C. , Roth, R. B. , Oeth, P. , Braun, A. , Kammerer, S. , et al. (2005). Role of ICAM1 in invasion of human breast cancer cells. *Carcinogenesis*, 26(5), 943- 950.
- [17] Rose, P. , Huang, Q. , Ong, C. N. , Whiteman, M. , . (2005). Broccoli and watercress suppress matrix metalloproteinase-9 activity and invasiveness of human MDA-MB-231 breast cancer cells. *Toxicol Appl Pharmacol*, 209, 105–13.
- [18] Pacheco, M. M. , Mourao, M. , Mantovani, E. B. , Nishimoto, I. N. , Brentani, M. M. (1998). Expression of gelatinases A and B, stromelysin-3 and matrilysin genes in breast carcinomas: clinico-pathological correlations. *Clin Exp Metastasis*, 16, 577-585.
- [19] Przybylowska, K. , Kluczna, A. , Zadrozny, M. , Krawczyk, T. , Kulig A, et al. (2006). Polymorphisms of the promoter regions of matrix metalloproteinases genes MMP-1 and MMP-9 in breast cancer. *Breast Cancer Res Treat*, 95, 65-72.
- [20] Garbett, E. A. , Reed, M. W. R. , Stephenson, T. J. , Brown, N. J. (2000). Proteolysis in human breast cancer. *J Clin Pathol Mol Pathol*, 53, 99-106.
- [21] Adams, L. S. , Phung, S. , Yee, N. , Seeram, N. P. , Li, L. , et al. (2010). Blueberry phytochemicals inhibit growth and metastatic potential of MDA-MB-231 breast cancer cells through modulation of the phosphatidylinositol 3-kinase pathway. *Cancer Res*, 70, 3594–3605.
- [22] Lee, H. S, Seo, E. Y, , Kang, N. E. , Kim, W. K. (2008). [6]-Gingerol inhibits metastasis of MDA-MB-231 human breast cancer cells. *J Nutr Biochem*, 9, 313–9.

- [23] Reuben, S. C. , Gopalan, A, Petit, D. M. , Bishayee, A. (2012). Modulation of angiogenesis by dietary phytoconstituents in the prevention and intervention of breast cancer. *Mol Nutr Food Res*, 56, 14–29.
- [24] Brown, L. F. , Berse, B. , Jackman, R. W., Tognazzi, K. , Manseau, E. J. , et al. (1993). Expression of vascular permeability factor (vascular endothelial growth factor) and its receptors in adenocarcinomas of the gastrointestinal tract. *Cancer Res*, 53, 4727-4735.
- [25] Ling, H. , Yang, H. , Tan, S. H. , Chui, W. K. & Chew, E. H. (2010). 6-Shogaol, an active constituent of ginger, inhibits breast cancer cell invasion by reducing matrix metalloproteinase-9 expression via blockade of nuclear factor-kB activation. *British Journal of Pharmacology*, 161, 763–1777.
- [26] Yodkeeree, S. , Ampasavate, C. , Sung, B. , Aggarwal, B. B. , Limtrakul, P. (2010). Demethoxycurcumin suppresses migration and invasion of MDA-MB-231 human breast cancer cell line. *European Journal of Pharmacology*, 627, 8–15.
- [27] Novak, U. , Cocks, B. G. , Hamilton, J. A. (1991). A labile repressor acts through the NFkB-like binding sites of the human urokinase gene. *Nucleic Acids Res*, 19, 3389-93.
- [28] Sliva, D. , Rizzo, M. T. , English, D. (2002). Phosphatidylinositol 3-kinase and NF-kappaB regulate motility of invasive MDA-MB-231 human breast cancer cells by the secretion of urokinase-type plasminogen activator. *J Biol Chem*, 277, 3150-7.
- [29] Wang, Y. , Dang, J. , Wang, H. , Allgayer, H. , Murrell, G. A. , Boyd, D. (2000). Identification of a novel nuclear factor-kappaB sequence involved in expression of urokinase-type plasminogen activator receptor. *Eur J Biochem*, 267, 3248-54.
- [30] Lerebours, F. , Vacher, S. , Andrieu, C. , Espie, M. , Marty, M. et al. (2008). NF-kappa B genes have a major role in Inflammatory Breast Cancer. *BMC Cancer*, 8, 41. doi:10.1186/1471-2407-8-41.
- [31] Wang, S. (2008). The promise of cancer therapeutics targeting the TNF-related apoptosis-inducing ligand and TRAIL receptor pathway. *Oncogene*, 27, 6207–6215.
- [32] Su, M. , Mei, Y. , Sinha, S. (2013). Role of the Crosstalk between Autophagy and Apoptosis in Cancer. *Journal of Oncology* 2013, 1-14. <http://dx.doi.org/10.1155/2013/102735>

- [33] Martin, K.R. (2006). Targeting apoptosis with dietary bioactive agents. *Experimental Biology and Medicine (Maywood)*, 231, 117-129.
- [34] Reed, J.C. (2003). Apoptosis-targeted therapies for cancer. *Cancer Cell*, 3, 17–22.
- [35] Brown, J. M. & Attardi, L. D. (2005). The role of apoptosis in cancer development and treatment response. *Nat Rev Cancer*, 5, 231–237.
- [36] William, G. H. , Stoeber, K. (2012). The cell cycle and cancer. *J Pathol*, 226(2), 352-64.
- [37] Pentimalli, F. , Giordano, A. (2009). Promises and drawbacks of targeting cell cycle kinases in cancer. *Discov Med* 8(43),177-80.
- [38] Gary, K. S. , & Manish, A. S. (2005). Targeting the Cell Cycle: A New Approach to Cancer Therapy. *J Clin Oncol* 23(36), 9408-9421.
- [39] Dai, M. , Al-Odaini, A. A, Fils-Aimé, N. , Villatoro, M. A. , Guo, J. , Arakelian, A. , Rabbani, S. A. , Ali, S. , Lebrun, J. J. (2013). Cyclin D1 cooperates with p21 to regulate TGFb-mediated breast cancer cell migration and tumor local invasion. *Breast Cancer Research*, 15, 1-14.
- [40] Malumbres, M. (2007). Cyclins and related kinases in cancer cells. *J BUON*, 12 Suppl 1, S45-52.
- [41] Hajduch, M. , Havlieek, L. , Vesely, J. , Novotny, R. , Mihal, V. , & Strnad, M. (1999). Synthetic cyclin dependent kinase inhibitors. New generation of potent anti-cancer drugs. *Adv Exp Med Biol*, 457, 341–353.
- [42] Sherr, C. J. , Roberts, J. M. (1999). CDK inhibitors: positive and negative regulators of G1-phase progression. *Genes Dev*, 13, 1501-1512.
- [43] Besson, A. , Dowdy, S. F. , Roberts, J. M. (2008). CDK inhibitors: cell cycle regulators and beyond. *Dev Cell*, 14, 159-169.
- [44] Coqueret, O. (2003). New roles for p21 and p27 cell-cycle inhibitors: a function for each cell compartment? *Trends Cell Biol*, 13(2), 65-70.
- [45] De Falco, M. , De Luca, A. (2010). Cell cycle as a target of antineoplastic drugs. *Curr Pharm Des*, 16(12), 417-26.
- [46] Gartel, A. L. , & Tyner, A. L. (2002). The Role of the Cyclin-dependent Kinase Inhibitor p21 in Apoptosis. *Tyner Mol Cancer Ther*, 1, 639-649.

- [47] Kim, J. K. , Diehl, J. A. (2009). Nuclear cyclin D1: an oncogenic driver in human cancer. *J Cell Physiol* 220, 292-296.
- [48] Massague, J. (2004). G1 cell-cycle control and cancer. *Nature*, 432, 298-306.
- [49] Ahmad, N. , Gupta, S. , & Mukhtar, H. (2000). Green tea polyphenol epigallocatechin 3-gallate differentially modulates nuclear factor kB in cancer cells versus normal cells. *Arch Biochem Biophys*, 376, 338–346.
- [50] Park, W. H. , Seol, J. G. , Kim, E. S. , Hyun, J. M. , Jung, C. W. , Lee, C. C. , Kim, B. K. , & Lee, Y. Y. (2000). Arsenic trioxide mediated growth inhibition in MC/CAR myeloma cells via cell cycle arrest in association with induction of cyclin dependent kinase inhibitor, p21, and apoptosis. *Cancer Res*, 60, 3065–3071.
- [51] Ahmad, N. , Adhami, V. M. , Afaq, F. , Feyes, D. K. , Mukhtar, H. (2001). Resveratrol Causes WAF-1/p21-mediated G1-phase Arrest of Cell Cycle and Induction of Apoptosis in Human Epidermoid Carcinoma A431 Cells. *Clinical Cancer Research*, 7, 1466–1473.
- [52] Buolamwini, J. K. (2000). Cell cycle molecular targets in novel anticancer drug discovery. *Curr Pharm Des*, 6, 379–392.
- [53] McDonald, E. R., & El Deiry, W. S. (2000). Cell cycle control as a basis for cancer drug development. *Int J Oncol*, 16, 871–886.
- [54] Senderowicz, A. M. , Headlee, D. , Stinson, S. F. , Lush, R. M. , Kalil, N., Villalba, L. , Hill, K. , Steinberg, S. M. , Figg, W. D. , Tompkins, A. , Arbuck, S. G. , and Sausville, E. A. (1998). Phase I trial of continuous infusion flavopiridol, a novel cyclin dependent kinase inhibitor, in patients with refractory neoplasms. *J Clin Oncol*, 16, 2986–2999.
- [55] Lin, C. H. , Lu, W. C. , Wang, C. W. , Chan, Y. C. , Chen, M. K. (2013). Capsaicin induces cell cycle arrest and apoptosis in human KB cancer cells. *BMC Complementary and Alternative Medicine*, 13(46). doi: 10.1186/1472-6882-13-46.
- [56] Sapra R. , Gupta V. , Bansal R. , Bansal P. (2012). Dietary phytochemicals in cell cycle arrest and apoptosis- an insight. *Journal of Drug Delivery and Therapeutics*, 2(2). Available online at <http://jddtonline.info>

- [57] Pan, M. H. & Ho, C. H. (2008). Chemopreventive effects of natural dietary compounds on cancer development. *Chem Soc Rev*, 37, 2558–2574.
- [58] Acosta, J. C. & Gil, J. (2012). Senescence: a new weapon for cancer therapy. *Trends Cell Biol*, 22(4), 211-9.
- [59] Rufini, A. , Tucci, P. , Celardo, I. , Melino, G. (2013). Senescence and aging: the critical roles of p53. *Oncogene*, 24;32(43), 5129-43.
- [60] Roninson, I. B. (2003). Tumor cell senescence in cancer treatment. *Cancer Res*, 63(11), 2705-2715.
- [61] Bringold, F, Serrano, M. (2000). Tumor suppressors and oncogenes in cellular senescence. *Exp Gerontol*, 35(3), 317–329.
- [62] Dimri, G. P. , Lee, X. , Basile, G. et al. (1995). A biomarker that identifies senescent human cells in culture and in aging skin in vivo. *Proc Natl Acad Sci U S A*, 92(20), 9363-9367.
- [63] Desai, A. A. , Stadler, W. M. (2006). Novel kinase inhibitors in renal cell carcinoma: progressive development of static agents. *Curr Urol Rep*, 7(1), 16–22.
- [64] Martin, L. , Schilder, R. J. (2006). Novel non-cytotoxic therapy in ovarian cancer: current status and future prospects. *J Natl Compr Canc Netw*, 4(9), 955–966.
- [65] Winkvist, E. , Waldron, T. , Berry, S. , Ernst, D. S. , Hotte, S. , Lukka, H. (2006). Non-hormonal systemic therapy in men with hormone-refractory prostate cancer and metastases: a systematic review from the Cancer Care Ontario Program in Evidence-based Care's Genitourinary Cancer Disease Site Group. *BMC Cancer*, 6, 112. doi: 10.1186/1471-2407-6-112
- [66] Schmitt, C. A. , Fridman, J. S. , Yang, M. et al. (2002). A senescence program controlled by p53 and p16INK4a contributes to the outcome of cancer therapy. *Cell*, 109(3), 335–346.
- [67] Roninson, I. B. , Broude, E. V. , Chang, B. D. (2001). If not apoptosis, then what? Treatment-induced senescence and mitotic catastrophe in tumor cells. *Drug Resist Updat*, 4, 303-313.
- [68] Lock, R. B. , Stribinskiene, L. (1996). Dual modes of death induced by etoposide in human epithelial tumor cells allow Bcl-2 to inhibit apoptosis without affecting clonogenic survival. *Cancer Res*, 56, 4006-4012.

- [69] Ruth, A. C. , Roninson, I. B. (2000). Effects of the multidrug transporter P-glycoprotein on cellular responses to ionizing radiation. *Cancer Res*, 60, 2576-2578.
- [70] Bhanot, A. , Sharma, R. Noolvi, M. N. (2011). Natural sources as potential anti-cancer agents: A review. *International Journal of Phytomedicine*, 3, 09-26.
- [71] Karikas, G. A. (2010). Anticancer and chemopreventing natural products: some biochemical and therapeutic aspects. *BUON*, 15(4), 627-38.
- [72] Kaczirek, K. , Schindl, M. , Weinhausel, A. , Scheuba, C. , Passler, C. , Prager, G. , Raderer, M. , Hamilton, G. , Mittlbock, M. , Siegl, V. , Pfragner, R. & Niederle, B. (2004). Cytotoxic activity of camptothecin and paclitaxel in newly established continuous human medullary thyroid carcinoma cell lines. *J Clin Endocrinol Metabol*, 89, 2397-240.
- [73] Butler, M. S. (2005). Natural products to drugs: natural product derived compounds in clinical trials. *Nat Prod Rep*, 22,162–195.
- [74] Bailly, C. (2009). Ready for a comeback of natural products in oncology. *Biochem Pharmacol*, 77, 1447–1457.
- [75] Rabi, T. & Bishaye, A. (2009). Terpenoids and breast cancer chemoprevention. Breast Cancer Research and Treatment. *Breast Cancer Res Treat*, 115, 223-239.
- [76] Reuben, S. C. , Gopalan, A. , Petit, D. M., & Bishayee, A. (2012). Modulation of angiogenesis by dietary phytoconstituents in the prevention and intervention of breast cancer. *Mol Nutr Food Res*, 56, 14–29.
- [77] Neergheen, V. S. , Bahorun, T. , Taylor, E. W. , Jen, L. S. , Aruoma, O. I. (2010). Targeting specific cell signaling transduction pathways by dietary and medicinal phytochemicals in cancer chemoprevention. *Toxicology*, 278(2), 229-41.
- [78] Noble, R. L. (1990). The discovery of the vinca alkaloids – chemotherapeutic agents against cancer. *Biochem Cell Biol*, 68, 1344-1351.
- [79] Stähelin, H. (1973). Activity of a new glycosidic lignan derivative (VP-16-213) related to podophyllotoxin in experimental tumors. *Eur J Cancer*, 9, 215-221.

- [80] Harvey, A. L. (1999). Medicines from nature: are natural products still relevant to drug discovery. *Trends Pharmacol Sci*, 20, 196-198.
- [81] Liu, L. F. (1989). DNA topoisomerase poisons as antitumor drugs. *Annu Rev Biochem*, 58, 351-375.
- [82] Wani, M. C. , Taylor, H. L. , Wall, M. E. et al. (1971). Plant antitumor agents. VI. The isolation and structure of taxol, a novel antileukemic and antitumor agent from *Taxus brevifolia*. *J Am Chem Soc*, 93, 2325-2327.
- [83] Creemers, G. J. , Bolis, G. , Gore, M. et al. (1996). Topotecan, an active drug in the second-line treatment of epithelial ovarian cancer. *J Clin Oncol*, 14, 3056-3061.
- [84] Bertino, J. R. (1997). Irinotecan for colorectal cancer. *Semin Oncol*, 24, S18-S23.
- [85] Liu, L. F. , Desai, S. D. , Li, T. K. et al. (2000). Mechanism of action of camptothecin. *Ann New York Acad Sci*, 922, 1-10.
- [86] Cragg, G. & Suffness, M. (1988). Metabolism of plant-derived anticancer agents. *Pharmacol Ther*, 37, 425-432.
- [87] Harmon, A. D. , Weiss, U. , Silverton, J. V. (1979). The structure of rohutukine, the main alkaloid of *Amoora rohituka* (syn. *Aphanamixis polystachya*) (Maliaceae). *Tetrahydron*, 20, 721-724.
- [88] Losiewicz, M. D. , Carlson, B. A, Kaur, G. et al. (1994). Potent inhibition of cdc2 kinase activity by the flavonoid L86-8275. *Biochem Biophys Res Commun*, 201, 589-595.
- [89] Worland, P. J. , Kaur, G. , Stetler-Stevenson, M. et al. (1993). Alteration of the phosphorylation state of p32cdc2 kinase by the flavone L86-8275 in breast carcinoma cells. *Biochem Pharmacol*, 46, 1831-1836.
- [90] Kelland, L. R. (2000). Flavopiridol, the first cyclin-dependent kinase inhibitor to enter the clinic: current status. *Ex Opin Inv Drugs*, 9, 2903-2911.
- [91] Powell, R. G. , Weisleder, D. , Smith, C. R. J. et al. (1970). Structures of harringtonine, isoharringtonine, and homoharringtonine. *Tetrahydron Lett*, 11, 815-818.
- [92] Kantarjian, H. M. , O'Brien, S. , Anderlini, P. et al. (1996). Treatment of myelogenous leukemia: current status and investigational options. *Blood*, 87, 3069-3081.

- [93] Zhou, D. C. , Zittoun, R. , Marie, J. P. (1995). Homoharringtonine: an effective new natural product in cancer chemotherapy. *Bull Cancer*, 82, 987-995.
- [94] Li, Y. Z. , Li, C. J. , Pinto, A. V. et al. (1999). Release of mitochondrial cytochrome c in both apoptosis and necrosis induced by  $\beta$ -lapachone in human carcinoma cells. *Mol Med*, 4, 232-239.
- [95] Vági, E. , Rapavi, E. , Hadolin, M. , Vàsàrhelyiné, P. K, Balázs, A. et al. (2005) Phenolic and triterpenoid antioxidants from *Origanum majorana* L. herb and extracts obtained with different solvents. *Journal of Agricultural and Food Chemistry*, 53, 17–21. doi: 10.1021/jf048777p.
- [96] Al-Harbi, N. O. (2011). Effect of marjoram extract treatment on the cytological and biochemical changes induced by cyclophosphamide in mice. *Journal of Medicinal Plants Research*, 5, 5479–5485. doi: 10.1158/0008-5472.can-09-3565.
- [97] Miron, T. L. , Plaza, M. , Bahrim, G. , Ibariez, E, Herrero, M. (2011). Chemical composition of biocactive pressurized extracts of Romanian aromatic plants. *Journal of Chromatography A*, 1218, 4918–4927. doi: 10.1016/j.chroma.2010.11.055.
- [98] Tsimogiannis, D. , Stavrakaki, M. , Oreopoulou, V. (2006). Isolation and characterisation of antioxidant components from Oregano (*Origanum heracleoticum*). *International Journal of Food, Science and Technology*, 41, 39–48. doi: 10.1016/j.chroma.2010.11.055.
- [99] Leeja, L. , Thoppil, J. E. (2007). Antimicrobial activity of methanol extract of *Origanum majorana* L. (Sweet marjoram). *J Environ Biol*, 28, 145–146. doi: 10.1016/j.chroma.2010.11.055
- [100] El-Ashmawy, I. M. , El-Nahas, A. F. , Salama, O. M. (2005). Protective effect of volatile oil, alcoholic and aqueous extracts of *Origanum majorana* on lead acetate toxicity in mice. *Basic Clin Pharmacol Toxicol*, 97, 238–243. doi: 10.1016/j.chroma.2010.11.055
- [101] El-Ashmawy, I. M. , Amal, S., Salama, O. M. (2007). Acute and long term safety evaluation of *Origanum majorana* essential oil. *Alex J Pharm Sci*, 21, 29–35. doi: 10.1016/j.chroma.2010.11.055
- [102] El-Ashmawy, I. M. , Saleh, A. , Salama, O. M. (2007). Effects of marjoram volatile oil and grape seed extract on ethanol toxicity in male rats. *Basic Clin Pharmacol Toxicol*, 101, 320–327. doi: 10.1111/j.1742-7835.2007.00125.x

- [103] Yazdanparast, R. , Shahriyary, L. (2008). Comparative effects of *Artemisia dracuncululus*, *Satureja hortensis* and *Origanum majorana* on inhibition of blood platelet adhesion, aggregation and secretion. *Vascul. Pharmacol*, 48, 32–37. doi: 10.1111/j.1742-7835.2007.00125.x
- [104] Lin, L. T. , Liu, L. T. , Chiang, L. C. , Lin, C. C. (2002). In vitro anti-hepatoma activity of fifteen natural medicines from Canada. *Phytotherapy Research*, 16, 440–444. doi: 10.1002/ptr.937
- [105] Binaschi, M. , Farinosi, R. , Borgnetto, M. E. et al. (2000). In vivo site specificity and human isoenzyme selectivity of two topoisomerase II poisoning anthracyclines. *Cancer Res*, 60, 3770-3776.
- [106] Patrick Y. (1997). Major microbial diversity initiative recommended. *Am Soc Microbiol News*, 63, 417-421.
- [107] Alberts, M. W. , Williams, R. T. , Brown, E. J. et al. (1993). KBP-Rapamycin inhibits a cyclin-dependent kinase activity and a cyclin D1-Cdk association in early G1 of an osteosarcoma cell line. *J Biol Chem*, 268, 22825-22829.
- [108] Schulte, T.W. , Neckers, L. M. (1998). The benzoquinone ansamycin 17-allylamino-17 demethoxygeldanamycin binds to HSP90 and shares important biologic activities with geldanamycin. *Cancer Chemother Harmacol*, 42, 273-279.
- [109] Cadenas, M. E. , Sandfrison, A. , Cutler, N. S. et al. (1998). Signal transduction cascades as targets for therapeutic intervention by natural products. *Trends Biotechnol*, 16, 427-433.
- [110] Adjei, A. A. (2000). Signal transduction pathway targets for anticancer drug discovery. *Curr Pharmaceut Design*, 6, 361-378.
- [111] Gupta, P. B. , Onder, T. T. , Jiang, G. , Tao, K. , Kuperwasser, C. , Weinberg, R. , Lander, E. S. (2009). Identification of Selective Inhibitors of Cancer Stem Cells by High-Throughput Screening. *Cell*, 138 (4), 645-659.
- [112] Wang, Y. (2011). Effects of Salinomycin on cancer stem cell in human lung adenocarcinoma A549 cells. *Med Chem*, 7(2), 106-11.
- [113] Zhi, Q. M, Chen, X. H. , Ji, J. , Zhang, J. N. , Li, J. F. , Cai, Q. , Liu, B. Y. , Gu, Q. L. , Zhu, Z. G. , Yu, Y. Y. (2011). Salinomycin can effectively kill ALDH (high) stem-like cells on gastric cancer. *Biomed Pharmacother*, 65(7), 509-15

- [114]Dong, T. T. , Zhou, H. M. , Wang, L. L. , Feng, B. , Lv, B. , Zheng, M. H. (2011). Salinomycin selectively targets 'CD133+' cell subpopulations and decreases malignant traits in colorectal cancer lines. *Ann Surg Oncol*, 18(6), 1797-804.
- [115]Huczynski, A. (2012). Salinomycin-A new cancer drug candidate. *Chem. Biol Drug Des*, 79, 235-238.
- [116]Riccioni, R. , Dupuis, M. L. , Bernabei, M. , Petrucci, E. , Pasquini, L. , Mariani, G. , Cianfriglia, M. , Testa, U. (2010). The cancer stem cell selective inhibitor Salinomycin is a p-glycoprotein inhibitor. *Blood Cells Mol Dis*, 45(1), 86-92.
- [117]Lu, D. , Choi, M. Y. , Yu, J. , Castro, J. E. , Kipps, T. J. , Carson, D. A. (2011). Salinomycin inhibits Wnt signaling and selectively induces apoptosis in chronic lymphocytic leukemia cells. *Proc Natl Acad Sci U S A*, 108(32), 13253-7.
- [118]Kim, K. Y. , Yu, S. N. , Lee, S. Y. , Chun, S. S. , Choi, Y. L. , Park, Y. M. , Song, C. S. , Chatterjee, B. , Ahn, S. C. (2011). Salinomycin-induced apoptosis of human prostate cancer cells due to accumulated reactive oxygen species and mitochondrial membrane depolarization. *Biochem Biophys Res Commun*, 413(1), 80-6.
- [119]Ketola, K. , Hilvo, M. , Hyötyläinen, T. , Vuoristo, A. , Ruskeepää, A. L. , Orešič, M. , Kallioniemi, O. , Iljin, K. (2012). Salinomycin inhibits prostate cancer growth and migration via induction of oxidative stress. *Br J Cancer*, 106(1), 99-106.
- [120]Zhang, G. N. , Liang, Y. , Zhou, L. J. , Chen, S. P. , Chen, G. , Zhang, T. P. , Kang, T. , Zhao, Y. P. (2011). Combination of Salinomycin and gemcitabine eliminates pancreatic cancer cells. *Cancer Lett*, 313(2), 137-44.
- [121]Kim, J. H. , Chae, M. , Kim, W. K. , Kim, Y. J. , Kang, H. S. , Kim, H. S. , Yoon, S. (2011). Salinomycin sensitizes cancer cells to the effects of doxorubicin and etoposide treatment by increasing DNA damage and reducing p21 protein. *Br J Pharmacol*, 162(3), 773-84.
- [122]Kim, W. K. , Kim, J. H. , Yoon, K. , Kim, S. , Ro, J. , Kang, H. S. , Yoon, S. (2011). Salinomycin, a p-glycoprotein inhibitor, sensitizes radiation-treated cancer cells by increasing DNA damage and inducing G2 arrest. *Invest New Drugs*, 30(4), 1311-8. doi: 10.1007/s10637-011-9685-6.

- [123]Kim, J. H. , Yoo, H. I. , Kang, H. S. , Ro, J. , Yoon, S. (2012). Salinomycin sensitizes antimitotic drugs-treated cancer cells by increasing apoptosis via the prevention of G2 arrest. *Biochemical and Biophysical Research Communications*, 418(1), 98-103.
- [124]Prudent, R. , Vassal-Stermann, E. , Nguyen, C. H. , Mollaret, M. , Viallet, J. et al. (2013). Azaindole derivatives are inhibitors of microtubule dynamics, with anti-cancer and anti-angiogenic activities. *Br J Pharmacol.*, 168, 673-85.
- [125]Debacq-Chainiaux, F. , Erusalimsky, J. D. , Campisi, J. , Toussaint, O. (2009). Protocols to detect senescence-associated beta-galactosidase (SA-beta-gal) activity, a biomarker of senescent cells in culture and in vivo. *Nat Protoc*, 4 (12), 1798–1806.
- [126]Meromsky, L. , Lotan, R. , Raz, A. (1986). Implications of endogenous tumor cell surface lectins as mediators of cellular interactions and lung colonization. *Cancer Res*, 46, 5270-5.
- [127]Zen, K. , Liu, D. Q. , Guo, Y. L. , Wang, C. , Shan, J. et al. (2008). CD44v4 Is a Major E Selectin Ligand that Mediates Breast Cancer Cell Transendothelial Migration. *PLOS ONE*, 3(3). e1826. doi:10.1371/ journal.pone.0001826. PubMed: 18350162.
- [128]Kleiner, D. E. , Stetler-Stevenson, W. G. (1994). Quantitative zymography: detection of picogram quantities of gelatinases. *Anal Biochem*, 218, 325-329. doi:10.1006/abio.1994.1186.
- [129]Liu, Y. N. , Lee, W. W. , Wang, C. Y. , Chao, T. H. , Chen, Y. et al. (2005). Regulatory mechanisms controlling human E-cadherin gene expression. *Oncogene*, 24, 8277-8290. doi:10.1038/sj.onc.1208991. PubMed: 16116478.
- [130]Leeja, L. , Thoppil, J. E. (2007). Antimicrobial activity of methanol extract of *Origanum majorana* L. (Sweet marjoram). *J Environ Biol*, 28(1). 145-146. PubMed: 17718003.
- [131]Green, C. E. , Liu, T. , Montel, V. , Hsiao, G. , Lester, R. D. et al. (2009). Chemoattractant Signaling between Tumor Cells and Macrophages Regulates Cancer Cell Migration, Metastasis and Neovascularization. *PLoS ONE*, 4(8), e6713. doi:10.1371/journal.pone.0006713. PubMed: 19696929.

- [132]Hendzel, M. J. , Wei, Y. , Mancini, M. A. , Van Hooser, A. , Ranalli, T. , Brinkley, B. R. , Bazett-Jones, D. P. , Allis, C. D., (1997). Mitosis-specific phosphorylation of histone H3 initiates primarily within pericentromeric heterochromatin during G2 and spreads in an ordered fashion coincident with mitotic chromosome condensation. *Chromosoma*, 106, 348-60.
- [133]Maurer M, Komina O, Wesierska-Gadek J. (2009). Roscovitine differentially affects asynchronously growing and synchronized human MCF-7 breast cancer cells. *Ann N Y Acad Sci*, 1171, 250–256.
- [134]Choi, H. J. , Fukui, M. , Zhu, B. T. (2011). Role of Cyclin B1/Cdc2 Up-Regulation in the Development of Mitotic Prometaphase Arrest in Human Breast Cancer Cells Treated with Nocodazole. *PLoS ONE*, 6(8), e24312. doi:10.1371/journal.pone.0024312
- [135]Quelle, D. E. , Ashmun, R. A. , Shurtleff, S. A. , Kato, J. , Bar-Sagi, D. , Russel, M. , & Sherr, C. J. (1993). Overexpression of mouse D-type cyclins accelerates G1 phase in rodent fibroblasts. *Genes Dev*, 7, 1559–1571.
- [136]Musgrove, E. A. , Lee, C. S. L. , Buckley, M. F. , & Sutherland, R. L. (1994). Cyclin D1 induction in breast cancer cells shortens G1 and is sufficient for cells arrested in G1 to complete the cell cycle. *Proc Natl Acad Sci USA*, 91, 8022–8026.
- [137]Tam, S. W. , Theodoras, A. M. , Shay, J. W. , Draetta, G. F. , & Pagano, M. (1994). Differential expression and regulation of cyclin D1 protein in normal and tumor human cells: association with cdk4 is required for cyclin D1 function in G1 progression. *Oncogene*, 9, 2663–2674.
- [138]Al Marzouqi N, Iratni R, Nemmar A, Arafat K, Ahmed Al Sultan M, Yasin J, Collin P, Mester J, Adrian TE, Attoub S. (2011). Fronoside A inhibits human breast cancer cell survival, migration, invasion and the growth of breast tumor xenografts. *Eur J Pharmacol*, 668(1-2), 25-34.
- [139]Ewald, J. A. , Desotelle, J.A. , Wilding, G. , Jarrard, D. F. (2010). Therapy-induced senescence in cancer. *J Natl Cancer Inst*, 102(20), 1536-46. Review.

- [140]Chang, B.D. , Broude, E.V. , Dokmanovic, M. , Zhu, H. , Ruth, A. , Xuan, Y, Kandel, E. S. , Lausch, E. , Christov, K. , Roninson, I. B. (1999). A senescence-like phenotype distinguishes tumor cells that undergo terminal proliferation arrest after exposure to anticancer agents. *Cancer Res*, 59(15), 3761-7.
- [141]Vergel, M. , Marin, J. J. , Estevez, P. , Carnero, A. (2010). Cellular senescence as a target in cancer control. *J Aging Res*, 2011. <http://dx.doi.org/10.4061/2011/725365>
- [142]Fuchs, D. , Heinold, A. , Opelz, G. , Daniel, V. , Naujokat, C. (2009). Salinomycin induces apoptosis and overcomes apoptosis resistance in human cancer cells. *Biochem Biophys Res Commun*, 390(3), 743-9.
- [143]Katayama, M. , Kawaguchi, T. , Berger, M. S. , Pieper, R. O. (2007). DNA damaging agent-induced autophagy produces a cytoprotective adenosine triphosphate surge in malignant glioma cells. *Cell Death Differ*, 14 (3), 548–558.
- [144]Lee, D. S. , Lee, M. K. , Kim, J. H. (2009). Curcumin induces cell cycle arrest and apoptosis in human osteosarcoma (HOS) cells. *Anticancer. Res*, 29 (12), 5039–5044.
- [145]Zhuang, Y. , & Miskimins, W. K. (2008). Cell cycle arrest in Metformin treated breast cancer cells involves activation of AMPK, downregulation of cyclin D1, and requires p27Kip1 or p21Cip1. *J Mol Signal*, 3-18. DOI:10.1186%2F1750-2187-3-18,
- [146]Tamm, I. , Wang, Y. , Sausville, E. , Scudiero, D. A. , Vigna, N. , Oltersdorf, T., Reed, J. C. (1998). IAP-family protein survivin inhibits caspase activity and apoptosis induced by Fas (CD95), Bax, caspases, and anticancer drugs. *Cancer Res*, 58, 5315–5320.
- [147]Shin, S. , Sung, B. J. , Cho, Y. S. , Kim, H. J. , Ha, N. C. , Hwang, J. I. Chung, C. W. , Jung, Y. K. , Oh, B. H. (2001). An anti-apoptotic protein human survivin is a direct inhibitor of caspase-3 and -7. *Biochemistry*, 40, 1117–1123. doi: 10.1021/bi001603q
- [148]Chandele, A. , Prasad, V. , Jagtap, J. C. , Shukla, R. , Shastri, P. R. (2004). Upregulation of surviving in G2/M cells and inhibition of caspase 9 activity enhances resistance in staurosporine-induced apoptosis. *Neoplasia*, 6, 29–40.
- [149]Reed, J. C. (2001). Apoptosis-regulating proteins as targets for drug discovery. *Trends Mol Med*, 7, 314–319.

- [150]Vogelstein, B. , Lane, D. , Levine, A. J. (2000). Surfing the p53 network. *Nature*, 408, 307–310.
- [151]Campisi, J. , , d'Adda di Fagagna, F. (2007). Cellular senescence: when bad things happen to good cells. *Nat Rev Mol Cell Biol*, 8 (9), 729–740, (Review).
- [152]Schwarze, S. R. , Shi, Y. , Fu, V. X. , Watson, P. A. , Jarrard, D. F. (2001). Role of cyclin-dependent kinase inhibitors in the growth arrest at senescence in human prostate epithelial and uroepithelial cells. *Oncogene* 20 (57). 8184–8192.
- [153]Han, Z. , Wei, W. , Dunaway, S. , Darnowski, J. W. , Calabresi, P. , Sedivy, J. , Hendrickson, E. A. , Balan, K. V. , Pantazis, P. , Wyche, J. H. . (2002). Role of p21 in apoptosis and senescence of human colon cancer cells treated with camptothecin. *J Biol Chem*, 277 (19), 17154–17160.
- [154]Romanov, V. S. , Abramova, M. V. , Svetlikova, S. B. , Bykova, T. V. , Zubova, S. G. , Aksenov, N. D. , A. J. Fornace A. J. , Pospelova, T. V. , Pospelov, V. A. (2010). p21(Waf1) is required for cellular senescence but not for cell cycle arrest induced by the HDAC inhibitor sodium butyrate. *Cell Cycle*, 9 (19), 3945–3955.
- [155]Larsson, O. C. Scheele, O. , Liang, Z. , Moll, J. , Karlsson, C. Wahlestedt, C. , (2004). Kinetics of senescence-associated changes of gene expression in an epithelial, temperature-sensitive SV40 large T antigen model. *Cancer Res*, 64 (2), 482–489.
- [156]Rebbaa, A, Zheng, X., Chou, P.M., Mirkin, B.L. (2003). Caspase inhibition switches doxorubicin-induced apoptosis to senescence. *Oncogene*, 22 (18), 2805–2811.
- [157]Chang, B. D. , Swift, M. E. , Shen, M. , Fang, J. ,Broude, E. V. Roninson, I. B. (2002). Molecular determinants of terminal growth arrest induced in tumor cells by a chemotherapeutic agent. *Proc. Natl. Acad. Sci. U. S. A.*, 99 (1), 389–394.
- [158]Wang, X. , Wong, S. C. , Pan, J. , Tsao, S. W. , Fung, K. H. , Kwong, D. L. , Sham J. S. , Nicholls, J. M. (1998). Evidence of cisplatin-induced senescent-like growth arrest in nasopharyngeal carcinoma cells. *Cancer Res*, 58 (22), 5019–5022.
- [159]Yeo, E. J. , Hwang, Y. C. , Kang, C. M. , Kim, I. H. , Kim, D. I. , Parka, J. S. , Choy, H. E. , Park, W. Y. , Park, S. C. (2000). Senescence-like changes induced by hydroxyurea in human diploid fibroblasts. *Exp Gerontol*, 35 (5), 553–571.

- [160]Michishita, E. , Nakabayashi, K. , Suzuki, T. , Kaul, S. C. , Ogino, H. , Fujii, M. , Mitsui, Y. , Ayusawa, D. (1999). 5-Bromodeoxyuridine induces senescence-like phenomena in mammalian cells regardless of cell type or species. *J Biochem*, 126 (6),1052–1059.
- [161]Kagawa, S. , Fujiwara, T. , Kadowaki, Y. , Fukazawa, T. , Sok-Joo, R. , Roth, J. A. , Tanaka, N. (1999). Overexpression of the p21 sdi1 gene induces senescence-like state in human cancer cells: implication for senescence-directed molecular therapy for cancer. *Cell Death Differ*, 8, 765–772.
- [162]Fang, L., Igarashi, M. , Leung, J. , Sugrue, M. M. , Lee, S. W. , Aaronson, S. A. (1999). p21Waf1/Cip1/Sdi1induces permanent growth arrest with markers of replicative senescence in human tumor cells lacking functional p53. *Oncogene*, 18 (18), 2789–2797.
- [163]Gao, F. H. , Hu, X.H. , Li, W. , Liu, H. , Zhang, Y. J. , Guo, Z. Y. , Xu, M. H. , Wang, S. T. , Jiang, B. , Liu, F. , Zhao, Y. Z. , Fang, Y. , Chen, F. Y. , Wu, Y.L. (2010). Oridonin induces apoptosis and senescence in colorectal cancer cells by increasing histone hyperacetylation and regulation of p16, p21, p27 and c-myc. *BMC Cancer*, 10, 6(10), 610. doi: 10.1186/1471-2407-10-610
- [164]Jadeski, L. C. , Hum, K. O. , Chakraborty, C. , Lala, P. K. (2000). Nitric oxide promotes murine mammary tumour growth and metastasis by stimulating tumour cell migration, invasiveness and angiogenesis. *Int J Cancer*, 86(1), 30-9.
- [165]Vakkala, M. , Kahlos, K. , Lakari, E. , Pääkkö, P. , Kinnula, V. , et al. (2000). Inducible nitric oxide synthase expression, apoptosis, and angiogenesis in in situ and invasive breast carcinomas. *Clin Cancer Res*, 6, 2408-16.
- [166]Switzer, C. H. , Glynn, S. A. , Ridnour, L. A. , Cheng, R. Y. , Vitek, M. P. , et al. (2011). Nitric oxide and protein phosphatase 2A provide novel therapeutic opportunities in ER-negative breast cancer. *Trends Pharmacol Sci.*, 32(11), 644-51.
- [167]Kuno, T. , Tsukamoto, T. , Hara, A, Tanaka, T. (2012). Cancer chemoprevention through the induction of apoptosis by natural compounds. *Journal of Biophysical Chemistry*, 3, 156–173. doi: 10.1210/jc.2003-031314
- [168]Teiten, M. H. , Gaascht, F. , Eifes, S. , Dicato, M. , Diederich, M. (2010). Chemopreventive potential of curcumin in prostate cancer. *Genes Nutr*, 5, 61–74. doi: 10.1007/s12263-009-0152-3

- [169]Gu, Y. H. , Leonard, J. (2006). *In vitro* effects on proliferation, apoptosis and colony inhibition in ER-dependent and ER independent human breast cancer cells by selected mushroom species. *Oncology Reports*, 15, 417–423. doi: 10.1158/0008-5472.can-09-3565
- [170]Lee, H. S. , Seo, E. Y. , Kang, N. E. , Kimb, W. K. (2008). [6]-Gingerol inhibits metastasis of MDA-MB-231 human breast cancer cells. *Journal of Nutritional Biochemistry*, 19, 313–319. doi: 10.1016/j.jnutbio.2007.05.008
- [171]Konopleva, M. , Zhao, S. , Xie, Z. , Segall, H. , Younes, A. , et al. (1999). Apoptosis Molecules and mechanisms. *Adv Exp Med Biol*, 457, 217–36.
- [172]Schulze-Osthoff, K. , Ferrari, D. , Los, M. , Wesselborg, S. , Peter, M. E. (1998). Apoptosis signaling by death receptors. *Eur J Biochem*, 254, 439–459.
- [173]Micheau, O. , Tschopp, J. (2003). Induction of TNF receptor I-mediated apoptosis via two sequential signaling complexes. *Cell*, 1142, 181–90. doi: 10.1016/S0092-8674(03)00521-X
- [174]Zou, H. , Li, Y. , Liu, X. , Wang, X. (1999). An APAF-1.cytochrome c multimeric complex is a functional apoptosome that activates procaspase-9. *J Biol Chem*, 274, 11549–56.
- [175]Gupta, S. (2003). Molecular signaling in death receptor and mitochondrial pathways of apoptosis (Review). *Int J Oncol*, 22, 15–20.
- [176]Zhu, H. , Huang, M. , Yang, F. , Chen, Y. , Miao, Z. H. , et al. (2007). R16, a novel amonafide analogue, induces apoptosis and G2-M arrest via poisoning topoisomerase II. *Mol Cancer Ther*, 6, 484–95.
- [177]Cai, Y. , Lu, J. , Miao, Z. , Lin, L. , Ding, J. (2007) Reactive oxygen species contribute to cell killing and P-glycoprotein downregulation by salvicine in multidrug resistant K562/A02 cells. *Cancer Biol Ther*, 611, 1794–9.
- [178]Rajendran, P. , Ho, E. , Williams, D. E. , Dashwood, R. H. (2011). Dietary phytochemicals, HDAC inhibition, and DNA damage/repair defects in cancer cells. *Clin Epigenetics*, 3(1), 4 doi:10.1186/1868-7083-3-4.
- [179]Norbury, C. J. , & Zhivotovsky, B. (2004). DNA damage-induced apoptosis. *Oncogene*, 23, 2797–808. doi: 10.1038/sj.onc.1207532

- [180]Ljungman, M. (2010). The DNA damage response—repair or despair? *Environ Mol Mutagen*, 51, 879–89. Review.
- [181]Vogel, C. , Hager, C. , Bastians, H. (2007). Mechanisms of Mitotic Cell Death Induced by Chemotherapy-Mediated G2 Checkpoint Abrogation. *Cancer Res*, 67, 339–345. doi: 10.1158/0008-5472.CAN-06-2548
- [182]Selivanova, G. (2001). Mutant p53: the loaded gun. *Curr Opin Investig Drugs*, 2, 1136–41. Review.
- [183]Fojo, T. (2002). p53 as a therapeutic target: unresolved issues on the road to cancer therapy targeting mutant p53. *Drug Resist Updat*, 55, 209–16. Review.
- [184]Bossi, G. , Lapi, E. , Strano, S. , Rinaldo, C. , Blandino, G. , et al. (2006). Mutant p53 gain of function: reduction of tumor malignancy of human cancer cell lines through abrogation of mutant p53 expression. *Oncogene*, 25, 304–9. doi: 10.1038/sj.onc.1209026
- [185]Wang, X. , Di Pasqua, A. J. , Govind, S. , McCracken, E. , Hong, C. , et al. (2011). Selective depletion of mutant p53 by cancer chemopreventive isothiocyanates and their structure-activity relationships. *J Med Chem*, 54, 809–16. doi: 10.1021/jm101199t
- [186]Han, J. , Kim, S. , Yang, J. H. , Nam, S. J. , Lee, J. E. (2012). TPA-induced p21 expression augments G2/M arrest through a p53-independent mechanism in human breast cancer cells. *Oncol Rep*, 27, 517–22. doi: 10.1021/jm101199t
- [187]Sambucetti, L. C. , Fischer, D. D. , Zabludoff, S. , Kwon, P. O. , Chamberlin, H. , et al. (1999) Histone deacetylase inhibition selectively alters the activity and expression of cell cycle proteins leading to specific chromatin acetylation and antiproliferative effects. *J Biol Chem*, 274, 34940–7. doi: 10.1021/jm101199t
- [188]Attoub, S. , Hassan, A. H. , Vanhoecke, B. , Iratni, R. , Takahashi, T. , et al. (2011). Inhibition of cell survival, invasion, tumor growth and histone deacetylase activity by the dietary flavonoid luteolin in human epithelioid cancer cells. *Eur J Pharmacol*, 651, 18–25. doi: 10.1021/jm101199t
- [189]Berx, G., Cleton-Jansen, A. M. , Nollet, F. , de Leeuw, W. J. , van de Vijver, M. , et al. (1995). E-cadherin is a tumour/invasion suppressor gene mutated in human lobular breast cancers. *EMBO J*, 14, 6107-15.

- [190] Mohammadzadeh, F. , Ghasemibasir, H. , Rajabi, P. , Naimi, A. , Eftekhari, A. , et al. (2009). Correlation of E-cadherin expression and routine immunohistochemistry panel in breast invasive ductal carcinoma. *Cancer Biomark*, 5, 1-8. doi: 10.3233/CBM-2009-0551.
- [191] Kowalski, P. J. , Rubin, M. A. , Kleer, C. G. (2003). E-cadherin expression in primary carcinomas of the breast and its distant metastases. *Breast Cancer Res*, 5(6), R217-22.
- [192] Cao, Q. , Yu, J. , Dhanasekaran, S. M. Kim, J. H. , Mani, R. S. , et al. (2008). Repression of E-cadherin by the polycomb group protein EZH2 in cancer. *Oncogene*, 27, 7274-84.
- [193] Kim, N. H. , Kim, S. N. , Kim, Y. K. (2011). Involvement of HDAC1 in E-cadherin expression in prostate cancer cells; its implication for cell motility and invasion. *Biochem Biophys Res Commun*, 404, 915-21.
- [194] Liotta, L. A. , Tryggvason, K. , Garbisa, S. , Hart, I., Foltz, C. M. , et al. (1980). Metastatic potential correlates with enzymatic degradation of basement membrane collagen. *Nature*, 284, 67-8.
- [195] Giajelli, C. , Theocharis, A. D. , Karamanos, N. K. (2011). Roles of matrix metalloproteinases in cancer progression and their pharmacological targeting. *FEBS J*, 278, 6-27. Review.
- [196] Bachmeier, B. E. , Nerlich, A. G. , Lichtinghagen, R. , Sommerhoff, C. P. (2001). Matrix metalloproteinases (MMPs) in breast cancer cell lines of different tumorigenicity. *Anticancer Res*, 21, 3821-8.
- [197] Koch, A. E. , Halloran, M. M. , Haskell, C. J. , Shah, M. R. , Polverini, P. J. (1995). Angiogenesis mediated by soluble forms of E-selectin and vascular cell adhesion molecule-1. *Nature*, 376, 517-9.
- [198] Nizamutdinova, I. T. , Lee, G. W. , Lee, J. S. , Cho, M. K., Son, K. H. , et al. (2008). Tanshinone I suppresses growth and invasion of human breast cancer cells, MDA-MB-231, through regulation of adhesion molecules. *Carcinogenesis*, 29, 1885-92.
- [199] Schröder, C. , Witzel, I. , Müller, V., Krenkel, S. , Wirtz, R. M. , et al. (2011). Prognostic value of intercellular adhesion molecule (ICAM)-1 expression in breast cancer. *J Cancer Res Clin Oncol*, 137, 1193-201.
- [200] Kerbel, R. , Folkman, J. (2002). Clinical translation of angiogenesis inhibitors. *Nat Rev Cancer*, 2, 727-39.
- [201] Kerbel, R.S. (2006). Antiangiogenic therapy: a universal chemosensitization strategy for cancer? *Science*, 312, 1171-5.

- [202] Relf, M. , LeJeune, S. , Scott, P.A. , Fox, S. , Smith, K. et al. (1997). Expression of the angiogenic factors vascular endothelial cell growth factor, acidic and basic fibroblast growth factor, tumor growth factor beta-1, platelet-derived endothelial cell growth factor, placenta growth factor, and pleiotrophin in human primary breast cancer and its relation to angiogenesis. *Cancer Res*, 57, 963-9.
- [203] Lee, Y. J. , Lin, W. L. , Chen, N. F. , Chuang, S. K. , Tseng, T. H. (2012). Demethylwedelolacton derivatives inhibit invasive growth in vitro and lung metastasis of MDA-MB-231 breast cancer cells in nude mice. *Eur J Med Chem*, 56, 361-7.
- [204] Li, C. , Guo, S. , & Tiemei, S. (2102). Role of NF- $\kappa$ B activation in matrix metalloproteinase 9, vascular endothelial growth factor and interleukin 8 expression and secretion in human breast cancer cells. *Cell Biochem Funct*, 31(3), 263-8. doi: 10.1002/cbf.2899
- [205] Perkins, N. D. (2012). The diverse and complex roles of NF- $\kappa$ B subunits in cancer. *Nature Reviews Cancer*, 12, 121-132. doi:10.1038/nrc3204.
- [206] Muntané, J. and De la Mata, M. (2010) Nitric oxide and cancer. *World J Hepatol*, 2, 337–344
- [207] Wang, C. , Trudel, L. J. , Wogan, G. N. , Deen, W. M. (2003). Thresholds of nitric oxidemediated toxicity in human lymphoblastoid cells. *Chem Res Toxicol*, 16, 1004-13.
- [208] Ambs, S. , Merriam, W. G. , Ogunfusika, M. O. , Bennett, W. P. , Ishibe, N. , et al. (1998). p53 and vascular endothelial growth factor regulate tumor growth of NOS2-expressing human carcinoma cells. *Nat Med*, 4, 1371-6.
- [209] Glynn, S. A. , Boersma, B. J. , Dorsey, T. H. , Yi, M. , Yfantis, H. G. , et al. (2010). Increased NOS2 predicts poor survival in estrogen receptor-negative breast cancer patients. *J Clin Invest*, 120, 3843-54.
- [210] Tadmouri, G. O. & Al-Sharhan, M. (2004). Cancers in the United Arab Emirates, Genetic Disorders in the Arab World: United Arab Emirates, (1), 59-61.